2006-07-31

Development of a Signal Processing Library for Extraction of SpO2, HR, HRV, and RR from Photoplethysmographic Waveforms

William S. Johnston
Worcester Polytechnic Institute

Development of a Signal Processing Library for Extraction of SpO_2, HR, HRV, and RR from Photoplethysmographic Waveforms

A Thesis

Submitted to the Faculty

of the

WORCESTER POLYTECHNIC INSTITUTE

in partial fulfillment of the requirements for the

Degree of Master of Science

by

William S. Johnston

Date: July 27, 2006

Approved:

Professor Yitzhak Mendelson, Major Advisor
Department of Biomedical Engineering

Professor R. James Duckworth, Committee Member
Department of Electrical and Computer Engineering

Professor William Michalson, Committee Member
Department of Electrical and Computer Engineering

ABSTRACT

Non-invasive remote physiological monitoring of soldiers on the battlefield has the potential to provide fast, accurate status assessments that are key to improving the survivability of critical injuries. The development of WPI's wearable wireless pulse oximeter, designed for field-based applications, has allowed for the optimization of important hardware features such as physical size and power management. However, software-based digital signal processing (DSP) methods are still required to perform physiological assessments. This research evaluated DSP methods that were capable of providing arterial oxygen saturation (SpO_2), heart rate (HR), heart rate variability (HRV), and respiration rate (RR) measurements derived from data acquired using a single optical sensor. *In vivo* experiments were conducted to evaluate the accuracies of the processing methods across ranges of physiological conditions. Of the algorithms assessed, 13 SpO_2 methods, 1 HR method, 6 HRV indices, and 4 RR methods were identified that provided clinically acceptable measurement accuracies and could potentially be employed in a wearable pulse oximeter.

ACKNOWLEDGEMENTS

I wish to thank the following people for their contributions and support during my research:

Prof. Yitzhak Mendelson for his expertise, assistance, and guidance throughout my endeavors at WPI.

Prof. R. James Duckworth and Prof. William Michalson for their unique perspectives and valuable suggestions.

Vladimir Floroff, Gary Comtois, and Paul Branche for their continuous assistance during my research and for helping to integrate my work into the overall project.

Suresh Atapattu for taking the time to help me with data analysis and providing critical reference values for my experiments.

Jenna Balistrini for her enthusiasm, research tips, and continuous support.

My family, especially my parents, for their unwavering love and support in everything I have pursued in life.

My friends in Worcester and at home for believing in me and helping me to enjoy life.

This work is supported by the U.S. Army Medical Research and Materiel Command under Contract No. DAMD17-03-2-0006. The views, opinions and/or findings contained in this report are those of the author and should not be construed as an official Department of the Army position, policy or decision unless so designated by other documentation.

TABLE OF CONTENT

LIST OF FIGURES

LIST OF TABLES

GLOSSARY OF ABBREVIATIONS

Abbreviation	Definition
μC	Microcontroller
BPF	Band-Pass Filter
DSP	Digital Signal Processing
ECG	Electrocardiogram
FFT	Fast Fourier Transform
Hb	Deoxyhemoglobin
HbO_2	Oxygenated Hemoglobin
HF	High Frequency
HPF	High-Pass Filter
HR	Heart Rate
HRV	Heart Rate Variability
IHR	Instantaneous Heart Rate
IR	Infrared
LED	Light Emitting Diode
LF	Low Frequency
LPF	Low-Pass Filter
PD	Photodetector
PDA	Personal Digital Assistant
PPG	Photoplethysmogram / Photoplethysmographic
PSPU	Photoplethysmogram Signal Processing Unit
R	Red
R	Ratio-of-Ratios
RIIV	Respiratory-Induced Intensity Variations
RR	Respiratory Rate
SaO_2	Arterial Oxygen Saturation
SpO_2	Estimate of Arterial Oxygen Saturation
WWPO	Wearable Wireless Pulse Oximeter

1. INTRODUCTION

Following serious trauma, it is critical to promptly acquire proper diagnosis and effective treatment in order to optimize a patient's chance of survival. In many situations, however, timely and efficient medical care is not readily available. An example of an extreme situation is the frontline of a military conflict. With individual soldiers often spread over a broad region, injuries potentially occurring suddenly and without warning, and a perpetually hostile environment, performing efficient triage and providing effective treatment to wounded combatants is exceedingly challenging.

As such, telemedicine applications have long been at the forefront of military research in an effort to improve the medical care received by casualties on the frontline. In recent years, the military has been working on a Warfighter Physiological Status Monitor (WPSM) [1] that will allow combat medics to monitor the physiological status of their soldiers, thereby potentially reducing medical response times and improving remote triage capabilities.

The uses of telemedical devices can also extend to non-military applications. High-risk occupations can often result in situations where performing triage on injured individuals is challenging. Firefighters and law enforcement are often placed in harms way on a daily basis, and in the midst of such chaotic environments, it is often difficult to determine when an individual is injured, let alone to estimate the severity of the injury. In urban or developed regions, events such as building collapses, floods, earthquakes, and other natural disasters often involve mass casualties. Even with highly-trained medical

professionals and emergency personnel, the sheer number of injuries in such a situation can make efficient triage and timely treatment difficult if not impossible.

A popular method of patient monitoring is pulse oximetry, due to its non-invasive nature. An additional benefit of this modality is the extensive amount of physiological information available through its use. While arterial oxygen saturation (SpO_2) and heart rate (HR) measurements are typically provided by pulse oximeters, heart rate variability (HRV) and respiration rate (RR) information can also be extracted from sensor data. This poses a significant advantage in the area of remote patient monitoring since providing all physiological measurements from a single sensor has allowed wearable monitoring devices to be miniaturized for portability and field use. However, despite advances in hardware optimization, the digital signal processing (DSP) methods required to perform such physiological measurements must still be developed for custom-designed devices.

In order to facilitate the development of a wearable medical monitoring system, the research performed here covered the first step in producing a software package capable of performing multiple physiological measurements based on pulse oximetry sensor data. Specifically, SpO_2, HR, HRV, and RR measurements were examined since they were known to provide critical patient information during medical diagnoses. The work consisted of assessing the accuracy of multiple processing methods that could be employed to measure each of the physiological parameters. Algorithms that provided clinically acceptable results under controlled conditions were placed in a library of potentially viable processing methods to allow for future assessments of their robustness during typical application conditions.

This thesis begins by discussing the needs of field medics and the potential impact of implementing a wearable monitoring system in field-based applications. Current and developing technologies in this research area are covered first, followed by an examination of the fundamental techniques for extracting physiological measurements from photoplethysmographic (PPG) waveforms. The latter half of this thesis outlines the experiments that were performed, how the acquired data were used to assess the signal processing algorithms that were tested, and finally, the results that were derived from each algorithm.

2. BACKGROUND

2.1 Military Medical Support

2.1.1 Medical Echelons:

As long as military conflicts exist, it is understood that soldiers sent into combat may be seriously wounded or killed. The United States military implements a structured medical response and evacuation system to provide life-saving support to troops on the battlefield. This system, outlined in Figure 2.1, allows for the presence of fast and effective medical care that is essential to maintaining the integrity of a squad, aids in the survival of critical injuries, and increases the success of a mission.

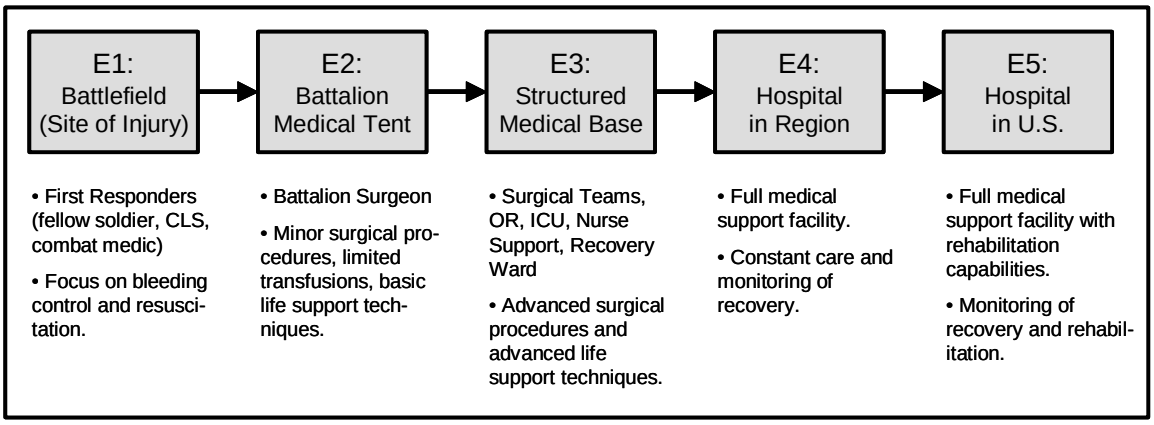

Figure 2.1. *Structure of military medical echelons.*

Following injury, a casualty is evacuated through multiple levels, or echelons, of medical care [2, 3]. The *first echelon* (E1) pertains to the treatment that is administered on the battlefield. Immediately following an injury, either the patient or the squad's combat lifesaver (CLS) administers very basic first aid with an emphasis on stopping any bleeding and beginning fluid resuscitation. If evacuation is not immediate, the combat

medic, a soldier with 10-weeks to 6-months of additional medical training, may arrive on the scene to provide more advanced treatment such as airway management, cardiopulmonary resuscitation (CPR), hemostasis, or medication including pain relievers or antibiotics. The *second echelon* (E2), the first evacuation stage for an injured combatant, is a mobile camp located near the frontline of a conflict. Here, casualties receive more critical care from the battalion surgeon, a physician with advanced medical training, and a group of support personnel. At this stage, minor surgical procedures can be performed along with limited blood and fluid transfusions and advanced life support techniques. Should a higher degree of care be required, the casualty is transported farther away from the frontline to the *third echelon* (E3), a corps surgical hospital (CSH) at a structured medical base. At this facility, full surgical teams can provide specialized medical care based on the specifics of a patient's injury. The resources are more advanced at this stage and include an operating room (OR), intensive care unit (ICU), nurse support, and recovery ward. The *fourth echelon* (E4) is a permanent hospital near the area of the conflict that has complete medical services and can maintain prolonged monitoring of the patient's recovery. The final *fifth echelon* (E5) is a permanent facility in the United States, where the patient can recover with the support of a full rehabilitation program.

2.1.2 Treatment on the Frontline:

On the frontline, the speeds of medical response and evacuation are vital. Combat medics require specific critical information in order to treat casualties quickly and stabilize them long enough to be transported to higher echelons of medical care. Due to limited medical

resources, minimal training, and potentially dangerous surroundings, the focus is on hemostasis, CPR, and evacuation.

Once a casualty has been identified, the medic or care-giver must locate the casualty and move to his position in order to provide treatment and initiate extraction from the area. Evaluation of the wounded combatant's physical condition then allows for a preliminary diagnosis to determine physiological stability. The basic vital signs that are of concern to a first responder are those that indicate the functional states of the circulatory and respiratory systems [2]. With an individual's physical condition assessed, triage is performed and the casualties are categorized according to the severity of their injuries and the need for specialized or advanced medical care.

2.2 Significance of a Wireless Monitoring System

Away from an organized medical facility, triage can often become inefficient. Passing casualty information by word-of-mouth, manually performing physiological measurements, and assessing casualties one at a time all require substantial amounts of time, energy, and resources. A wireless sensor network could potentially improve the quality of medical care in the field by accelerating the flow of medically relevant information. Providing vital information to a medic could reduce the amount of time spent performing tasks such as manual measurements, triage on multiple casualties, and physically moving between casualties to assess individual conditions.

By using wearable wireless sensors to monitor individuals, a medic could be alerted to potential problems or injuries soon after they occur, reducing a caregiver's response time in an emergency. During assessment of a casualty, obtaining multiple

physiological measurements from wearable sensors could free a medic from performing manual measurements and allow him to focus on stabilizing a patient and providing treatment.

Remote monitoring of multiple casualties could also allow for more effective triage. It can often be difficult or even impossible to track the conditions of numerous patients even when they are all in one location. During military conflicts, casualties can be spread over a wide area and having a medic constantly moving between them to provide ongoing assessments is extremely inefficient. By receiving vital physiological measurements and alerts by exception as to which individuals are critically wounded, medics could perform remote triage on numerous patients simultaneously from a single location.

In a combat environment, remote monitoring even has the potential to keep medics themselves from becoming injured or killed. In hostile environments, it can often be dangerous for a medic to move to a casualty's location. Performing medical assessments using wireless sensors could aid in determining whether an injured soldier is alive or dead before performing a rescue. Attempting to reach a combatant that has already died puts unnecessary risk on the medic and other personnel.

2.3 Current State of Developing Technologies

In an effort to improve the medical care provided to combatants, the military has long been looking to implement a personal status monitoring system capable of tracking the physiological conditions of soldiers [1]. Different groups have developed systems that allow for remote monitoring, data processing, and control of information flow. Several

systems have been specifically designed with military applications in mind, while others are aimed at home-based care and in-hospital monitoring.

A research team from Dartmouth College and Dartmouth Hitchcock Medical Center, for example, is currently developing an Automated Remote Triage and Emergency Management Information System, known as ARTEMIS, for use by the military [4-7]. The system is based on a wireless sensor network and pulse oximetry data from individual soldiers. Algorithms employed by portable devices, such as a personal digital assistant (PDA), are designed to perform automated physiological assessments of combatants based on the measurements provided by the sensors. Information derived from these assessments is then relayed to multiple echelons of medical care through a mobile communications network.

A group at Kansas State University has also been developing a non-invasive physiological monitoring system based on pulse oximeter and electrocardiogram (ECG) modules [8-11]. Designed to facilitate home care, hospital patient observation, and veterinary and livestock monitoring, the system employs a wireless link between each wearable data logger and a central base station. The base station is configured to transfer data to off-site locations, such as a doctor's office, via the internet, providing the capability of remote patient monitoring.

In addition to photoplethysmogram (PPG) and ECG data, assessing an individual's physical activities has also become increasingly important. Many wearable medical systems are designed to monitor activity using accelerometers, gyroscopes, and tilt sensors [12-15]. Patient activity levels, posture, speed of movement, and falling events measured by these sensors can provide important information to caregivers.

Much work has also been dedicated to the development of various sensor modalities. Acoustic sensors [16, 17] designed at the Army Research Laboratory in Adelphi, MD, are capable of extracting a variety of physiological measurements by analyzing sounds produced by the human body. A ring-based pulse oximeter sensor [18] being developed by a research team at MIT has the potential to combat motion artifacts during signal acquisition. Advanced implantable and ingestible sensors [19] are also currently being designed.

Providing patients with freedom of mobility while maintaining continuous monitoring is a rapidly growing desire of medical professionals. Wearable devices such as the AMON physiological monitor [20, 21] and the Nonin WristOx® 3100 [22] have been designed with these goals in mind. These wristwatch-style units allow caregivers to track physiological changes in high-risk patients while freeing users from the constraints of tethered equipment and stationary instruments. Hardware features vary between devices depending upon how monitoring is performed. For example, the AMON utilizes a wireless data link to transmit measurements and signals to medical professionals on demand, while the WristOx® stores data locally in non-volatile memory so it can be extracted and analyzed at a later point in time.

2.4 The WPI Wearable Wireless Pulse Oximeter Project

The wearable wireless pulse oximeter (WWPO) system in development at WPI is being designed to allow monitoring of multiple individuals who would potentially be dispersed over a wide region. The system, outlined in Figure 2.2, consists of a wireless network that connects wearable sensor modules to a central monitoring unit such as a PDA. The

wearable sensor modules perform non-invasive monitoring using an optical pulse oximeter sensor and accelerometers so that a medic or care giver using a PDA is provided with physiological information from the individuals within the device's coverage area.

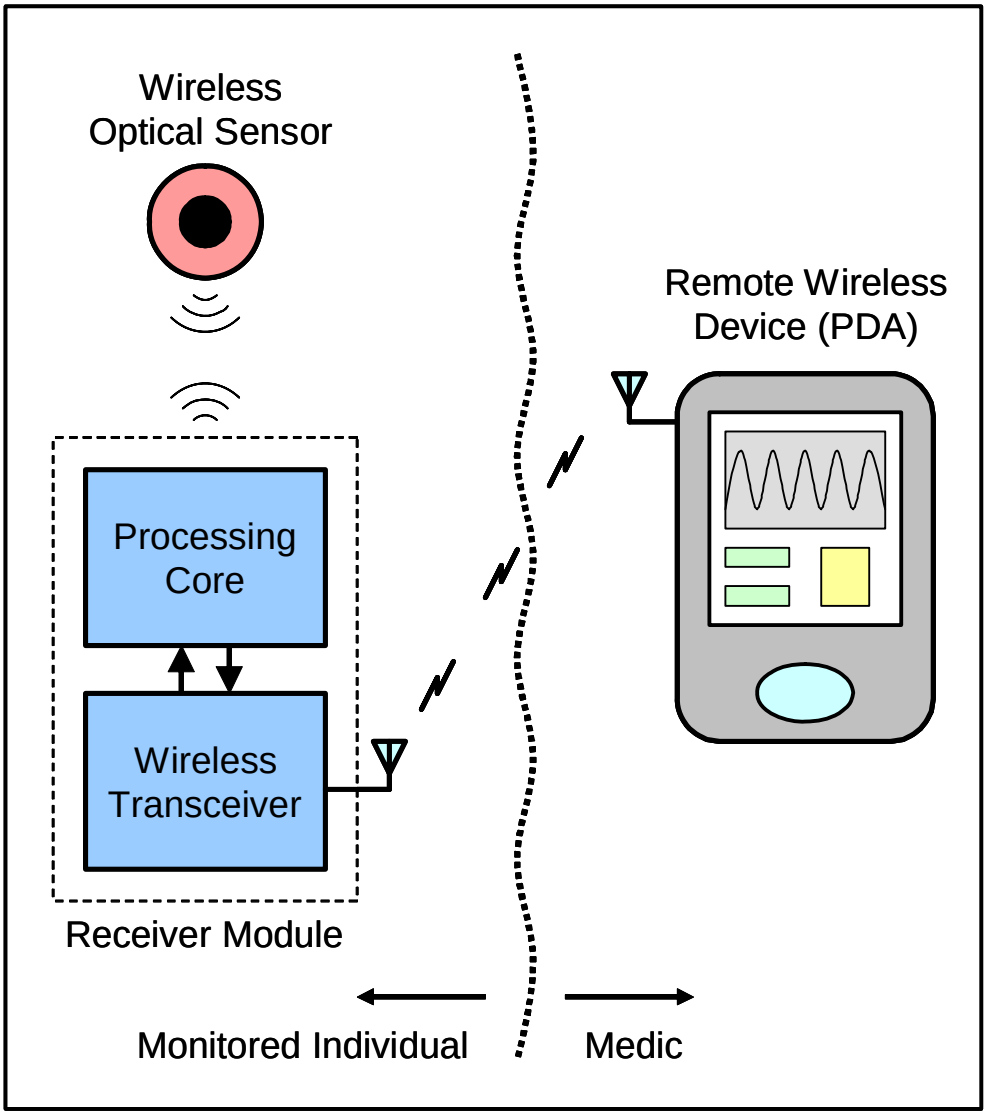

Figure 2.2. *Functional diagram of the WPI WWPO.*

While recent technological developments have allowed for the miniaturization of medical devices such as pulse oximeters [23-26], significant hurdles still exist when attempting to implement these off-the-shelf units in field-based applications. The sizes

and weights of some 'portable' modules are unacceptable for use by individuals in the field, and substantial power requirements significantly limit the duration of usability of more compact devices. In addition, the measurement of multiple physiological parameters typically requires the use of multiple sensors, corresponding to an increase in hardware cost, weight encumbrance, and maintenance. Therefore, the development of a miniature, low-power, WWPO capable of monitoring multiple physiological parameters is a desirable solution.

Although compact and efficient solutions currently exist for performing certain physiological measurements, the flexibility of commercially available development options is limited. Products such as the BCI-4320 and the Xpod® and ipod® available from Nonin, while designed for integration into larger systems, are self-contained and not easily modified. Thus, desirable changes to key features such as physical size and power consumption cannot be made. As such, the WWPO system in development at WPI employs a custom-designed microcontroller (μC) based hardware platform that has allowed such key features to be optimized for portable field-based applications.

However, limitations in commercially available software have required custom-designed solutions to be developed for this new hardware platform. In order to identify software-based processing methods capable of performing the desired physiological measurements, the PPG waveforms acquired from a pulse oximeter sensor had to be examined. The physiological factors affecting the form of the PPGs were key to extracting medically-relevant physiological measurements.

3. OPTICALLY-BASED PHYSIOLOGICAL MEASUREMENTS

By incorporating multiple measurements into a clinical evaluation, a more accurate assessment of an individual's status can be obtained. Due to the numerous factors that affect its form, the PPG signal contains information pertaining to various physiological parameters. Several of these parameters are commonly used in medical diagnoses and include SpO_2, HR, HRV, and RR. Presenting such medical information simultaneously to medics could improve diagnostic abilities and enhance treatment regimes in the field. In addition, utilizing a single sensor to obtain all physiological measurements would simplify data processing, extend battery life, and reduce cost and encumbrance by minimizing the hardware worn by an individual.

3.1 The Photoplethysmographic Signal

PPG signals are commonly used in medical settings to obtain vital physiological information. These waveforms, recorded using optical sensors, contain information pertaining to such factors as blood oxygen content [27-30], cardiovascular activity [31-33], and respiratory patterns [31, 33-35]. Typically, PPG signals are recorded and analyzed by pulse oximeters to provide SpO_2 and HR measurements.

Plethysmographic waveforms represent changes in blood volume in a given region of tissue. Optical sensors are commonly employed as a practical way of obtaining these waveforms through non-invasive means. Such optical sensors consist of a light source, typically a light-emitting diode (LED), and a photodetector (PD) element. The

light source is used to illuminate a region of tissue and the PD measures the amount of light exiting the tissue at a different location.

Most illuminated constituents, such as bone, muscle, venous blood, and various other cellular structures, absorb a constant amount of light, since their volumes and densities do not change over short periods of time. The volume of the arterial blood, however, is modulated by the beating of the heart. Each time the heart contracts, an additional bolus of blood is forced through the arterial pathways. With this variation in arterial volume comes a proportional variation in light absorption that can be measured by an optical sensor. An increase in arterial blood volume causes a corresponding decrease in the amount of light that reaches the PD. The amount of light absorbed by the tissues contains two significant aspects, as shown in Figure 3.1a. The first is the constant absorbance, or DC component, influenced by the nonvascular tissues and residual arterial and venous blood volumes. The second is a modulated absorbance, or AC component, caused by the variations in arterial blood volume. Together, they affect the amount of light that illuminates the PD to produce a pulsatile waveform, as shown in Figure 3.1b.

3.2 Theory of SpO_2 Measurement

Injuries sustained in a combat environment often directly affect a soldier's cardiac and pulmonary systems, many times causing blood loss, hemothorax, pneumothorax, and other dangerous conditions [2]. Such conditions can lead to hypoxemia, depriving vital organs of oxygen and endangering the casualty's life. SpO_2 measurements are routinely employed to detect these hypoxic events before irreversible damage is caused to tissues and organs.

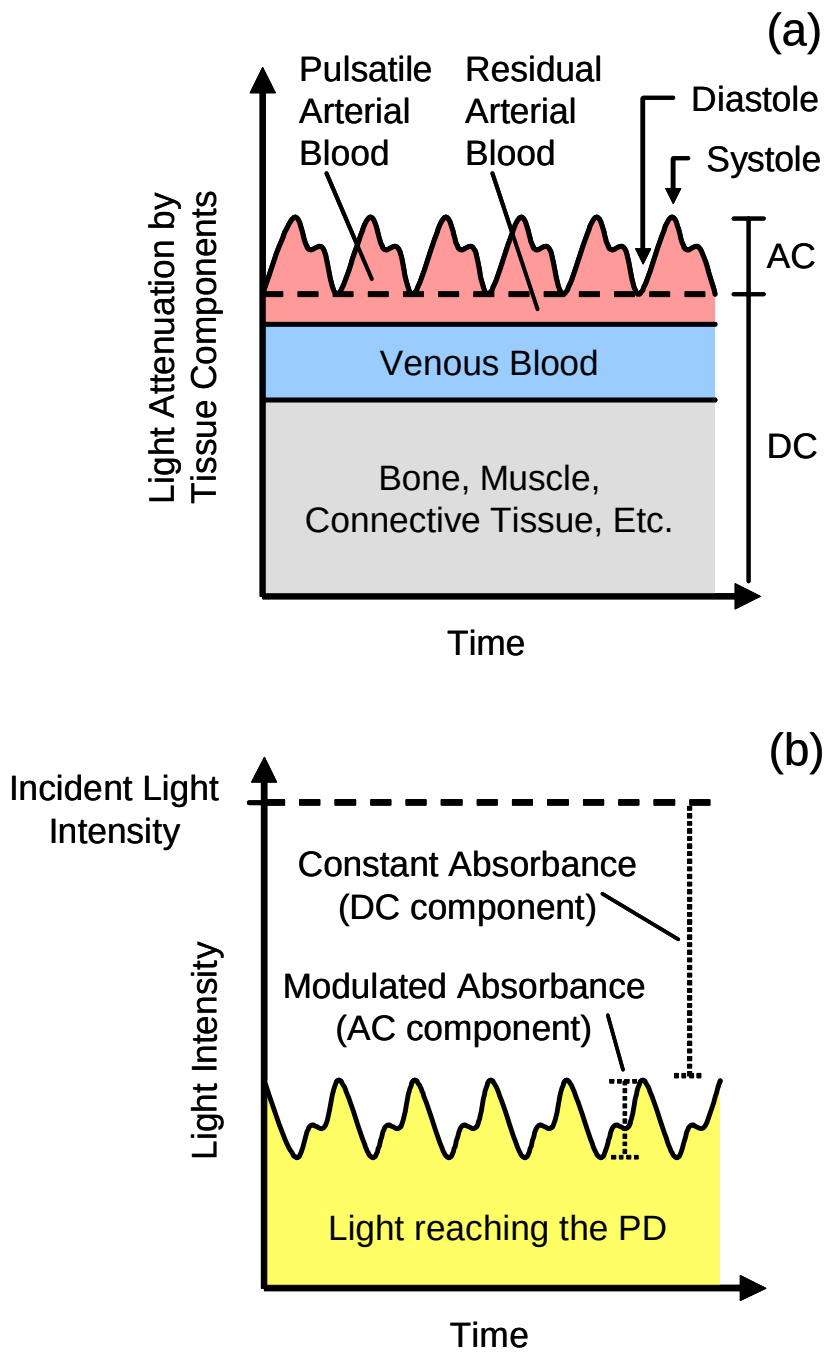

Figure 3.1. *Graphical representations of (a) the light absorbance of tissue components and (b) the resulting light intensity illuminating the PD.*

3.2.1 Hemoglobin Light Attenuation:

Noninvasive optical estimation of arterial oxygen saturation (SaO_2) by pulse oximetry is based on the light absorption properties of blood. Deoxyhemoglobin (Hb), which carries approximately 98% of the blood's oxygen supply, changes its light absorption characteristics when it binds with oxygen. Pulse oximetry exploits this optical difference between Hb and oxygenated hemoglobin (HbO_2) to estimate the percentage of arterial blood saturated with oxygen. As shown in Figure 3.2, the absorption spectrums of Hb and HbO_2 differ significantly in the visible and near-infrared region of the electromagnetic spectrum. Hb has a substantially higher absorption profile between 600 and 805 nm, while HbO_2 has a slightly higher absorption profile between 805 and 1000 nm. Wavelengths in the red (R) and infrared (IR) regions around 660 and 900 nm are typically used in most pulse oximetry applications [36], although variations are common among device manufacturers.

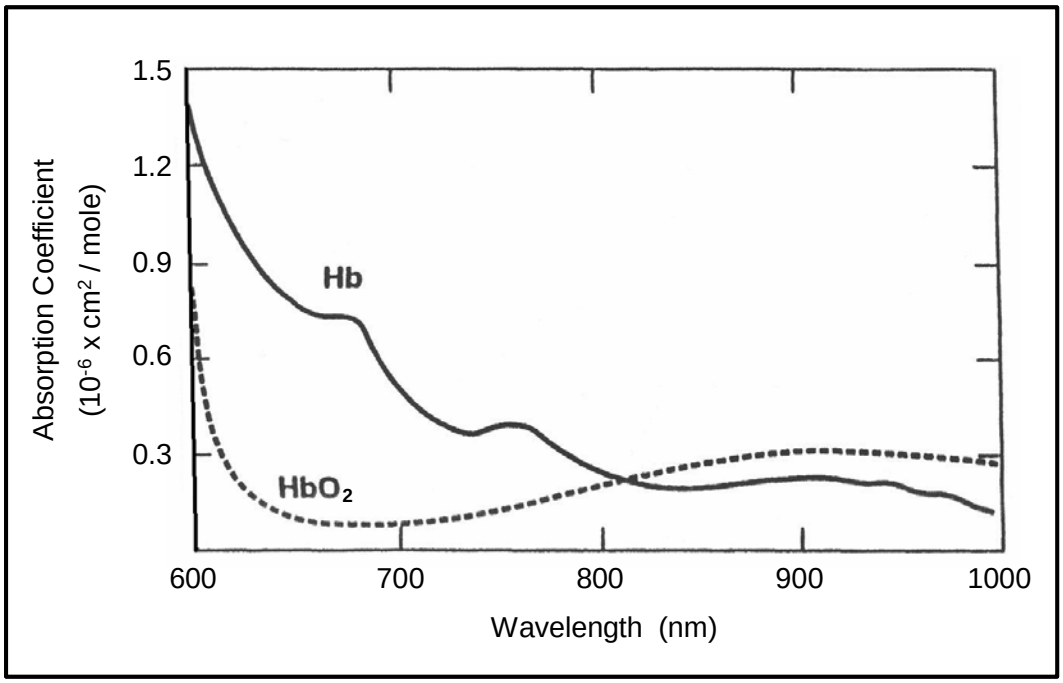

Figure 3.2. *Optical absorption spectra of Hb and HbO_2 in the R and IR regions [37].*

Blood with a low amount of oxygen contains an increased level of Hb and a decreased level of HbO_2. As a result, the blood absorbs more light at R wavelengths and less light at IR wavelengths. Conversely, blood with a high amount of oxygen contains a reduced level of Hb and an increased level of HbO_2. The blood then absorbs less light at R wavelengths and more light at IR wavelengths. These wavelength-based absorption characteristics make it possible to measure changes in SaO_2 using optical means.

3.2.2 Measurement Derivation:

The ratio of R-to-IR light (R/IR) absorbed by arterial blood changes with SaO_2 in an inversely proportional manner, as shown in Figure 3.3. As such, Equation 3.1 can be used to approximate this relationship and to calculate SpO_2:

$$SpO_2 = A - B \bullet (R/IR) \qquad (3.1)$$

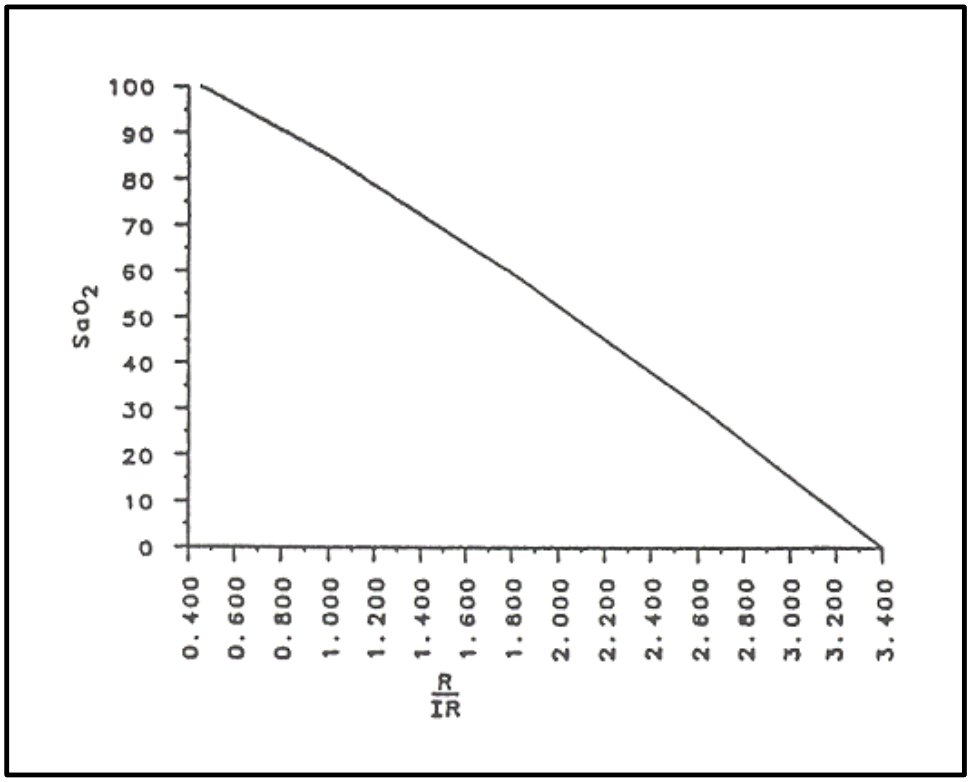

Figure 3.3. *Empirically-derived relationship between SaO_2 and the measured R/IR ratio [28].*

where (R/IR) is the ratio of R and IR light absorbed by the arterial blood, A and B are calibration coefficients, and SpO_2 is the estimate of SaO_2. In pulse oximetry, two PPG signals are recorded simultaneously: one at a R wavelength and one at an IR wavelength. The amplitude of the AC component in a signal corresponds to the amount of light absorbed by the arterial blood. By measuring the pulsatile amplitude of both signals, the amount of light absorbed by arterial blood at each wavelength can be estimated and used to calculate the ratio R/IR.

The PPG signals can be affected by a number of physiological and physical factors. LED intensities, PD wavelength sensitivity, and thickness or density of a tissue region for example, can alter the relative amplitudes of the two PPG signals. As a result, the amplitudes of the two AC components must be normalized. A graphical representation of this procedure is shown in Figure 3.4. Equation 3.2 depicts the equivalent mathematical function:

$$\boldsymbol{R} = (R/IR) = \frac{\left(\frac{AC_R}{DC_R}\right)}{\left(\frac{AC_{IR}}{DC_{IR}}\right)} \qquad (3.2)$$

where AC_R is the AC amplitude of the R signal, DC_R is the DC offset of the R signal, AC_{IR} is the AC amplitude of the IR signal, DC_{IR} is the DC offset of the IR signal, and $\boldsymbol{R}$ is the resulting "ratio-of-ratios". Combining Equations 3.1 and 3.2 results in Equation 3.3, which estimates SaO_2 based on normalized R and IR PPG signals.

$$SpO_2 = A - B \bullet \boldsymbol{R} \qquad (3.3)$$

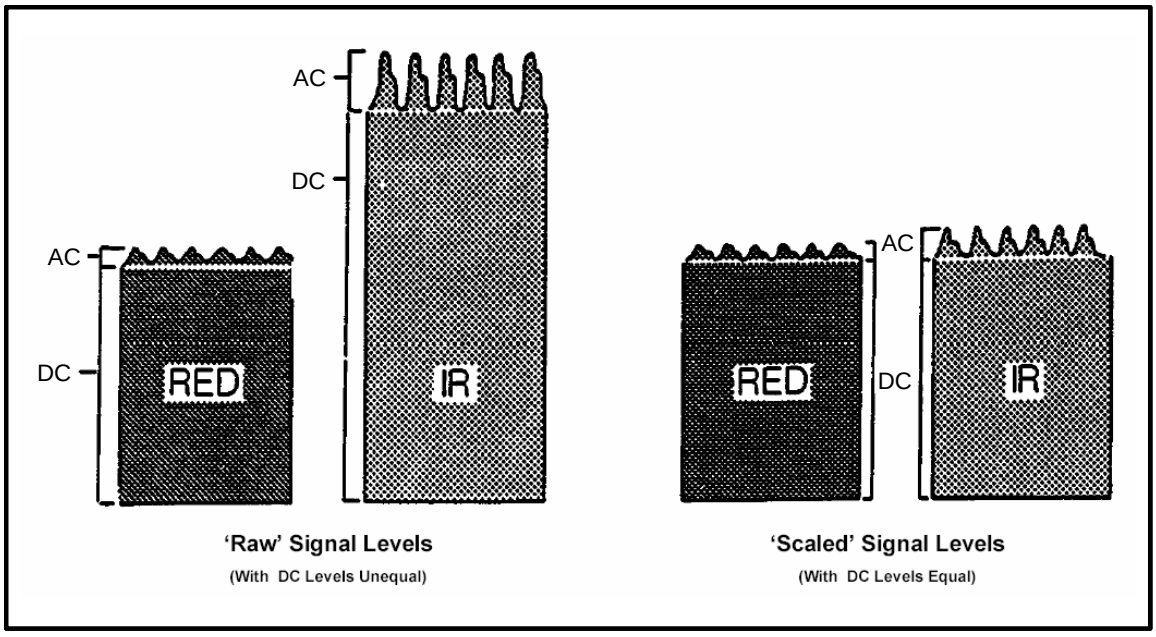

Figure 3.4. *Graphical normalization of R and IR PPG signals to allow for direct comparison of the AC components [38].*

where ***R*** is defined by Equation 3.2, A and B are coefficients derived through empirical calibration, and SpO_2 is the resulting estimate of SaO_2.

It should be noted that the relationship between ***R*** and SpO_2 is not perfectly linear. However, most clinical work does not require measurements over the full range of SaO_2. The region from 70 – 100% saturation is typically the most relevant to care-givers for SpO_2 measurements in adults. Since the relationship in this region is very close to linear, it can be approximated using the linear Equation 3.3. The resulting accuracy in the region of interest is typically ±2% [28], which is acceptable for most clinical work.

3.2.3 SpO_2 Measurement Methods:

An SpO_2 measurement based on PPG signals requires a calculation of the normalized ***R*** ratio. While the form of Equation 3.3 remains constant, a variety of methods exist for obtaining the values used to calculate ***R***, in particular the amplitudes of the AC

components of the R and IR PPG signals. Most commercial devices utilize simple algorithms, while a few advanced models employ more complex assessment methods.

Direct amplitude measurements of the pulsatile components in time-domain PPG signals are some of the simplest methods used for estimating an AC value. As depicted in Figure 3.5b, measuring the amplitudes of individual pulses [23, 39] can be used to provide accurate AC values. An alternative method, shown in Figure 3.5a, is to use the point-to-point differentials between consecutive data points [40] to measure relative amplitude changes between R and IR PPGs. The advantages of these methods are their high processing speeds and the minimal resources required to implement the algorithms. However, since minor variations typically exist between consecutive measurements, averaging is used to smooth the final results [41].

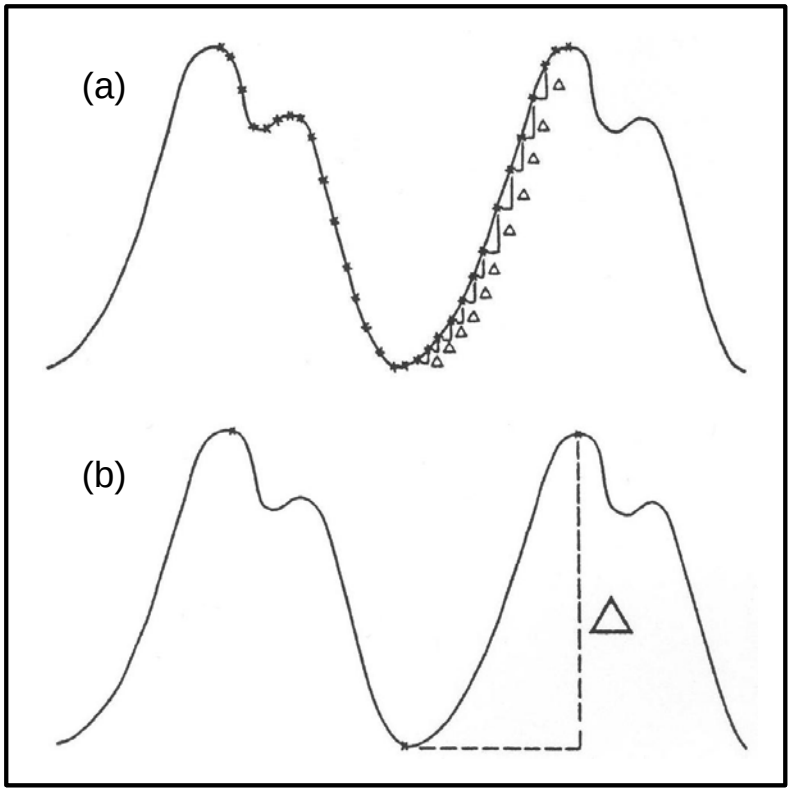

Figure 3.5. *AC amplitude estimation based on (a) point-to-point differentials and (b) peak-nadir differences [28].*

Various research groups have investigated alternative methods for computing SpO_2. Rusch and Scharf [41-44] and Kim et al. [45] have examined spectral analysis as a potential means of performing pulse oximetry measurements. Sinusoidal-based transforms can be used to convert PPG signals into the frequency domain. The AC and DC amplitudes of the PPGs are then estimated based on the heights of the 0 Hz and cardiac spectral peaks, as shown in Figure 3.6. The results from these studies have shown that spectral analysis boasts potential improvements over time-based computations, including greater measurement accuracy, insensitivity to high frequency noise, and better stability in the presence of light motion artifacts. A number of pulse oximeter manufacturers, including Ohmeda [46], Nellcor [47], and Masimo [48, 49] have also noted that spectral analysis is a potential method of measuring SpO_2.

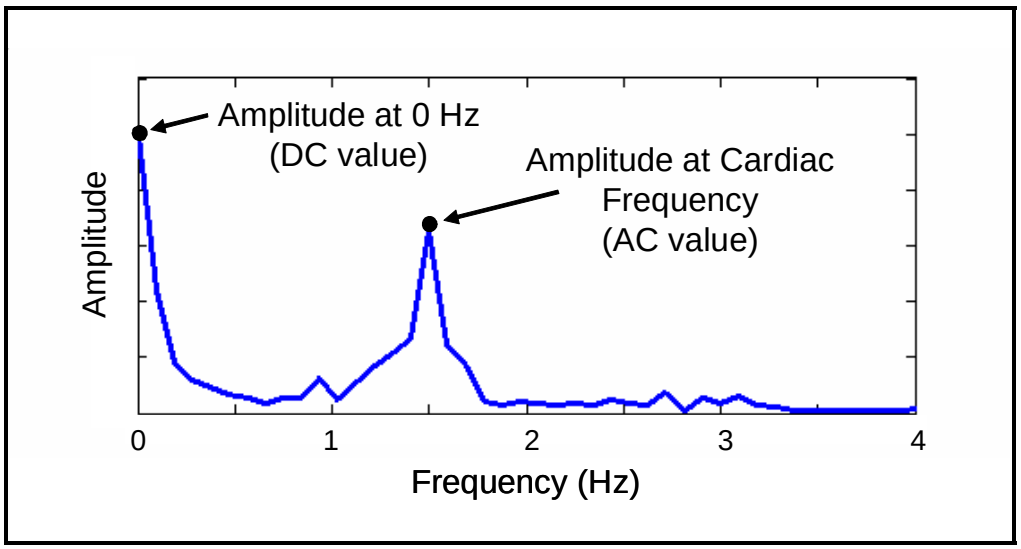

Figure 3.6. *Fourier transform of a PPG signal showing estimates of the AC and DC components.*

Ohmeda has also described a technique for estimating SpO_2 based on regression analysis [50-54]. The process involves first calculating the derivatives of the R and IR

PPGs, and normalizing them with their respective DC values. The normalized derivatives are used to generate a regression line as shown in Figure 3.7, where the R data points are used as the X values and the IR data points are used as the Y values. The slope of the resulting regression line correlates to SpO_2. Unlike the standard ***R*** ratio, the relationship between regression slope and SpO_2 is proportional; namely, a steep slope reflects a high SpO_2, and a shallow slope reflects a low SpO_2.

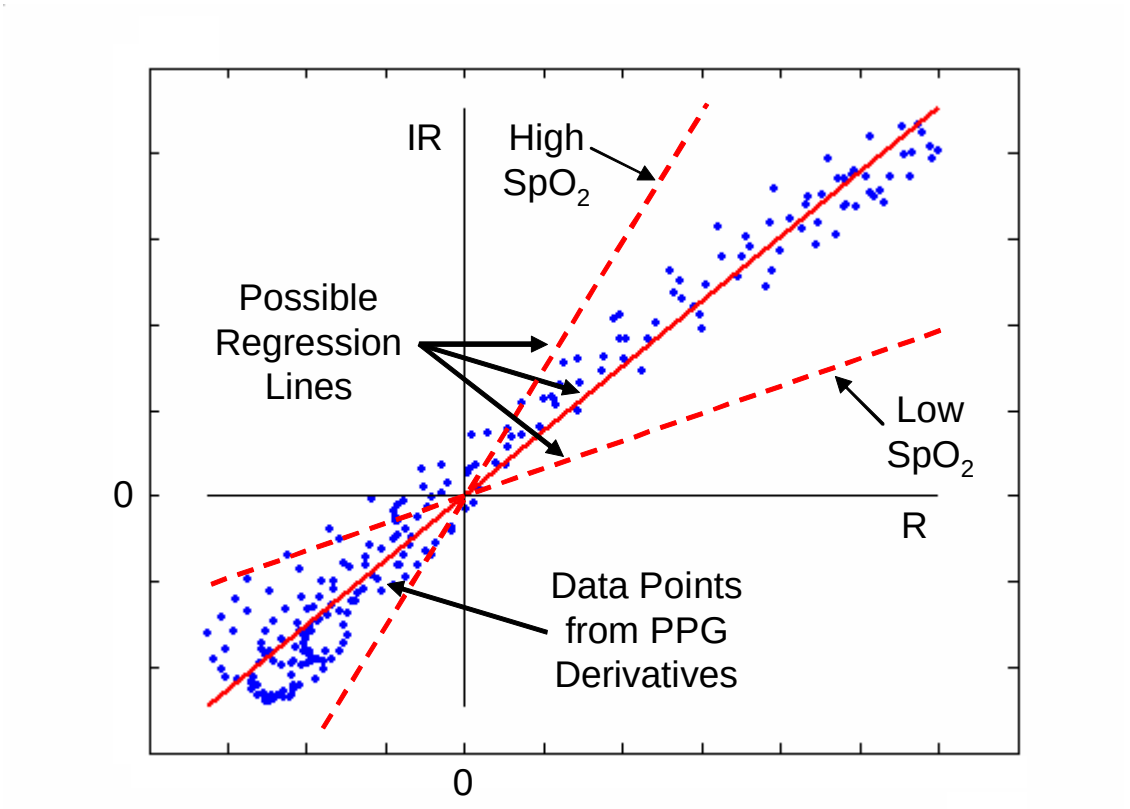

Figure 3.7. *Regression analysis using PPG derivatives and showing the effects of SpO_2 changes on the regression line.*

Wavelet transforms have also been shown to provide a significant amount of information when applied to the analysis of PPG signals [55, 56]. However, the difficulties associated with this type of analysis include large amounts of data, extensive

processing, and results that are difficult to interpret. As such, the role of wavelet transforms in the analysis of PPGs is still being studied.

Masimo has developed an advanced method of performing pulse oximetry measurements, denoted as SET® processing, that is based on multiple complex algorithms [57-59]. The adaptive DSP algorithms are dynamically selected and adjusted based on the measurement situation. This system was developed to improve measurement stability and provides more accurate results in the presence of motion artifacts [60, 61].

3.3 Theory of HR Measurement

HR is a vital measurement during any form of trauma assessment as it provides an estimate of the current stability of a patient. This type of measurement is therefore very important for a combat medic's ability to rapidly assess a casualty's stability [2].

3.3.1 Cardiac Contributions to the PPG:

When the heart contracts during systole, an additional bolus of blood is forced through the systemic circulation. These periodic fluctuations in arterial blood volume introduce a pulsatile component into the PPG signal, as shown in Figure 3.8. Individual pulses correspond to heart contractions, with the positive peaks occurring during systole and the negative peaks occurring at the end of diastole. It should also be noted that the frequency of the pulsatile component is also of significance, as it corresponds to the subject's HR.

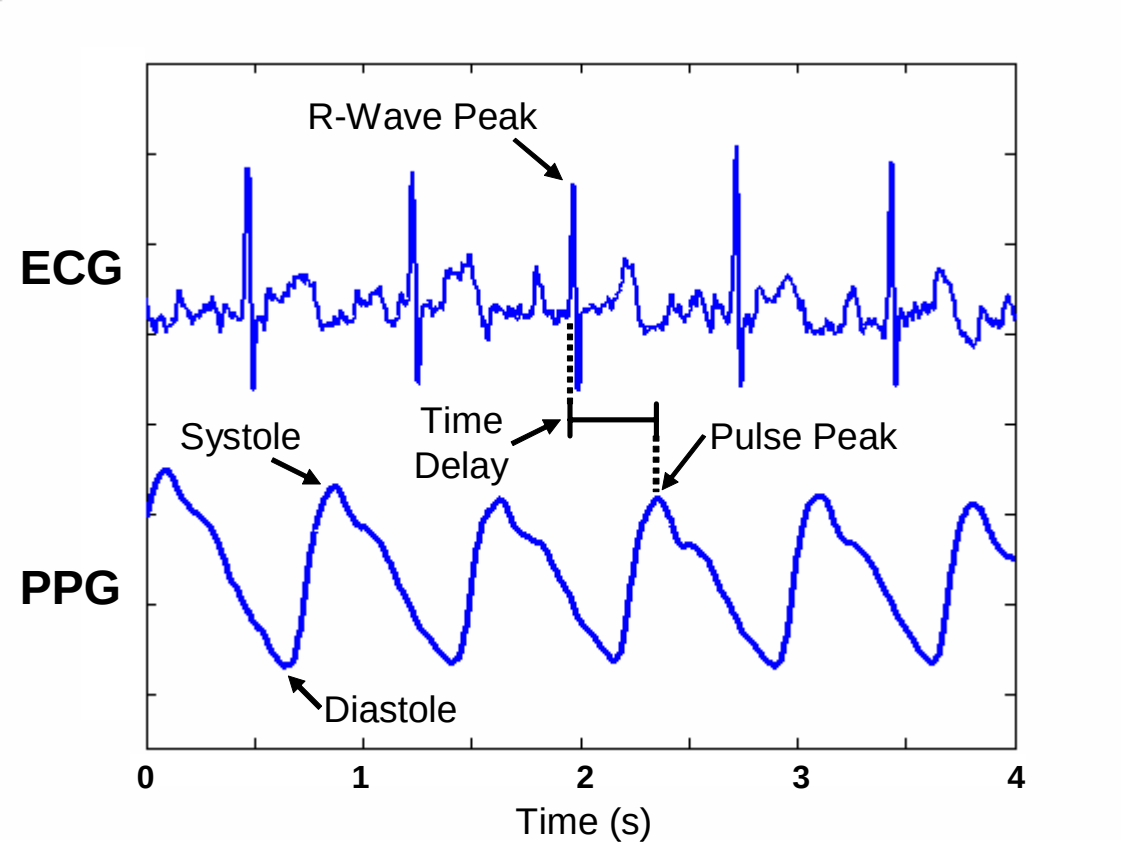

Figure 3.8. *Influence of cardiac activity on the shape of the PPG.*

3.3.2 HR Measurement Methods:

Due to the strong influence of cardiac activity on the pulsatile nature of arterial blood flow, HR measurements can readily be estimated based on the PPG signal. As such, pulse oximeters measure HR in addition to SpO_2.

Manufacturers such as Hewlett-Packard [62], Masimo Corporation [63-65], and Vitalsines International [66] have noted that PPG derivatives can be used to identify pulse peaks and estimate HR. As depicted in Figure 3.9, the derivative of a PPG signal can be employed to locate the sharp upward slope at the beginning of a cardiac event. The subsequent zero-crossing, indicating a slope transition, is used to determine the location of the peak. This method has the advantage of being consistent and robust.

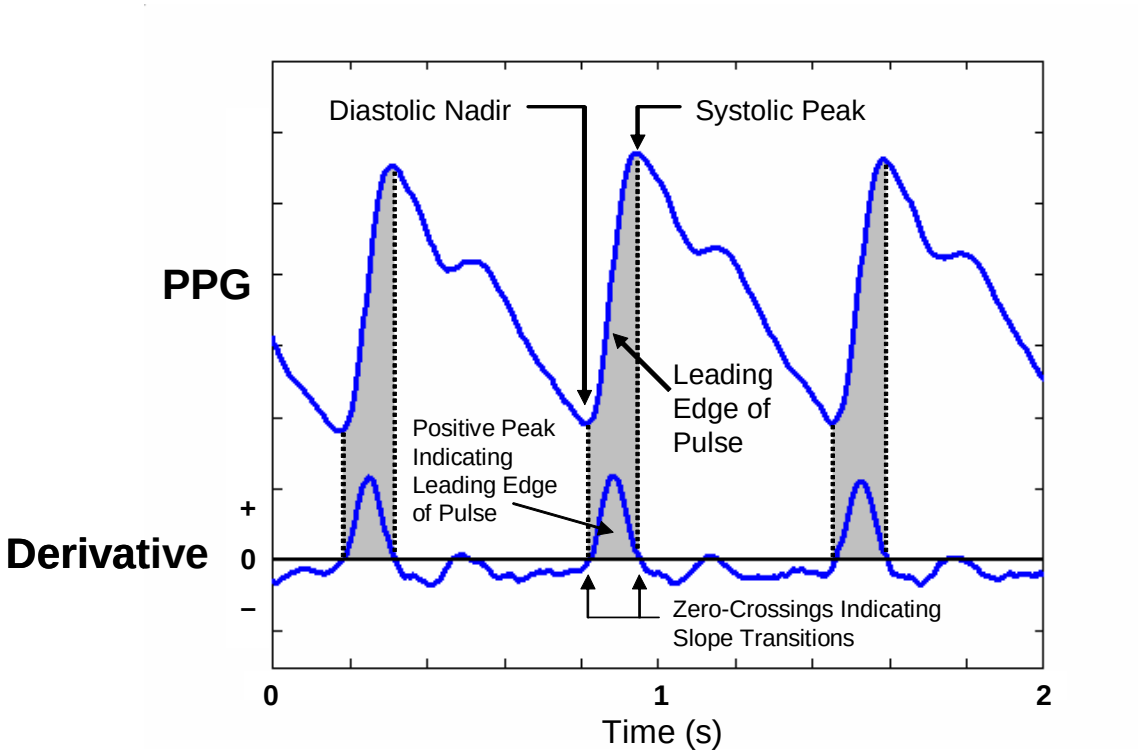

Figure 3.9. *Use of derivatives in identifying the leading slope of a PPG and the following systolic peak.*

Individual pulse peaks can also be located by identifying local minima or maxima in the PPG signal. As shown in Figure 3.10, each point in the signal is assessed with respect to the surrounding points. If the center point is lower or higher than all surrounding points, a local minimum or maximum has been located, possibly indicating a pulse peak. The width of the processing window determines the sensitivity of the peak detection, with narrow windows detecting smaller, more subtle peaks that a wide window would overlook. The optimal window width is dependent upon the relative frequency of the peaks that are to be identified. This method has the disadvantages of poorer stability and accuracy [67] compared to other methods.

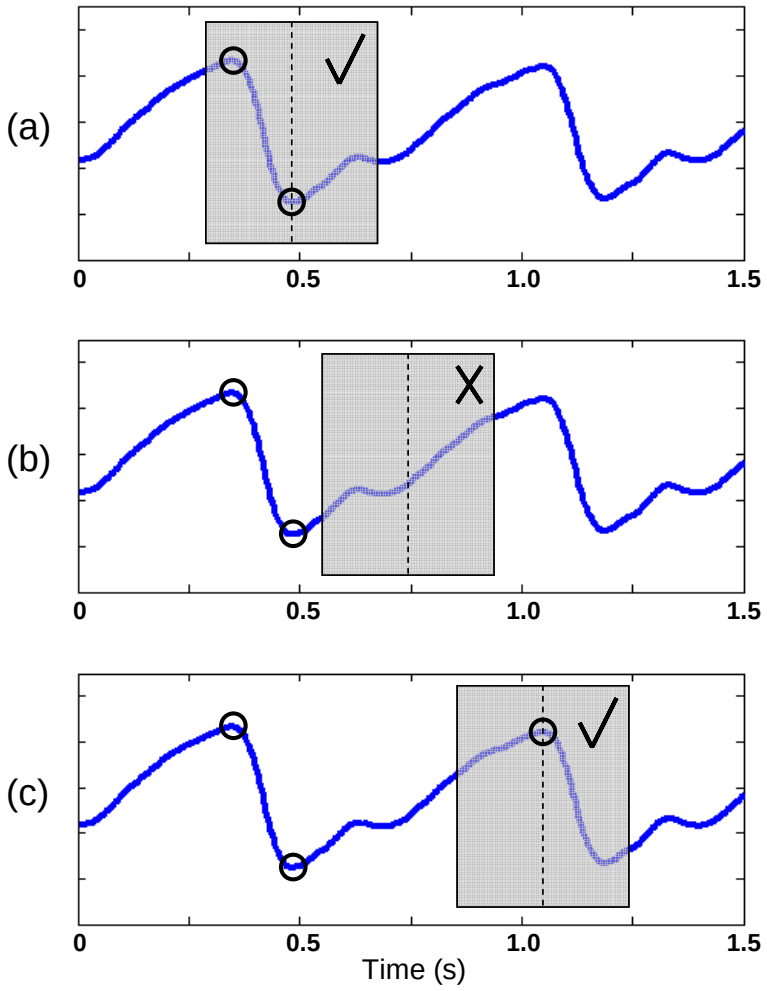

Figure 3.10. *Identifying local maxima and minima in a PPG using a window: (a) local minimum found, (b) no local maximum or minimum, (c) local maximum found.*

Different research groups have also taken the initiative to improve measurement accuracy by developing advanced processing techniques. As mentioned previously, the frequency of the PPG's pulsatile component is a reflection of HR. Rusch and Scharf [41-44] and Reuss and Bahr [68] have noted that HR measurements can be extracted using spectral analysis. Sinusoidal-based transforms of the PPG signal, as depicted in Figure 3.11, typically contain a high-amplitude spike located at the cardiac frequency. The

potential of increased accuracy over conventional time-based assessments has also been noted by manufacturers such as Nellcor [47, 69].

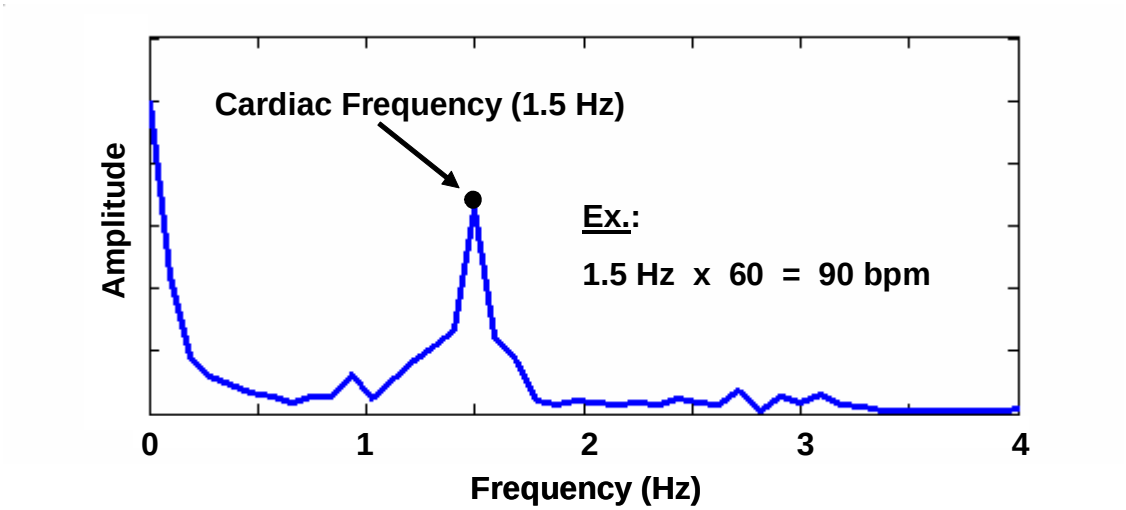

Figure 3.11. *Fourier transform of a PPG signal showing cardiac spectral line.*

3.4 Theory of HRV Measurement

HRV measurements can provide a considerable amount of information pertaining to an individual's physiological state. HRV is predominantly a reflection of activity in the autonomic nervous system. As such, it is commonly used to monitor sympathetic activation [70, 71]. This is important to medical professionals because shifts in sympathetic and parasympathetic activity can indicate specific physiological conditions or events. During periods of shock or significant blood loss, for example, the sympathetic nervous system becomes more active in order to regulate arterial blood pressure [72]. Similarly, airway obstructions [73], and even sudden changes in emotional states [74], can be detected through changes in sympathetic tone. With respect to long-term monitoring and diagnosis, prolonged mental stress and cardiovascular disorders are

known to induce distinctly different HR fluctuation patterns when compared to measurements from normal individuals [75-77].

Possibly the most useful application of HRV is as a pre-hospital triage tool. Abnormal or fluctuating HRV indices are often an indication of poor or negative patient outcomes [78]. Low HRVs can also be used as markers of impending physiological deterioration and are an independent predictor of sudden cardiac death [79]. In a battlefield setting, efficient casualty management is essential to maximizing a patient's chances of surviving a critical injury. HRV could provide combat medics with important information regarding a casualty's stability, allowing the most critical individuals to be treated and evacuated first, improving patient survival.

Since there is currently no universal agreement as to the best index of HRV [79], various methods of assessment are employed based on the clinical setting. HRV assessments can be grouped in two general categories: long-term and short-term. Long-term evaluations typically assess data that have been collected over the course of several hours or days, while short-term evaluations assess only the most recent few minutes of data. For clinical research and to allow for comparisons between studies, however, the standard data size for long- and short-term studies are 24 hours and 5 minutes, respectively [71].

Short-term HRV evaluations are considerably important when performing triage or monitoring potentially unstable patients, where correct prediction of imminent physiological deterioration can increase an individual's chances of survival during an injury. Short-term HRV assessments, summarized in Table 3.1, are based on the lengths of heart beat intervals (NN intervals). The most common indices derived from NN

intervals are SDNN, SDSD, COV and RMSSD [80-82]. These measurements respond proportionally to fluctuations in HR and are capable of tracking fast changes in a patient's status during real-time monitoring [83]. Other indices for short-term assessment

Table 3.1. *Summary of short-term HRV indices.*

Index	**Definition**
SDNN	Standard Deviation of NN Intervals
SDSD	Standard Deviation of Successive Differences
RMSSD	Root-Mean-Square of Successive Differences
SDANN	Standard Deviation of Average NN Intervals
SDNN Index	Mean of 5-minute SDNNs over 24 hours
COV	Coefficient of Variance
NN50	NN Intervals Greater than 50 ms
pNN50	Proportion of NN Intervals Greater than 50 ms
pNN6.25%	Proportion of NN Intervals with a Difference 6.25% of Mean Interval

also exist [84, 85], but are less common and typically confined to clinical research environments. SDANN and SDNN index, for example, estimate the change in HR over a period of 5 minutes, while NN50, pNN50, and pNN6.25% specifically reflect changes in vagal tone over a similar length of time.

In a hospital setting, patient diagnosis and monitoring based on HRV are typically long-term in nature. Several hours of ECG are recorded and assessed using spectral analysis. Spectral decomposition of the recorded signals is provided by transforms such as the Discrete Fourier Transform (DFT), harmonic wavelet transform (HWT), or power spectral density (PSD) [86-88], as depicted in Figure 3.12. Low frequency signal fluctuations, identifiable in these transforms, correspond to activity in the autonomic

nervous system. Sympathetic activity is characterized by the power in the 0.01 – 0.15 Hz region (LF), while parasympathetic activity is characterized by the power in the 0.15 – 0.5 Hz region (HF) [71, 76]. The power ratio LF/HF is by far one of the most common indices that is obtained through spectral analysis, although a number of other ratios are occasionally extracted [73, 80, 89, 90]. Regardless of the particular ratio used, a single parameter is provided which directly reflects changes in sympathetic and parasympathetic activity.

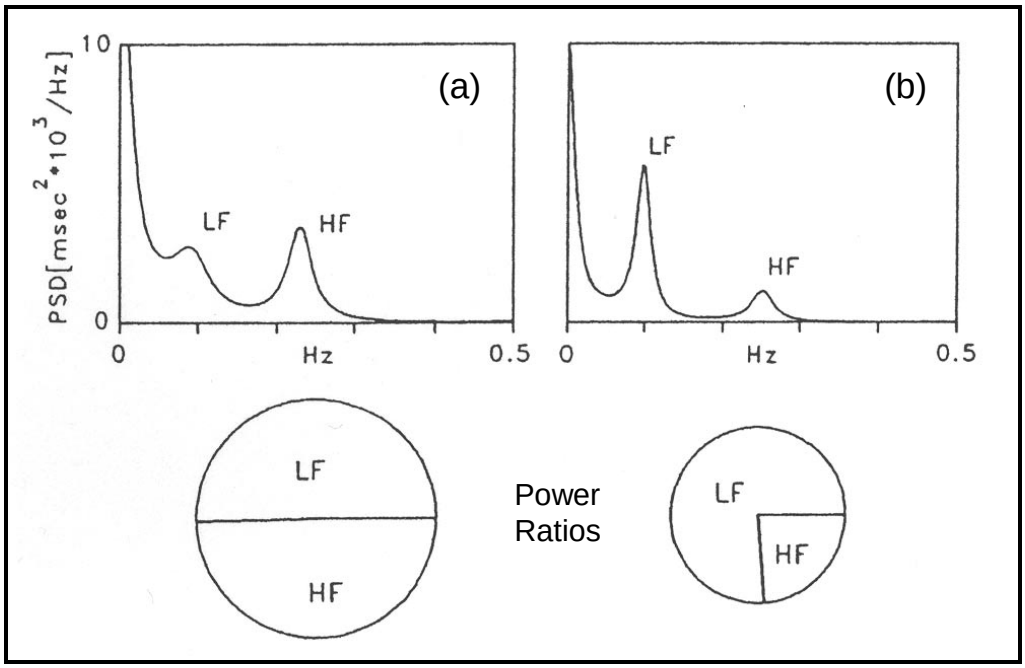

Figure 3.12. *PSD showing LF and HF components and corresponding power ratios for periods when a subject was (a) laying down and (b) standing upright [71].*

3.5 Theory of RR Measurement

The RR measurement is a vital diagnostic tool. During injury or trauma, substantially elevated or reduced RR values can indicate impending detrimental changes to an

individual's status [2]. As such, these measurements have been found to be a useful triage tool prior to arrival at a medical facility and vital to medical personnel in the field [91].

Many methods currently exist for monitoring the RR of a subject. Most methods measure either direct airflow through the mouth and/or nasal passages, or the expansion of the chest or abdomen due to respiratory effort [92, 93]. The sensors utilized for these measurements typically consist of thermistors and pressure transducers for sensing the temperature and pressure changes due to oral and nasal airflow, ECG or comparable electrodes to measure variations in thoracic impedance, or resistive straps and pressure bulbs to record expansion of the chest and/or abdomen. These methods of monitoring respiratory activity are ill-suited for use in a harsh battlefield environment, since moderate activity levels can affect their accuracy. In addition, the hardware employed is often unwieldy and can hinder soldiers from performing normal activities.

The activity of the pulmonary system directly influences the flow and volume of blood in the cardiovascular pathways. As a result, the PPG signal is affected by respiratory activity. Due to the complexity of the cardio-pulmonary interactions, such activities cause several distinct changes to the PPG waveforms. With these considerations in mind, pulse oximeter sensors have proven to be a potential alternative for RR monitoring [94].

3.5.1 Cardio-Pulmonary Interactions:

A spontaneous respiratory cycle induces pressure changes in the intrathoracic cavity [31]. During inspiration, contraction of the diaphragm and expansion of the rib cage induce a pressure drop in the chest cavity. Air is pulled from the external environment into the lungs while blood is drawn into the pulmonary vessels from the venous pathways through

the right side of the heart. As a result, a drop in the peripheral venous pressure occurs. On the left side of the heart, stroke volume decreases as blood pools in the pulmonary vessels, while beat intervals are shortened due to constriction of the heart by the lungs. Conversely, during expiration, the opposite physiological reactions occur. The increase in intrathoracic pressure and compression of the pulmonary vessels cause the peripheral venous pressure to rise. Blood is forced into the left side of the heart, increasing stroke volume, while beat-to-beat intervals increase in duration.

Nitzan et al. [34] have shown that, due to the nature of cardio-pulmonary interactions and their effects on cardiovascular blood flow, three prominent fluctuations in the PPG signal can be linked to respiratory activity. Fluctuations and variations in the baseline, the pulse amplitudes, and the pulse intervals (i.e., cardiac period) of a PPG signal are strongly influenced by respiratory activity. Examples of these effects are shown in Figure 3.13.

Other groups, such as Johansson et al. [35, 95-97] and Chang et al. [98], have examined respiratory-induced intensity variations (RIIV) in the PPG and their correlations with various physiological changes. They found that baseline modulations in the PPG signals are closely correlated with multiple aspects of cardio-pulmonary interaction including changes in blood pressure and tidal volume. In addition, variations in breathing style such as thoraco-abdominal separation differences, apnea, and airway obstruction induce distinctly identifiable changes in the RIIVs.

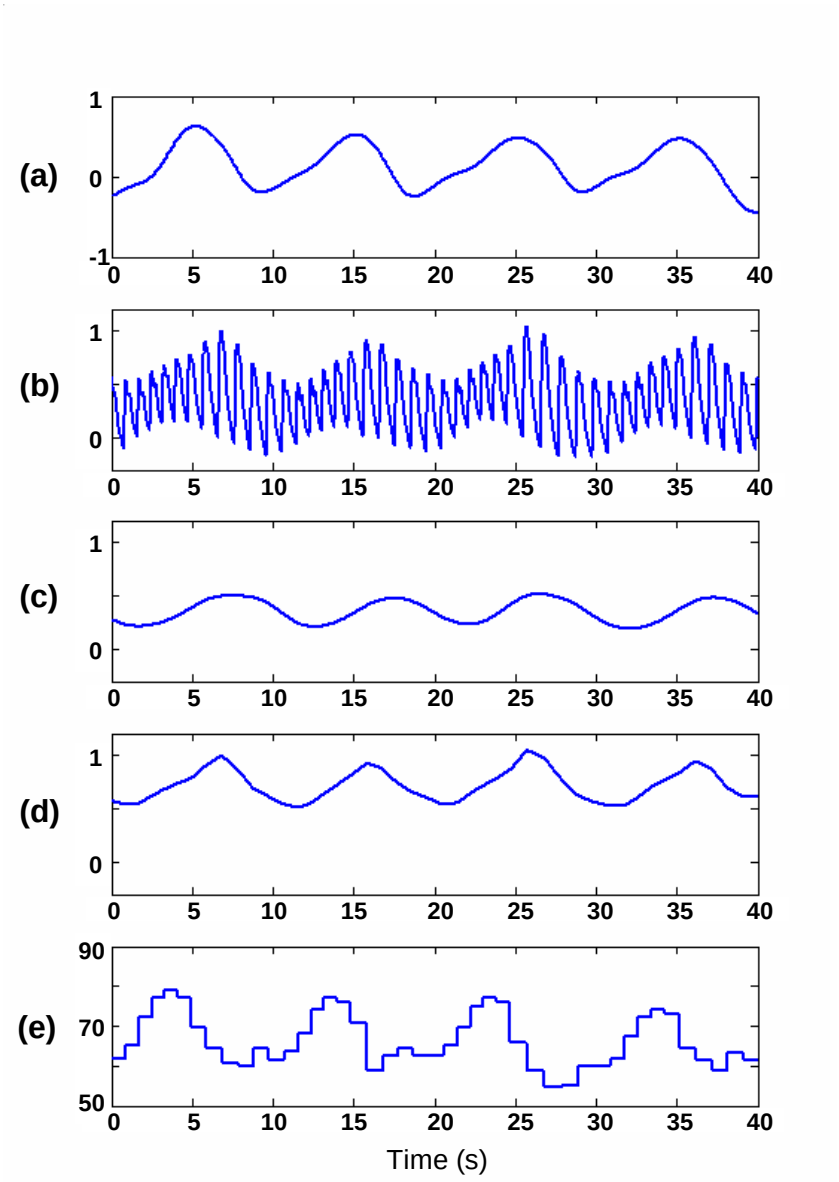

Figure 3.13. *Effects of cardio-pulmonary interactions on the PPG: (a) respiratory waveform, (b) PPG waveform, (c) baseline modulation, (d) peak amplitude modulation, (e) HR modulation.*

Ahlstrom et al. [99] and Zhang et al. [100] have also observed that cardiac frequency fluctuations have strong correlations to respiratory patterns. They have shown that measurements obtained through PPG analysis are typically more accurate compared to other cardiovascular assessments based on pulse transit time (PTT) and ECG.

3.5.2 RR Measurement Methods:

Two separate steps are typically required to obtain RR measurements from PPG signals. The first step involves extracting a waveform from the PPG signal that accurately represents respiratory activity. The second step consists of analyzing the waveform to determine the RR. Different groups have investigated various methods of performing both waveform extraction and analysis.

Low-frequency baseline modulations are one of the most readily observed effects of cardio-pulmonary interactions in the PPG. Since RR typically resides within a limited range of frequencies, filters can be readily employed to isolate corresponding baseline fluctuations. Barschdorff and Zhang [101], for example, used a simple analog low-pass filter (LPF) to remove signal components that did not correspond to respiratory frequencies. The resulting waveform was then processed using a Fast Fourier Transform (FFT) to assess respiratory frequency, as depicted in Figure 3.14b. Conversely, Nakajima et al. [33] chose to employ a dynamic set of software-based digital high-pass filters (HPF) and LPFs to isolate RIIVs. Post-processing consisted of performing peak detection to measure the durations of each respiratory cycle. This time-based processing technique is shown in Figure 3.14a.

Experiments performed in various labs [94, 98] and work done by Nitzan et al. [34] and Murray and Foster [31] have shown that the peak amplitude fluctuations of the PPG can also be readily employed to provide RR information. The positive envelope of the PPG can reflect breathing patterns and be used to identify the predominant respiratory frequency through time- or spectral-based analysis.

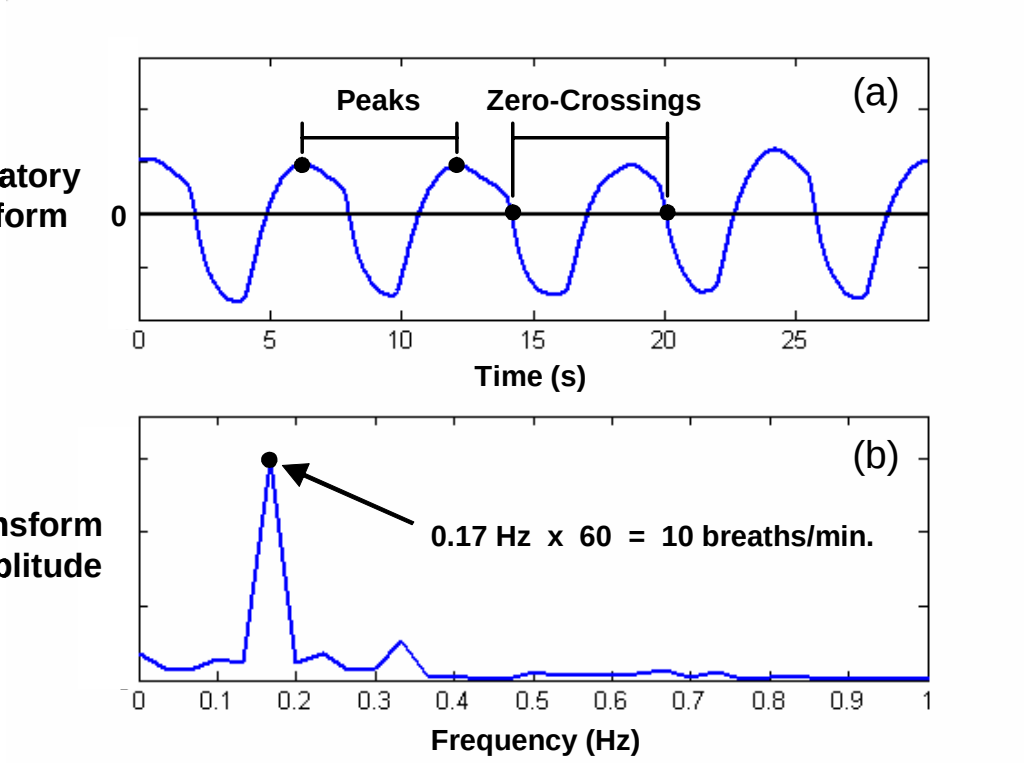

Figure 3.14. *The two primary methods of assessing respiratory waveforms: (a) measuring individual breathing cycle intervals and (b) performing spectral analysis.*

As noted by Nitzan et al. [34], cardiac period fluctuations contain a substantially higher amount of power when compared to baseline and amplitude modulations in the PPG signal. Whitney and Solomon [102] have demonstrated that these cardiac fluctuations can be extracted and used to measure RR. Their post-processing methods were based around spectral analysis. FFTs and periodograms were used to assess the respiratory frequencies of the waveforms and provided accurate results.

4. RESEARCH OBJECTIVES

While steady progress has been made in the development of an optimized hardware structure for a wearable pulse oximeter, limitations in commercially available software solutions still exist. The processing software employed by manufacturers to perform physiological measurements can be expensive, proprietary, and does not provide all the measurement features desired in a wearable pulse oximeter. As a result, the newly-developed hardware platform designed at WPI requires custom-developed software routines to perform physiological measurements based on sensor data. Therefore, the goal of this research was the development of a library of software-based processing methods that could be employed to advance the development of the WPI wearable pulse oximeter that is being designed for military and mass casualty applications. The specific research objectives were to:

Objective 1: Evaluate and characterize a set of software-based processing methods capable of measuring SpO_2 based on a set of PPG signals.

Objective 2: Evaluate and characterize a set of software-based processing methods capable of measuring HR based on a set of PPG signals.

Objective 3: Evaluate and characterize a set of software-based processing methods capable of measuring HRV based on a set of PPG signals.

<u>Objective 4:</u> Evaluate and characterize a set of software-based processing methods capable of measuring RR based on a set of PPG signals.

The primary steps necessary to achieve each of these objectives were to:

- Compile a list of processing methods that could potentially perform the given measurement.
- Perform a set of *in vivo* experiments to record PPG waveforms and corresponding reference measurements for the physiological measurement of interest.
- Assess the accuracies of the methods using the recorded PPG waveforms and reference values.

5. SUPPORT EQUIPMENT

5.1 Recording Hardware

5.1.1 BIOPAC Data Acquisition System:

A BIOPAC data acquisition system was used to record PPG signals during most experiments and to obtain reference measurements for HR, HRV, and RR. The central monitoring unit was a model MP100 Workstation controlled using the AcqKnowledge v3.7.3 software program running on a Windows operating system. The primary advantages of this recording system were the types of sensor modules available for use and its ability to record data simultaneously from multiple sources. The flexibility of the software controls for setting sampling rates and automatic recording intervals was also a benefit. The general setup of the BIOPAC system is shown in Figure 5.1.

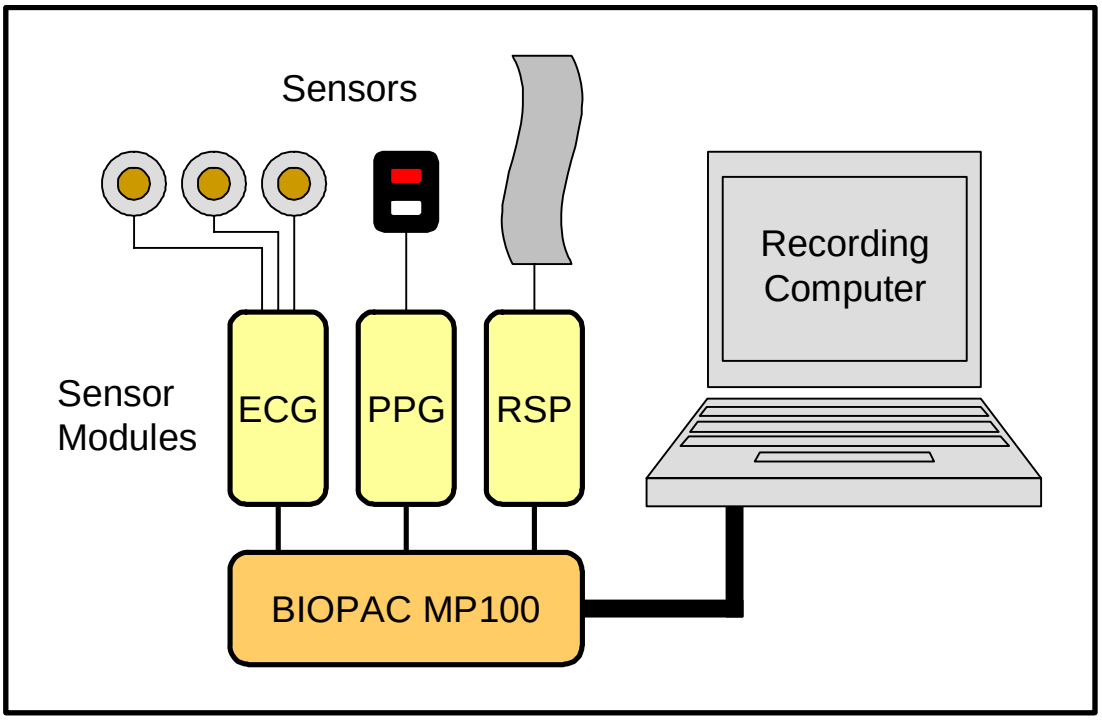

Figure 5.1. *General recording setup for experiments using a BIOPAC recording system.*

Three sensor modules were used during the various experiments to record physiological signals. An ECG100 module was used to record ECGs from a standard Lead I setup. A PPG100 module was connected to a TSD100B infrared (IR) optical reflectance sensor to record PPG waveforms. An RSP100 module was used to record signals from a TSD101 Pneumotrace® chest strap that provided information regarding breathing patterns.

5.1.2 Photoplethysmogram Signal Processing Unit:

The photoplethysmogram signal processing unit (PSPU) is a hardware-based signal processing device that uses an optical pulse oximeter sensor to acquire PPG-related waveforms. The unit was used during SpO_2-based experiments to provide R and IR PPG signals. Different hardware units could not be used during such experiments since they provided only one PPG signal, which was insufficient for monitoring SpO_2. The general structure of the PSPU is shown in Figure 5.2.

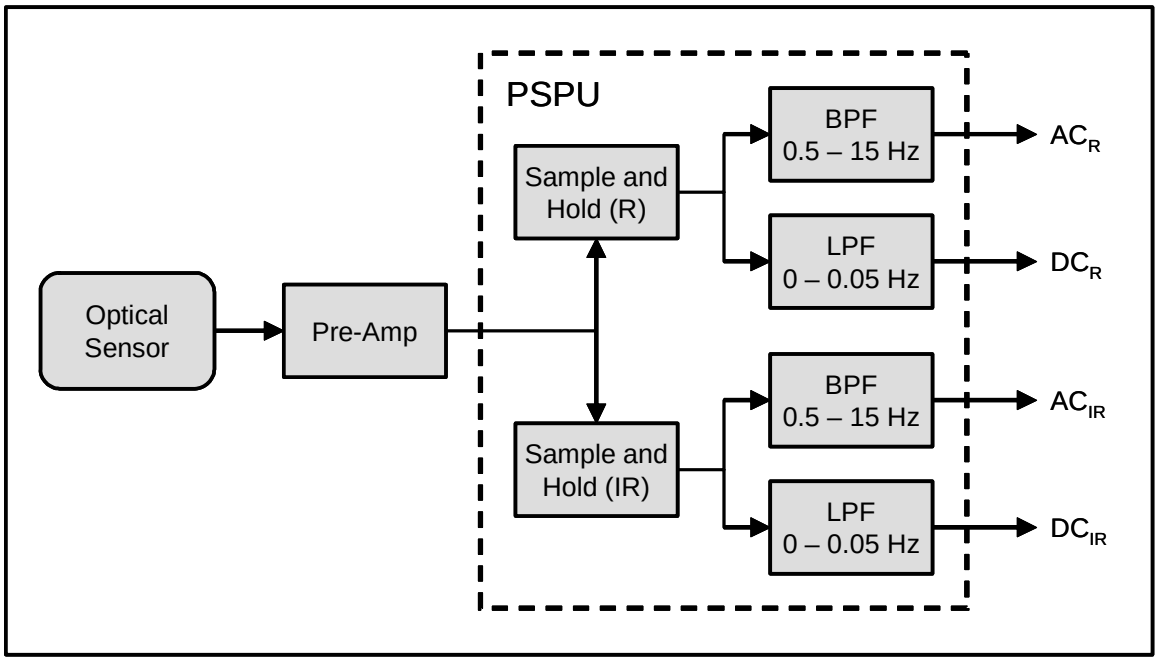

Figure 5.2. *General structure of the PSPU.*

5.1.3 Nonin Xpod®:

A Nonin Xpod® pulse oximeter module, model number 3012, was utilized to provide reference SpO_2 measurements during experiments. The Xpod® was used over other reference oximeters due to its readily available serial data stream. The unit provided continuous measurement data through an RS-232 serial interface that was easily monitored using computer-based recording software.

5.2 Software Environments

5.2.1 LabVIEW:

The LabVIEW programming environment, Version 7.1, was used for data acquisition and display. Simple construction of software-based interfaces and ready access to analog and serial inputs made this environment ideal for recording data from multiple sources that used different communication mediums, a task that would have been difficult with other software platforms.

5.2.2 Matlab:

Matlab, version 6.5, provided a flexible workspace in which to perform offline data analysis. The ability to work with large data sets, formulate custom programs, and graph and display waveforms and results for visual inspection allowed for efficient analysis procedures when assessing the accuracies of the various processing methods. Software filters employed in certain analyses were designed and constructed using Matlab's FDATool program since the filter coefficients could be easily transferred to and implemented in the core Matlab environment.

6. EXPERIMENTAL SETUPS

6.1 SpO_2 Experiments

R and IR PPG data, as well as reference SpO_2 measurements, were required to assess the accuracy of the SpO_2 processing methods. A series of *in vivo* experiments were performed to obtain data over a range of SpO_2 values typically monitored for clinical purposes.

6.1.1 Experimental Setup:

A Nonin Xpod® pulse oximeter was used to obtain reference SpO_2 values from a transmission-mode optical sensor attached to the subject's index finger since this is the gold standard for monitoring SpO_2 levels. A Nonin reflectance-mode optical sensor was also secured to the subject's forehead using an elastic headband. This sensor was monitored by the photoplethysmogram signal processing unit (PSPU) which could provide both R and IR waveforms required to perform an SpO_2 measurement. Since the data being recorded consisted of both analog signals and serial data, a LabVIEW program was used to acquire and store the data from both sources simultaneously. Figure 6.1 depicts the experimental setup. Separate AC and DC signals corresponding to the R and IR PPG signals were recorded from the PSPU at a rate of 75 s/s, the sampling rate used by the sensor control routine in WPI's custom pulse oximeter. Reference SpO_2 values were recorded from the Xpod® once a second.

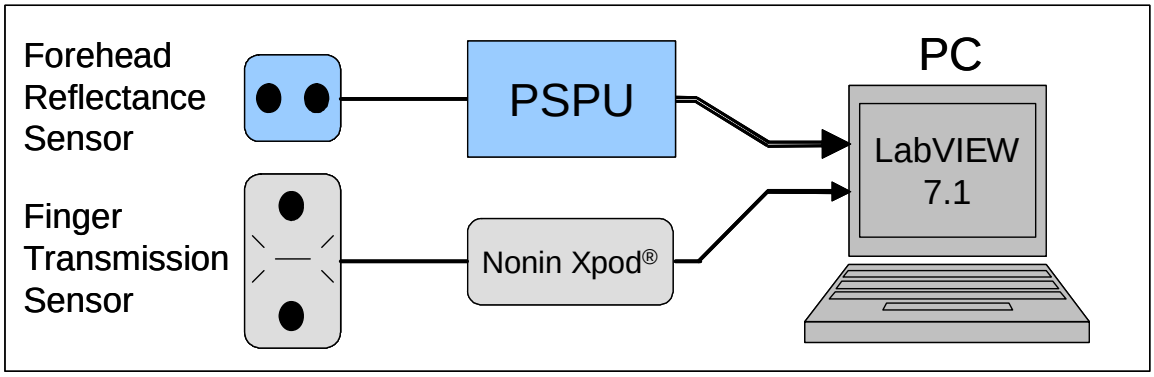

Figure 6.1. *Experimental setup to acquire SpO_2 data.*

6.1.2 In Vivo Experiments:

Data were acquired from 3 healthy male volunteers, ages 24 – 25. During data recording, subjects were seated comfortably in a chair with their arms resting on the armrests. To assess the relationship between reference SpO_2 values and measured SpO_2 values, each subject was instructed to perform a breath-holding maneuver to induce a noticeable drop in SpO_2. A 20 second baseline reading was recorded while each subject was breathing spontaneously. Following the baseline recording, each subject was instructed to hyperventilate for about 15 seconds, and then hold his breath for as long as possible to induce hypoxemia. Following the breath-holding period, each subject resumed spontaneous breathing for 20 seconds to allow the SpO_2 readings to return to normal. SpO_2 values were monitored during each pause in breathing to ensure that a drop in the oxygen level was noticeable. If a significant drop in SpO_2 was not induced, the data were discarded and the experiment was repeated. A total of three successful data sets were recorded.

6.2 HR Experiments

PPG data, as well as reference HR measurements, were required to assess the accuracy of the HR processing methods. A series of *in vivo* experiments were performed to obtain data over a range of HR values typical of healthy individuals.

6.2.1 Experimental Setup:

The BIOPAC data acquisition system was used in this experimental setup since it was capable of recording PPG and ECG signals simultaneously. An optical sensor, held in place on the subject's forehead by an elastic band, provided an IR PPG waveform since only a single PPG signal was required to perform HR measurements. Disposable ECG electrodes were also attached to the subject and used to record standard Lead I ECG waveforms. Figure 6.2 depicts the experimental setup. The waveforms were recorded at a rate of 200 s/s since the ECG signals required a high sampling rate due to their high frequency components. Since the BIOPAC system did not perform any advanced signal processing, the ECG waveforms had to be processed offline in Matlab in order to provide reference HR measurements.

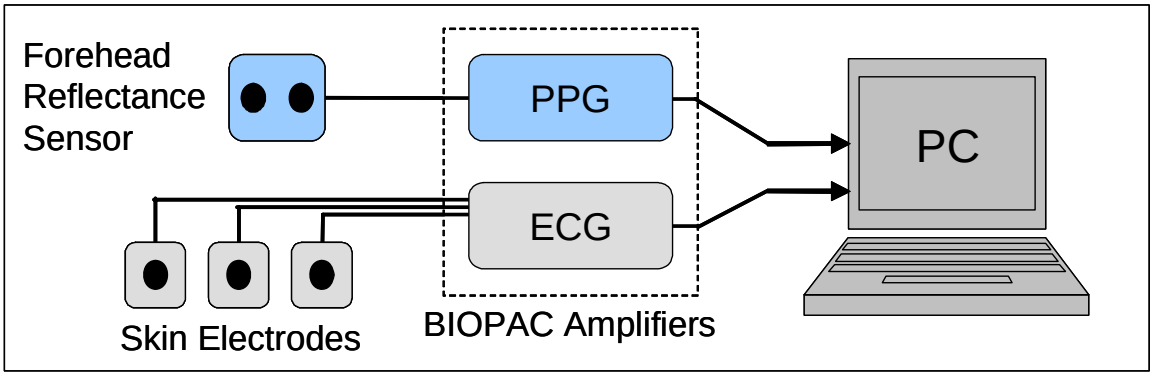

Figure 6.2. *Experimental setup to record HR and HRV data.*

6.2.2 In Vivo Experiments:

Data were acquired from 3 healthy male volunteers, ages 23 – 25. To assess various levels of HR, two recording sessions were performed. During the first session, 9 recordings were made while each subject was resting comfortably in a chair. Each recording lasted 3 minutes. During the second session, subjects were instructed to perform light exercises in order to increase their HR. A 1 minute recording was made to establish a baseline. Each subject was asked to jog in place for 30 seconds, after which another 1 minute baseline recording was made. Lastly, each subject was asked to jog in place for 60 seconds before a final 1 minute baseline recording was made. Each subject performed 3 consecutive exercise-based experiments.

6.3 HRV Experiments

PPG data and reference measurements were required to assess the accuracy of the HRV processing methods. A series of *in vivo* experiments were performed to obtain data over a range of HRV values typical of healthy individuals.

6.3.1 Experimental Setup:

The recording setup for the HRV experiments was identical to the one used in the HR experiments and is depicted in Figure 6.2. The waveforms were recorded at a rate of 200 s/s since the ECG signals required a high sampling rate due to their high frequency components. Since the BIOPAC system did not perform any advanced signal processing, the ECG waveforms were analyzed offline by a LabVIEW-based software program [84, 85] that provided reference HRV values for the experiments.

6.3.2 In Vivo Experiments:

Data were acquired from 22 healthy volunteers, 19 males and 3 females, ages 20 – 36. To assess various levels of HRV, 3 controlled breathing exercises were performed. Twenty-seven recordings were made while each subject was resting comfortably and breathing at a normal tidal rate. Recordings were also acquired while 5 subjects were instructed to hold their breath for about 30 seconds. Lastly, recordings were also made while 5 subjects took short but deep breaths for about 30 seconds. Each experimental recording lasted a total of 5 minutes, the standard interval used for short-term HRV assessments.

6.4 RR Experiments

PPG data and reference RR measurements were required to assess the accuracy of the RR processing methods. A series of *in vivo* experiments were performed to obtain data over a range of RR values typical of healthy individuals.

6.4.1 Experimental Setup:

The BIOPAC data acquisition system was used in this experimental setup since it was capable of recording PPG and respiratory waveforms simultaneously. An optical sensor, held in place on the subject's forehead by an elastic band, provided an IR PPG waveform since only a single PPG signal was required to perform RR measurements. An elastic Pneumotrace™ respiration transducer was secured around the subject's chest using Velcro tabs in order to acquire a reference signal indicative of the subject's breathing pattern. Figure 6.3 depicts the experimental setup. The waveforms were recorded at a rate of 75 s/s, the sampling rate used by the sensor control routine in WPI's custom pulse oximeter. Since the BIOPAC system did not perform any advanced signal processing, the

respiratory waveforms obtained from the chest strap had to be processed offline in Matlab in order to provide reference RR measurements.

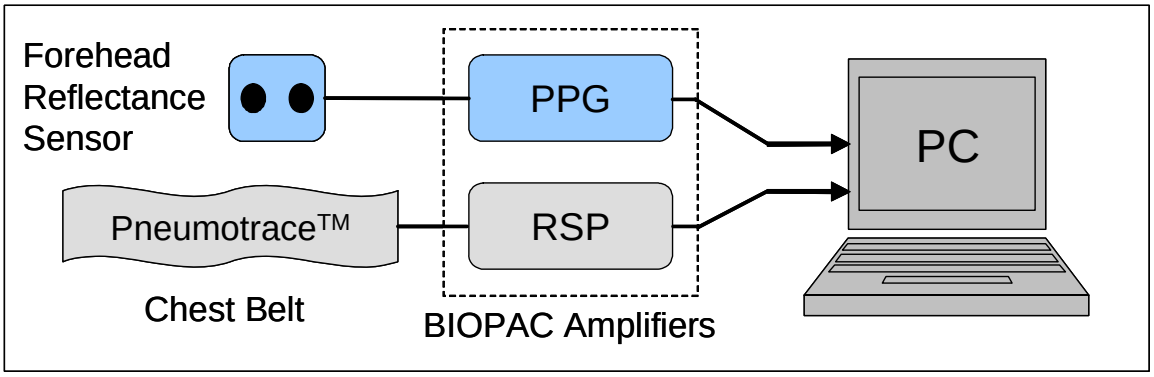

Figure 6.3. *Experimental setup to record RR data.*

6.4.2 In Vivo Experiments:

Data were acquired from 5 healthy volunteers, 4 males and 1 female, ages 21 – 55. During the time that data were recorded, subjects were seated comfortably in a chair with their arms resting on the armrests. Preliminary readings were observed visually to ensure that the sensors were producing strong and stable PPGs during spontaneous breathing. Subjects were asked to refrain from talking, coughing, swallowing, sneezing, and any other activity that could interrupt their breathing patterns. Before each session, preliminary readings from each sensor were inspected visually to confirm that the signal amplitude remained acceptable. Adjustments to the sensors were then made as needed.

During each 90-second recording session, each subject was instructed to maintain a constant breathing rate and a spontaneous tidal volume. An analog clock was used for timing, with tape marks indicating the starting points of each breathing cycle. Each subject performed the experiment 15 times by breathing from 6 to 20 breaths-per-minute, resulting in a total of 75 recordings.

6.5 A Note on Experiment Subjects

Due to some limitations in the number of subjects that were available for the *in vivo* experiments, some subjects were required to provide multiple data sets in addition to performing physical activities to alter their physiological states. Fortunately, this study characterized the correlations between processing method measurements and reference measurements instead of the differences between individual subjects. The recorded data were used to assess measurement accuracies across a range of physiological levels, for example, HRs between 60 and 120 bpm. Since these assessments were based on pairs of measurements each obtained simultaneously from a single individual, the specific subject providing the data was not relevant. The number and ages of subjects in an experiment were therefore unimportant as they did not influence the comparisons between measurements and reference values. If further experiments were to be performed to characterize the differences in physiological levels between individuals, then the specific number of subjects would be relevant.

7. PROCESSING METHOD ASSESSMENTS

7.1 Assessment Procedures

The data obtained from the *in vivo* experiments were used to evaluate the measurement accuracies of the processing methods. The accuracy assessments were performed in Matlab since the environment could handle large data sets and also allowed the processing methods to be implemented in individual program files (see Appendix A). With this software platform, the processing methods were used to analyze the PPG signals recorded during the experiments. For purposes of comparison, all processing methods that provided a given type of measurement (e.g., HR) analyzed the same recordings. The resulting measurements obtained from each method were plotted against corresponding reference measurements to assess accuracy. The accuracy of a method was described using the R^2 value, bias, and the standard error of the estimate (SEE). Student's t-test was used to determine if a significant difference existed between each set of measured values and corresponding reference values; $p < 0.05$ was considered significant.

7.2 SpO_2 Processing Methods

Of the processing methods described in section 3.2, not every method was selected for evaluation. Since the measurement techniques had to be implemented in a μC environment with limited resources, SET® processing was not tested because this algorithm requires extensive resources to perform its analyses. Wavelet transforms were removed from the assessment list as well since they are still being examined with regards

to their usefulness in pulse oximetry [46, 57-58]. Spectral analysis potentially required large amounts of memory and computation time [43-44], however, an optimized analysis [45] form was employed in order to reduce processing overhead. As a result, this method was further evaluated as a potential method of measuring SpO2. Table 7.1 lists the SpO_2 processing methods tested in this section.

7.2.1 SpO_2 Calculation:

Analysis of PPG signals to determine SpO_2 involved two initial steps: measurement of the DC and AC components. Once these values were obtained from both the R and IR PPGs, the ratio ***R*** was calculated using Equation 3.2. The instantaneous ***R*** values produced by a given processing method were plotted against corresponding instantaneous reference SpO_2 values obtained from the Nonin Xpod®. The linear regression equation derived from the comparison was used to convert the ***R*** values to SpO_2 values, providing the final measurements for the processing method. Table 7.2 summarizes the results of the assessments.

7.2.2 Analysis Windows:

Several processing methods performed analyses based on PPG segments that were selected using a rectangular window. In order to ensure accurate results, a full pulse cycle had to be present within the window. The minimum HR of interest was 30 bpm, corresponding to a beat duration of 2 seconds. To guarantee that at least one positive and one negative pulse peak was present in any given window, the window width was set to 3 seconds. All window-based processing methods employed a 3-second window.

Table 7.1. *List of processing methods capable of providing SpO_2 measurements.*

Processing Method	General Description
DC Measurement:	
Moving Average [41]	The mean value of a section of PPG.
LPF	The result of a low-pass filtered PPG.
Window Minimum	The minimum value in a section of PPG.
AC Measurement:	
PPG Differentials [23, 28, 39]	The mean amplitude difference between consecutive sample points in a PPG.
Pulse Amplitudes [28, 40]	A measure of the peak-to-peak amplitude of individual cardiac pulses.
Regression Analysis [51-54]	The regression slope generated by comparing R and IR PPG derivatives.
Window Analysis	The difference between the maximum and minimum values in a section of PPG.
AC and DC Measurement:	
Spectral Analysis [41-45]	A measure of the power contained in the cardiac frequency and DC offset.

7.2.3 DC Measurements:

Three different processing methods were employed to measure the DC components of PPG signals. The baselines and average offsets of the signals could both be used to estimate these DC values and were used to normalize the AC measurements obtained through other methods.

The first method was a moving average. A 3-second window of the most recent PPG samples was averaged to produce a DC value. This calculation was performed as required by the AC processing methods.

The second method used a LPF to track the DC level of a PPG. The chosen filter was an IIR Butterworth which allowed for a reduced number of coefficients compared to FIR filters and a smooth passband with no significant ripple. A cutoff of 0.1 Hz was used to remove the high-frequency pulsatile component generated by cardiac activity. A 5^{th} order filter was required to maintain stability.

The third processing method followed the baseline of the PPG. The minimum value in a 3-second window of the most recent PPG samples was used as a DC value. This calculation was performed as required by the AC processing methods.

7.2.4 AC Measurements:

Five different processing methods were employed to measure the pulsatile amplitudes of the R and IR PPGs. Once measured, the AC values were normalized using the results obtained from the above DC measurements. The normalized AC measurements were used to calculate ***R*** values which were converted to SpO_2 values based on the empirical relationship between ***R*** and SpO_2. Four of the AC measurement methods were paired with each of the three DC measurement methods, as shown in Table 7.2, resulting in a set of 13 unique processing methods that provided SpO_2 measurements once every second.

7.2.5 PPG Differentials:

Using differentials to estimate AC amplitude first involved calculating the absolute derivative of a PPG, as demonstrated in Figure 7.1. During a single analysis, 3 seconds of the absolute derivative were averaged to produce an AC measurement. AC values from R and IR PPGs were normalized with their respective DC values and used to calculate the ***R*** values. To assess method accuracy, the calculated ***R*** values were converted to SpO_2 measurements and plotted against corresponding reference SpO_2 values, as shown in Figures 7.2 – 7.3.

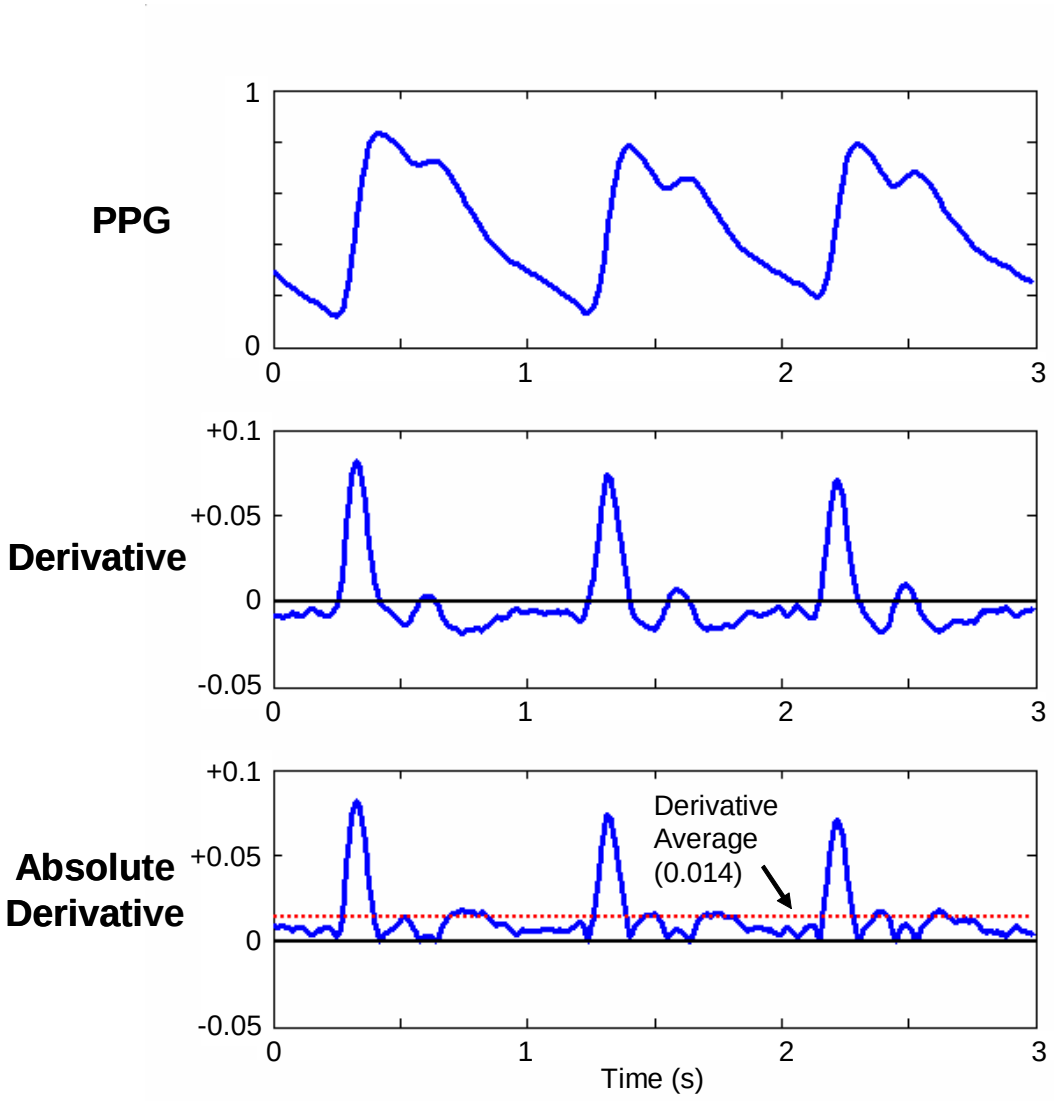

Figure 7.1. *Relative PPG with corresponding derivative and absolute derivative. The marked derivative average is used as an AC value.*

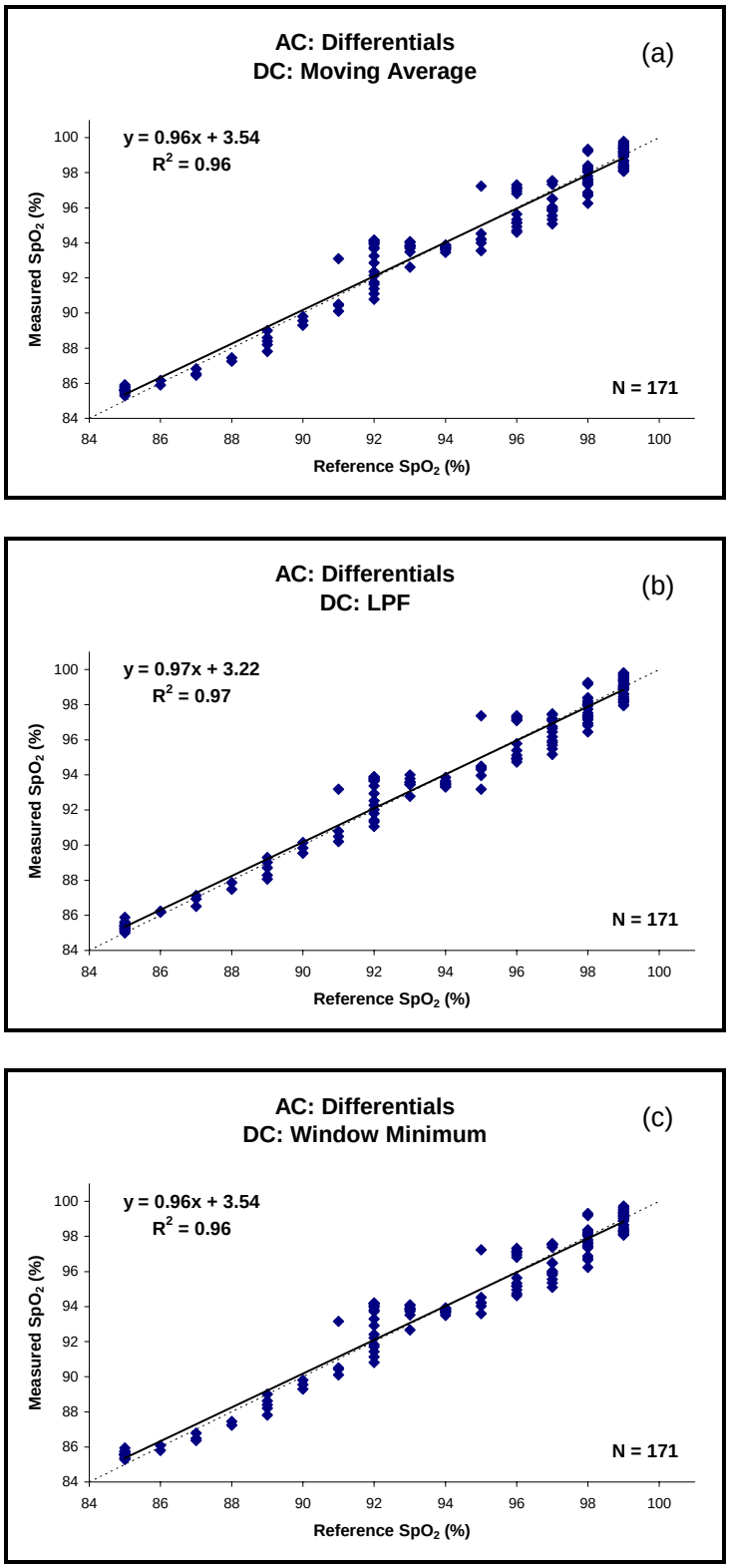

Figure 7.2. *SpO_2 measurements based on PPG differentials normalized using (a) a moving average, (b) LPF, and (c) window minimum. Regression lines (—) and lines of identity (---) are shown for comparison.*

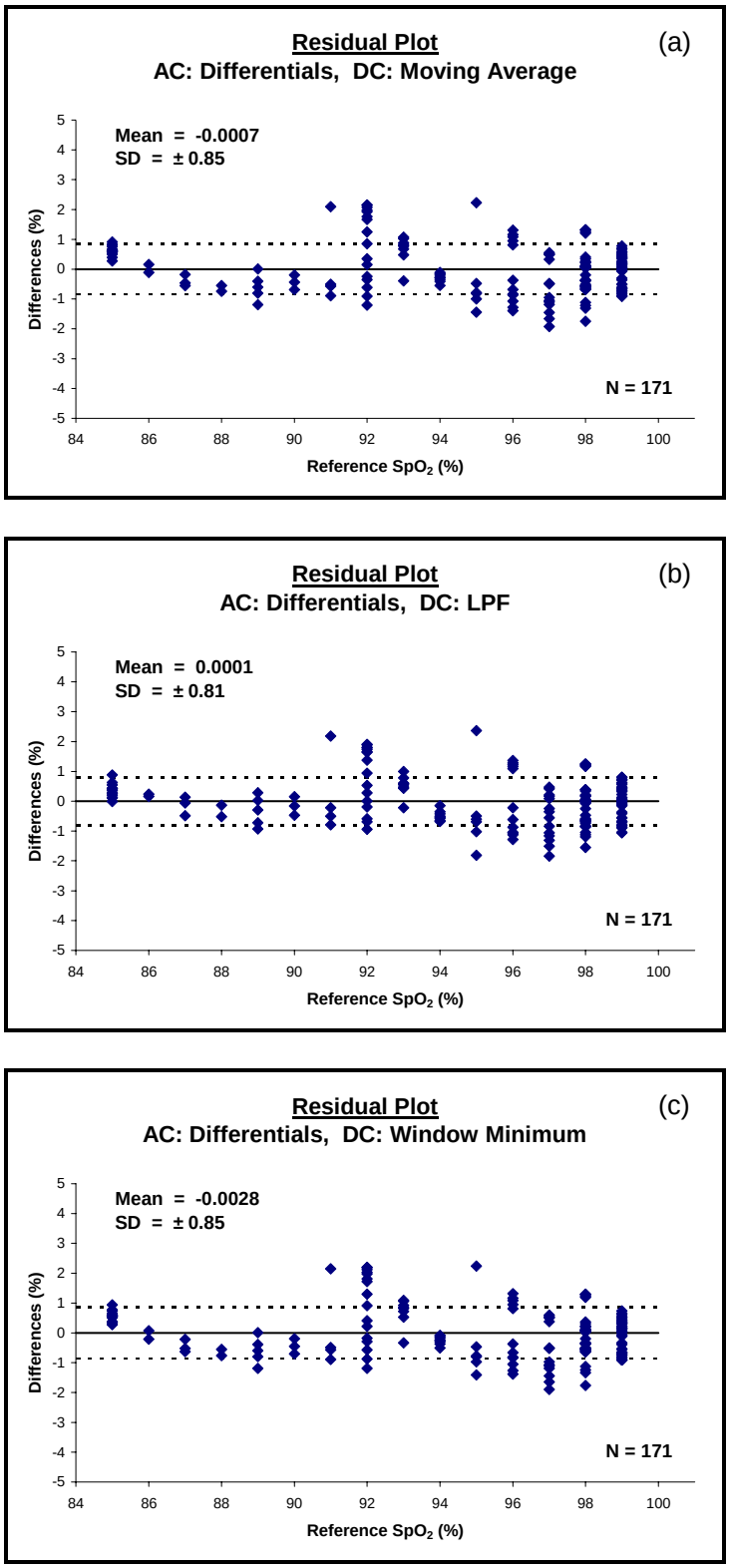

Figure 7.3. *Residual data plots from SpO_2 measurements based on PPG differentials normalized using (a) a moving average, (b) LPF, and (c) window minimum.*

7.2.6 Pulse Amplitudes:

Individual pulses of a PPG were first identified using signal derivatives. As demonstrated in Figure 7.4, the amplitude difference between the peak and nadir of a pulse was measured and used as an AC value. AC values from the R and IR PPGs were normalized with their respective DC values and used to calculate ***R*** values. To assess method accuracy, the calculated ***R*** values were converted to SpO_2 measurements and plotted against reference SpO_2 values, as shown in Figures 7.5 – 7.6.

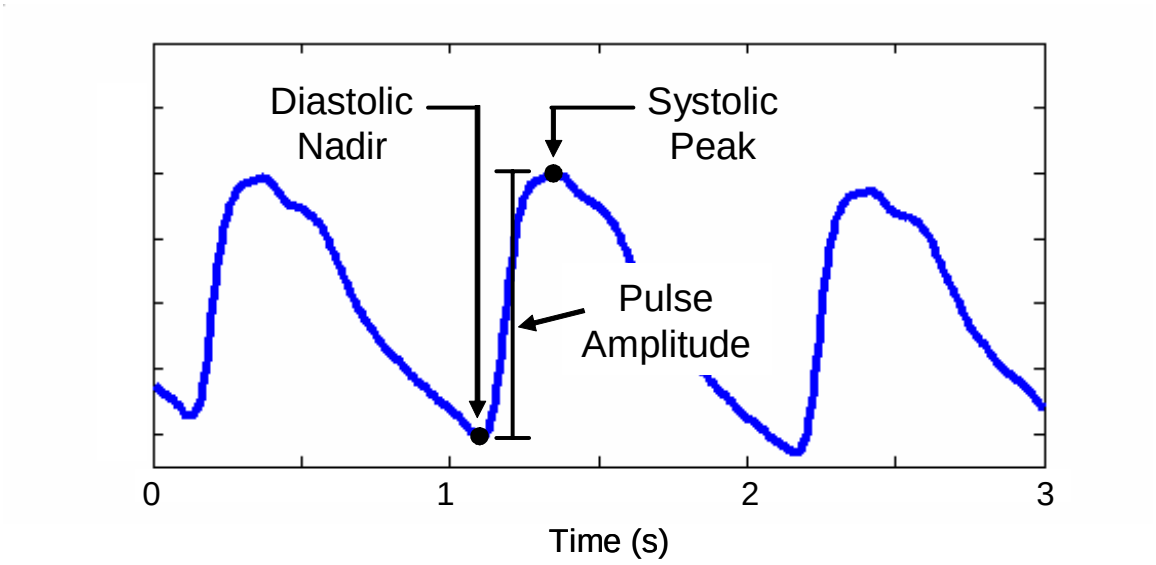

Figure 7.4. *The amplitude of a pulse measured as the difference between the peak and the nadir.*

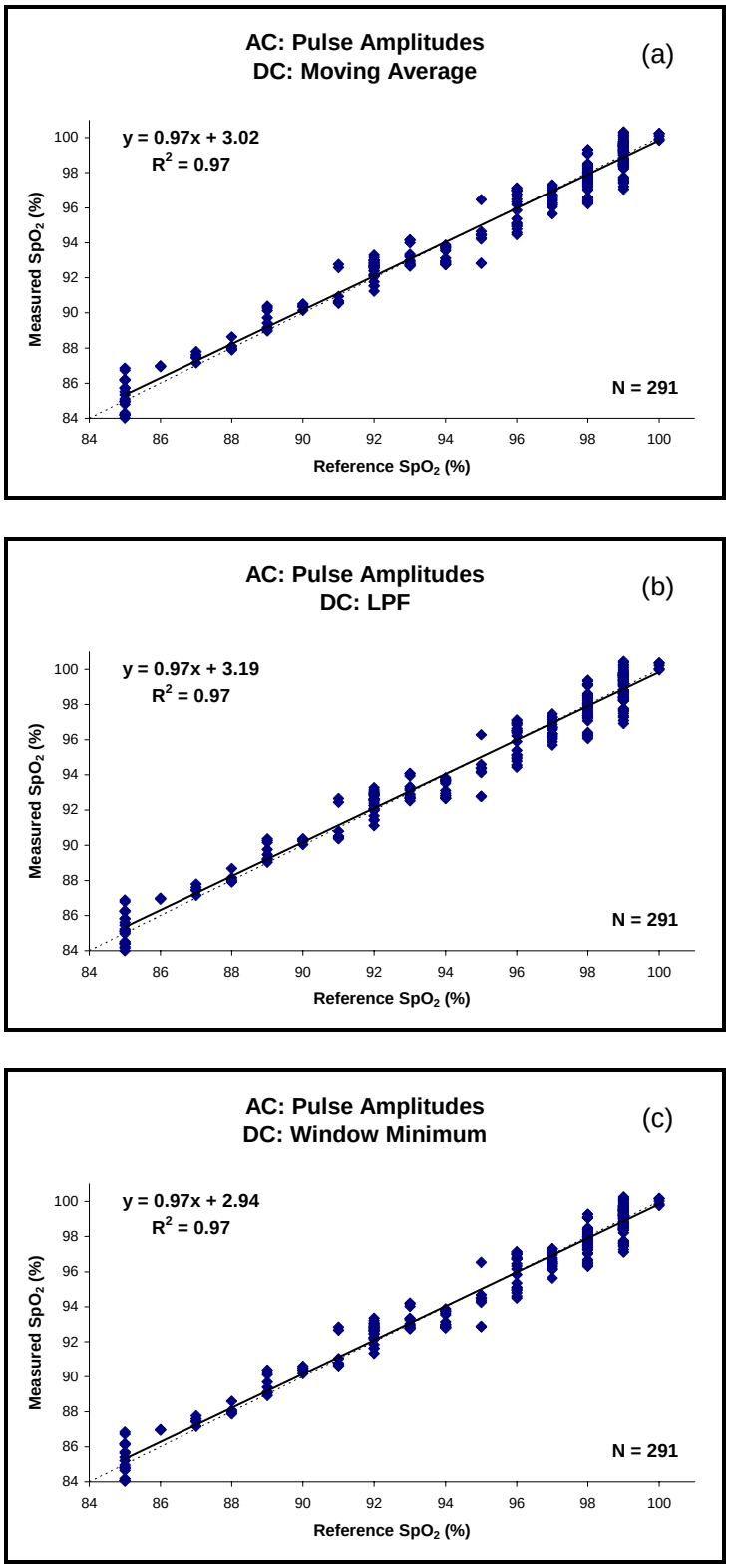

Figure 7.5. *SpO_2 measurements based on pulse amplitudes normalized using (a) a moving average, (b) LPF, and (c) window minimum. Regression lines (—) and lines of identity (---) are shown for comparison.*

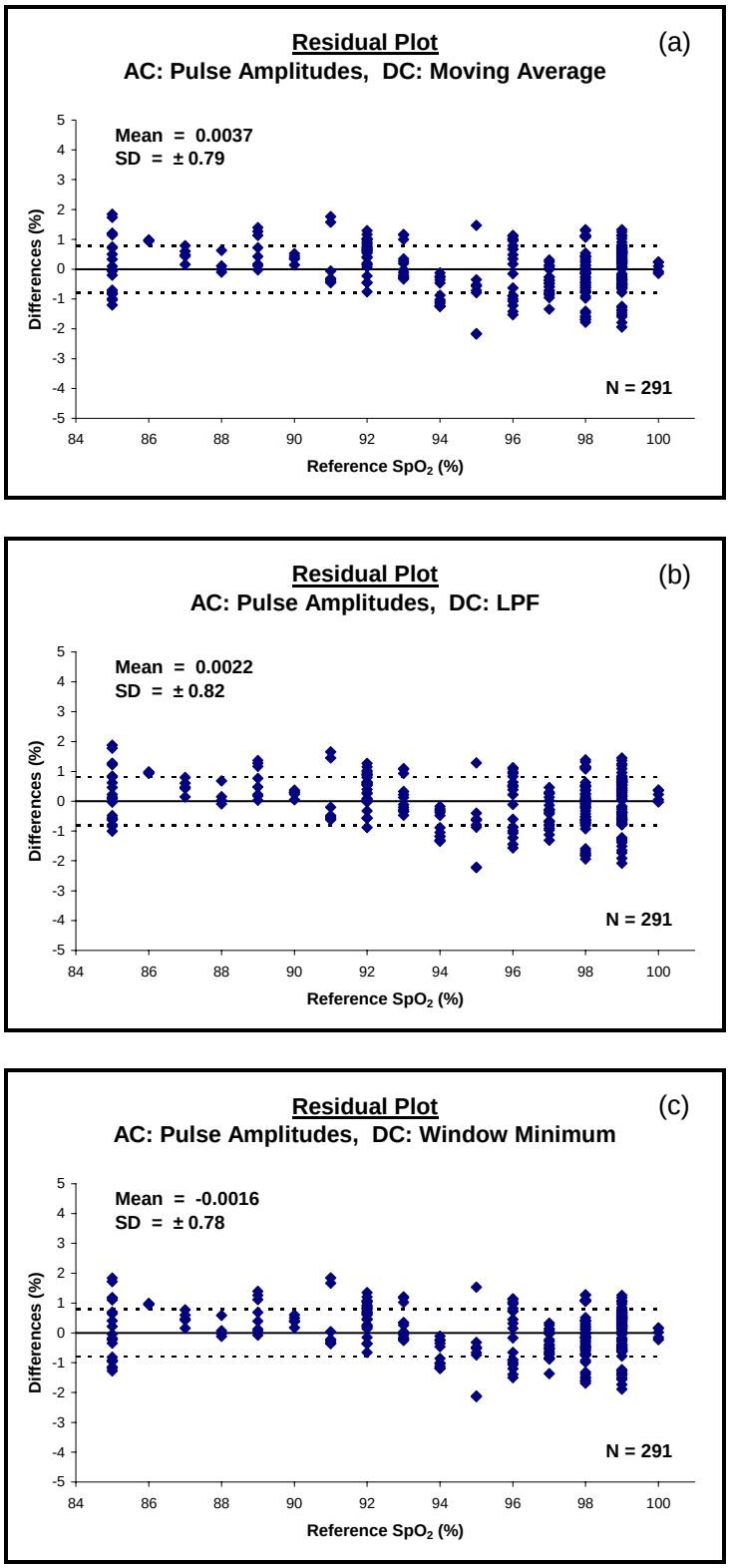

Figure 7.6. *Residual data plots from SpO_2 measurements based on pulse amplitudes normalized using (a) a moving average, (b) LPF, and (c) window minimum.*

7.2.7 Regression Analysis:

Regression analysis involved comparing the derivatives of the R and IR signals. During a single analysis, the most recent 3 seconds of both derivatives were normalized with their respective DC values. As demonstrated in Figure 7.7, the normalized derivatives were used to calculate a regression slope with the R values plotted on the x-axis and the IR values plotted on the y-axis. The regression slope was converted to an angle measurement and used in place of an ***R*** value when deriving the empirical SpO_2 relationship. Method accuracy was assessed by plotting measured SpO_2 values against corresponding reference SpO_2 values, as shown in Figures 7.8 – 7.9.

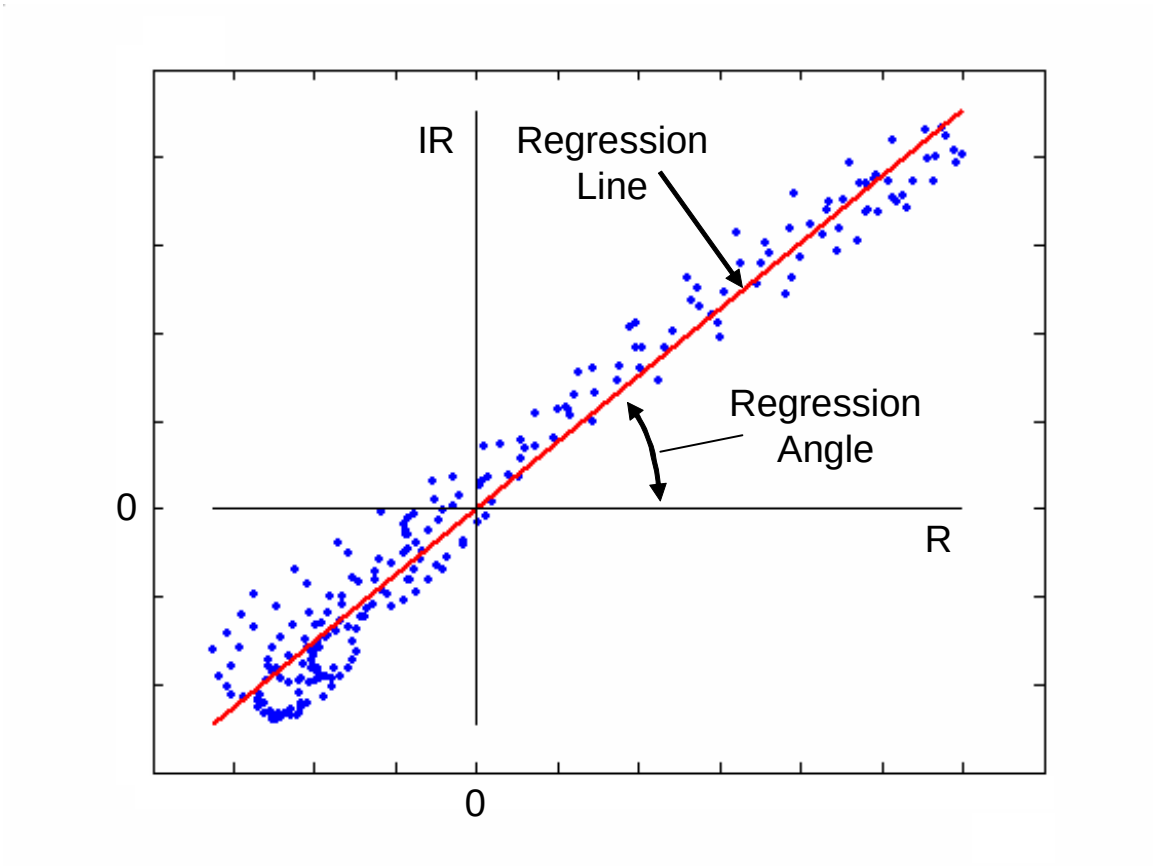

Figure 7.7. *Regression analysis of R and IR derivatives.*

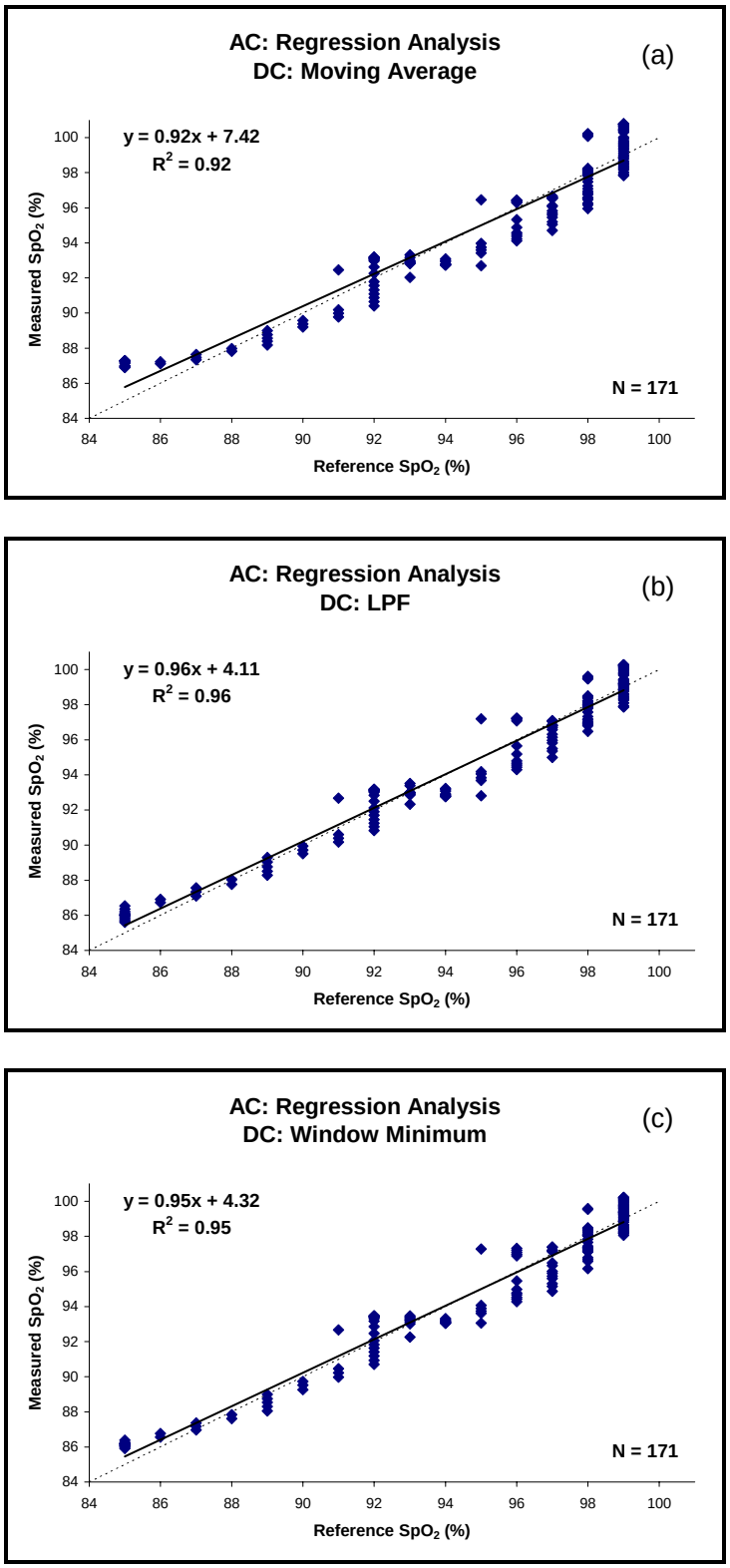

Figure 7.8. *SpO_2 measurements based on regression analysis normalized using (a) a moving average, (b) LPF, and (c) window minimum. Regression lines (—) and lines of identity (---) are shown for comparison.*

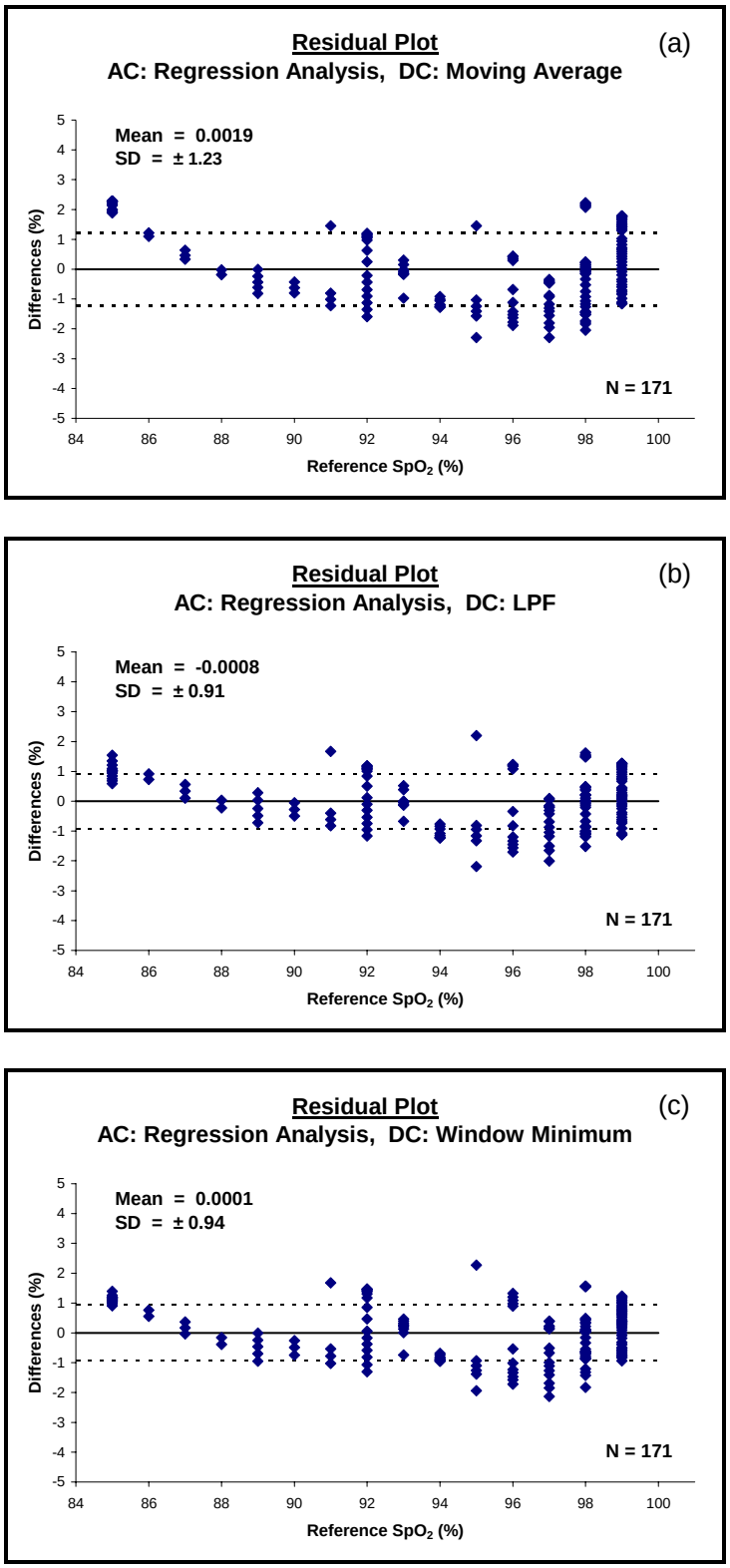

Figure 7.9. *Residual data plots from SpO_2 measurements based on regression analysis normalized using (a) a moving average, (b) LPF, and (c) window minimum.*

7.2.8 Window Analysis:

During a single analysis, a 3-second window spanning the most recent data points in a PPG was assessed. As shown in Figure 7.10, the difference between the maximum and minimum values in the window was used as an AC value. AC values from the R and IR PPGs were normalized with their respective DC values and used to calculate the ***R*** values. To assess method accuracy, the calculated ***R*** values were converted to SpO_2 measurements and plotted against corresponding reference SpO_2 values, as shown in Figures 7.11 – 7.12.

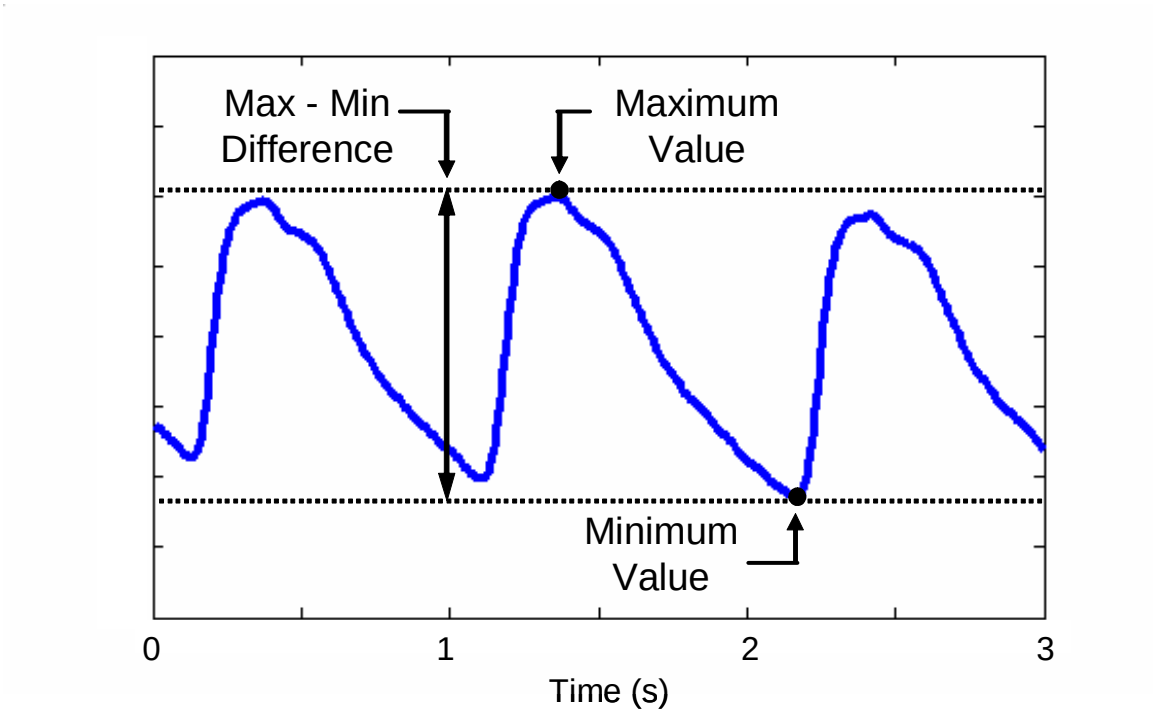

Figure 7.10. *The difference between the maximum and minimum values in a 3-second window.*

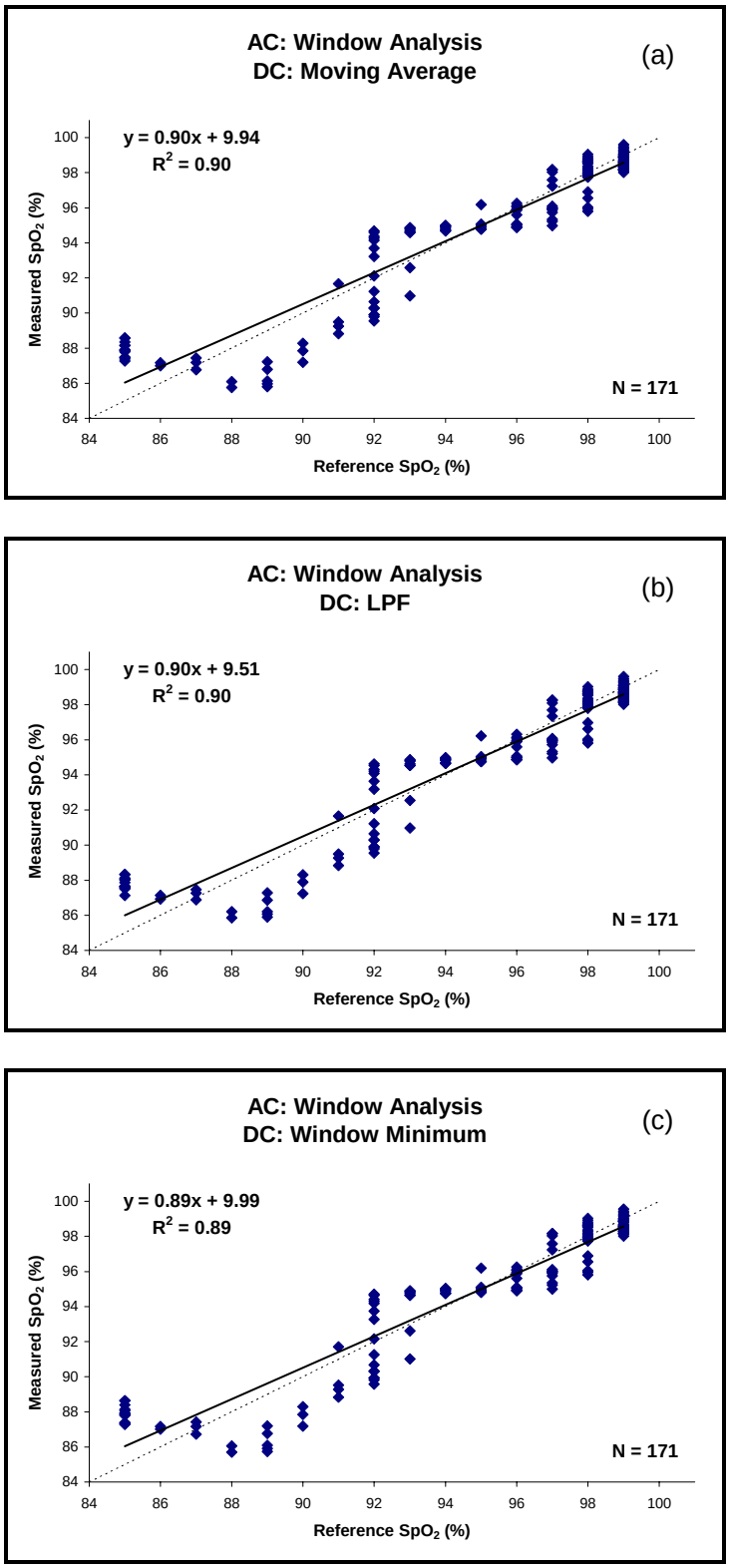

Figure 7.11. *SpO_2 measurements based on a window analysis normalized using (a) a moving average, (b) LPF, and (c) window minimum. Regression lines (—) and lines of identity (---) are shown for comparison.*

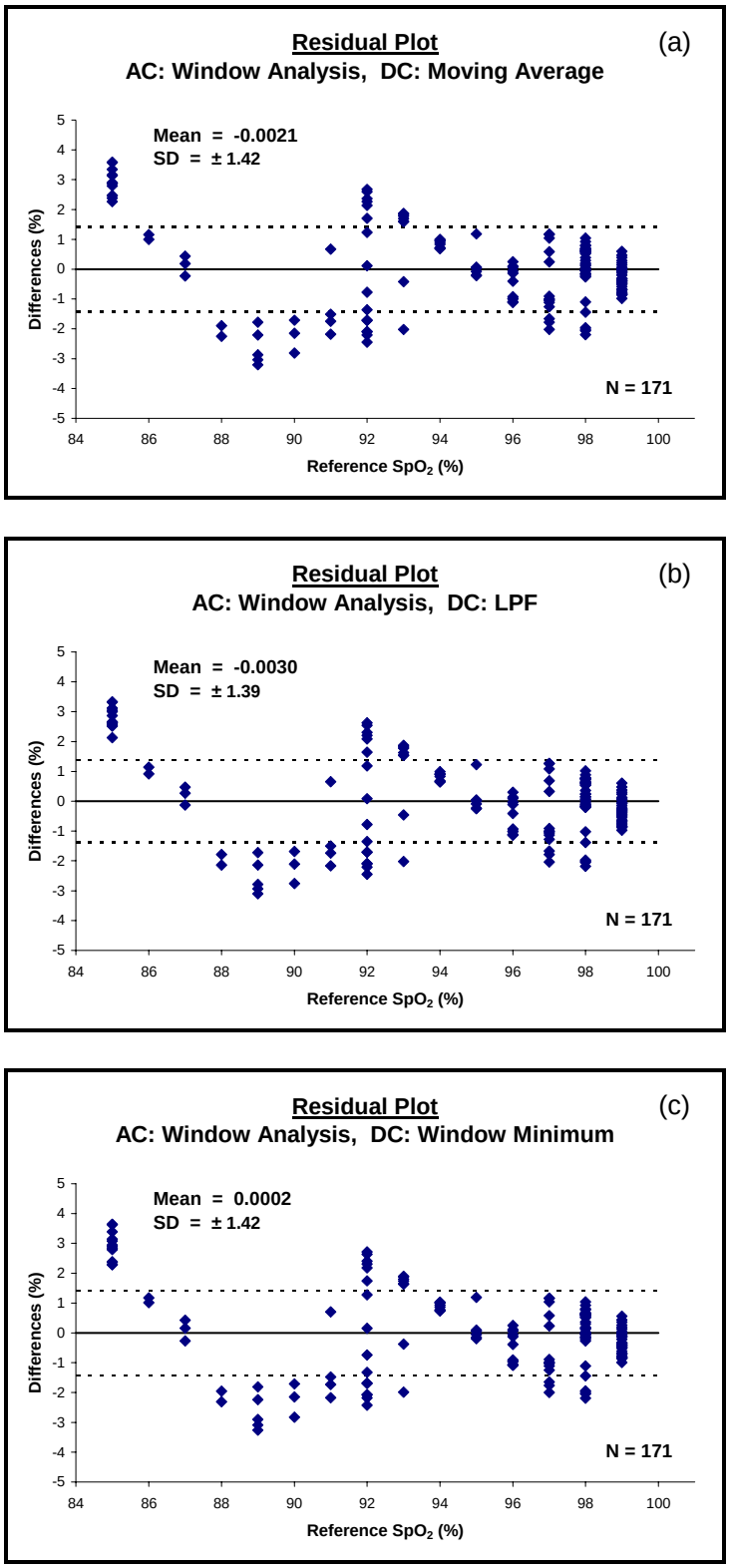

Figure 7.12. *Residual data plots from SpO_2 measurements based on window analysis normalized using (a) a moving average, (b) LPF, and (c) window minimum.*

7.2.9 Spectral Analysis:

An optimized analysis form was employed during spectral analysis. The optimization consisted of processing every 5th data point in the PPG using a 64-point FFT. This resulted in a transform that assessed 4.3 seconds of a PPG signal while still providing information over the full span of the cardiac frequency range (0.5 – 5 Hz). As shown in Figure 7.13, the AC value from the transformed PPG was considered to be the amplitude of the highest peak in the cardiac frequency range. This value was normalized using the amplitude of the 0 Hz (DC) component. Spectral analysis was performed on both the R and IR PPGs to obtain the normalized AC values. The normalized AC measurements were used to calculate the corresponding ***R*** values. To assess method accuracy, the calculated ***R*** values were converted to SpO_2 measurements and plotted against reference SpO_2 values, as shown in Figures 7.14 – 7.15.

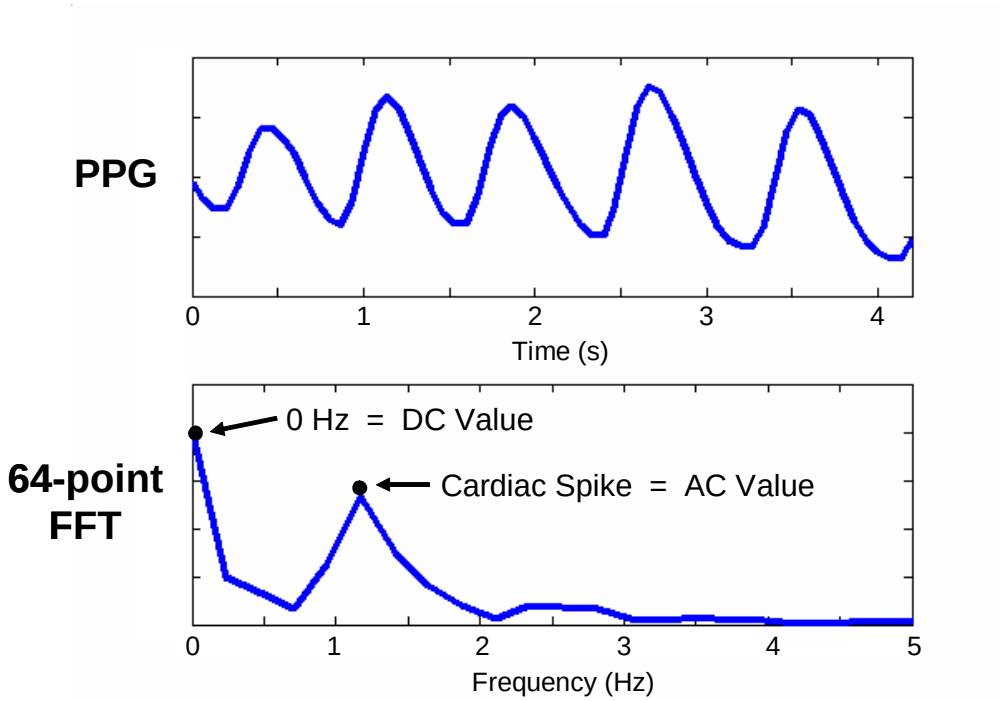

Figure 7.13. *PPG and corresponding FFT with marked amplitudes used as AC and DC values. Note that the top waveform consists of every 5th data point from the original signal, essentially making it a PPG that has been sampled at a rate of 15 Hz.*

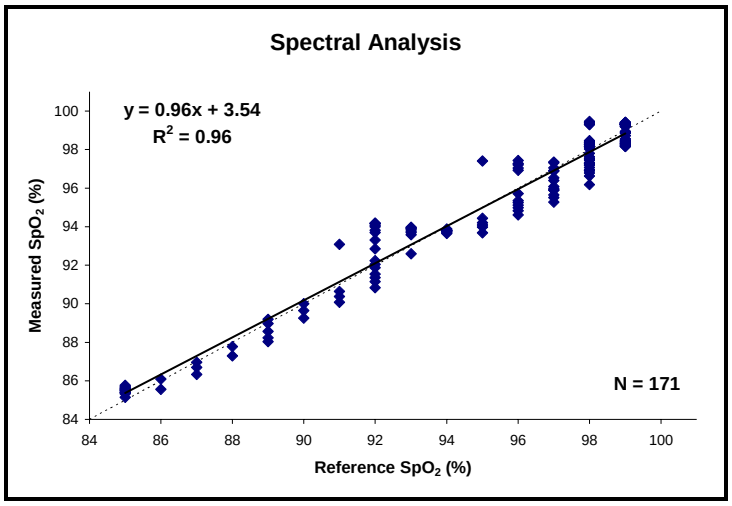

Figure 7.14. *SpO_2 measurements based on spectral analysis with resulting regression line (—) and line of identity (---).*

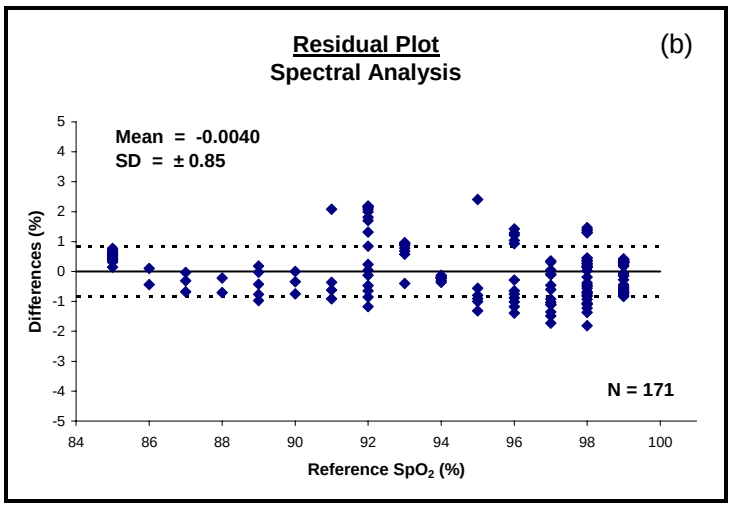

Figure 7.15. *Residual data plot from SpO_2 measurements based on spectral analysis.*

Table 7.2. *Assessment results for SpO_2 processing methods.*

AC Measurements	DC Measurements	R^2 Value	Bias (%)	SEE (%)
Differentials	Moving Average	0.96	-0.0007	0.84
	LPF	0.97	0.0001	0.82
	Window Minimum	0.96	-0.0028	0.91
Pulse Amplitudes	Moving Average	0.97	0.0037	0.82
	LPF	0.97	0.0022	0.91
	Window Minimum	0.97	-0.0016	0.81
Regression Analysis	Moving Average	0.92	0.0019	1.37
	LPF	0.96	-0.0008	1.11
	Window Minimum	0.95	0.0001	0.96
Window Analysis	Moving Average	0.90	-0.0021	1.38
	LPF	0.90	-0.0030	1.41
	Window Minimum	0.89	0.0002	1.44
Spectral Analysis	Spectral Analysis	0.96	-0.0040	0.84

7.3 HR Processing Methods

The processing methods described in section 3.3 required only one PPG signal to perform assessments of HR activity. IR PPGs were selected for analysis due to their consistently larger amplitudes compared to corresponding R PPGs. The IR PPGs recorded during the HR experiments were divided into 1-minute segments. All segments were processed by each method to obtain average HR measurements. Table 7.3 lists the processing methods used to measure average HR based on the PPGs. Table 7.4 summarizes the results of the assessments.

Table 7.3. *List of processing methods capable of providing HR measurements.*

Processing Methods	General Description
Moving Window [67]	The comparison of each consecutive point in a PPG to its surrounding values in order to locate local maxima or minima.
Signal Derivative [62-66]	Using the derivative of the PPG to identify the steep slopes at the leading edges of cardiac pulses.
Spectral Analysis [41-44, 68]	Estimation of HR based on the predominant cardiac frequency.

7.3.1 Moving Window:

An adaptive window with a varying width was used to locate individual pulse peaks in the PPG signals. The window scanned a PPG signal by moving 1 data point at a time. After each move, the maximum value in the window was located. If the maximum value was in the center of the window, that data point was marked as a peak. To account for variations in HR, the width of the processing window was adjusted every time a peak was located. The new window width was set to half the length of the previous beat-to-beat interval, as demonstrated in Figure 7.16b. This reduced the chances of a peak being overlooked while maintaining a reduced sensitivity to noise and signal irregularities.

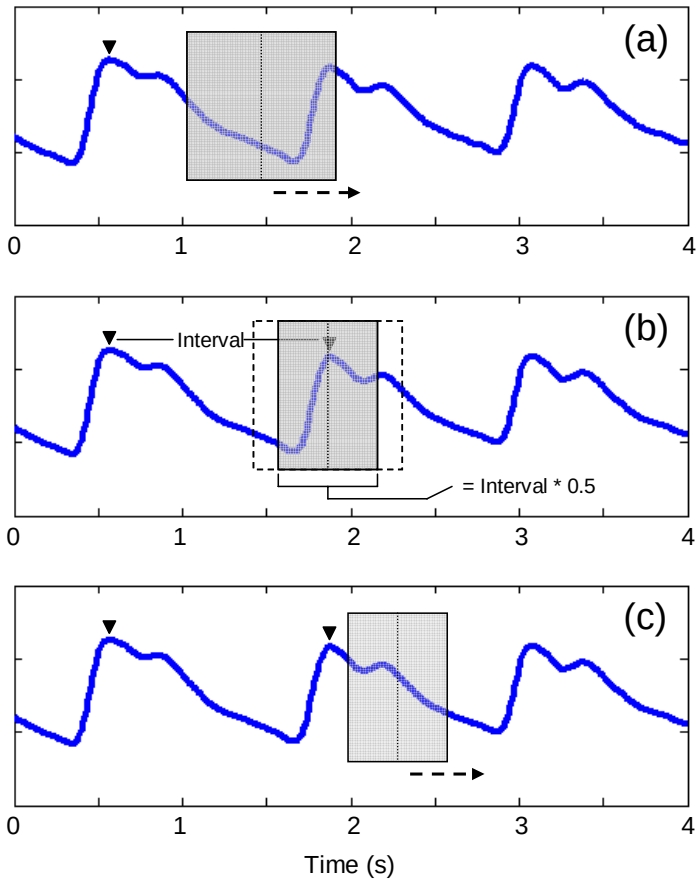

Figure 7.16. *Using an adaptive window to locate pulse peaks. (a) Searching for a peak. (b) Adapting the window's width after locating a peak. (c) Searching for next peak using the new window.*

The number of identified peaks in each 60-second recording were counted and provided a measure of the average HR in beats-per-minute. To assess method accuracy, HR measurements from the data sets were plotted against corresponding reference HR values obtained through the BIOPAC, as shown in Figures 7.17 – 7.18.

7.3.2 Signal Derivative:

The derivatives of the PPG signals were used to identify individual pulse peaks. The derivative of a PPG was assessed 1 data point at a time by comparing the point to a threshold value. When the value of a point exceeded the threshold, it indicated that the

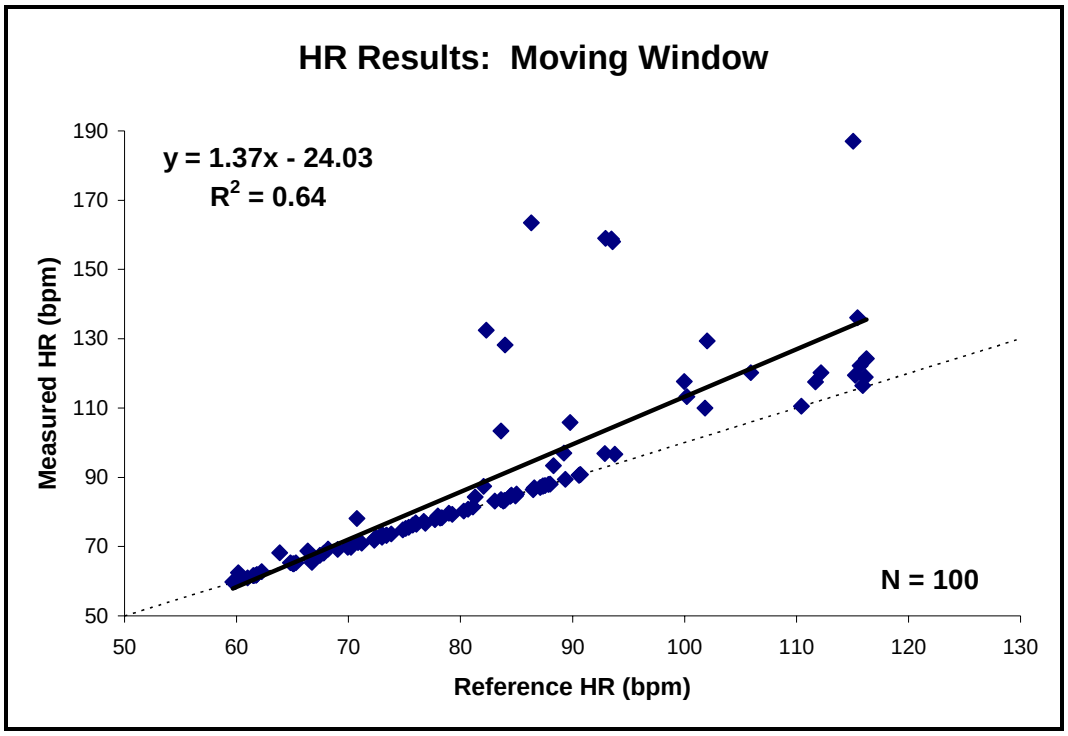

Figure 7.17. *HR measurements obtained using an adaptive moving window with resulting regression line (—) and line of identity (---).*

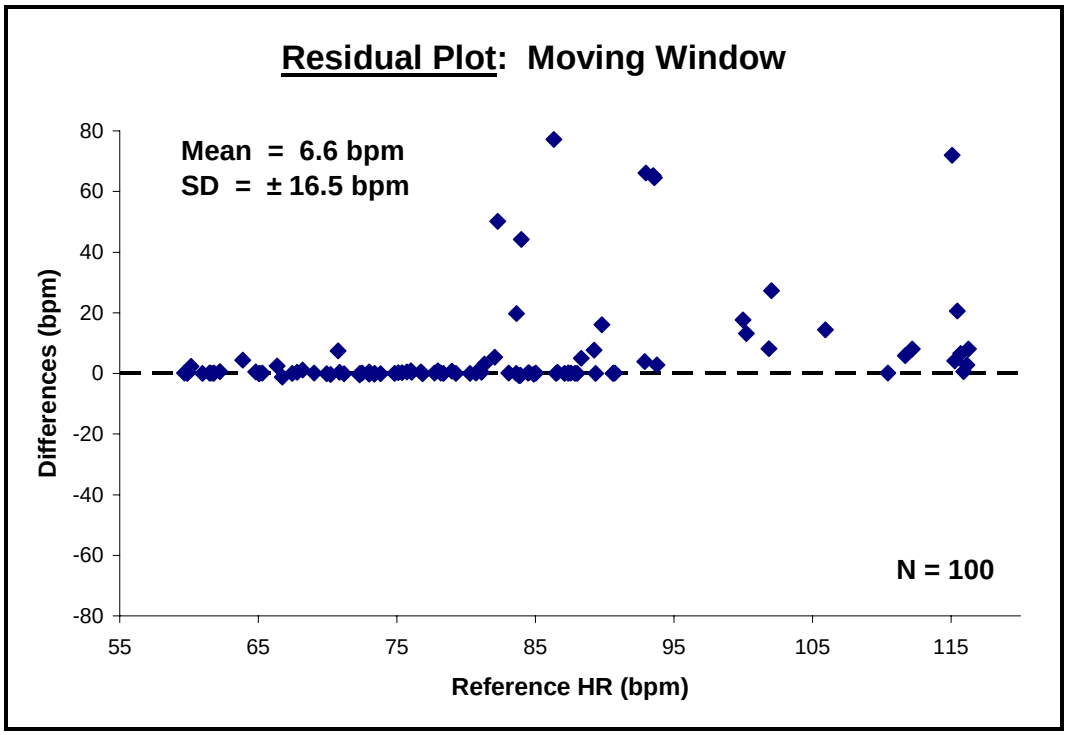

Figure 7.18. *Residual data plot from HR measurements based on an adaptive moving window.*

steep slope at the leading edge of a pulse had been located. The following zero-crossing in the derivative was marked as a peak. Figure 7.19 shows an example of peaks identified in this way. To account for variations in slope intensity due to changes in HR and pulse shape, the threshold was adjusted every time a peak was located. The new threshold was set to half the height of the current pulse's maximum slope. This minimized noise and minor signal irregularities from being identified, while the chances of missing a leading pulse edge due to a shallow slope were also reduced.

The number of identified peaks in each 60-second recording were counted and provided a measure of the average HR in beats-per-minute. To assess method accuracy, HR measurements from the data sets were plotted against corresponding reference HR values obtained through the BIOPAC, as shown in Figures 7.20 – 7.21.

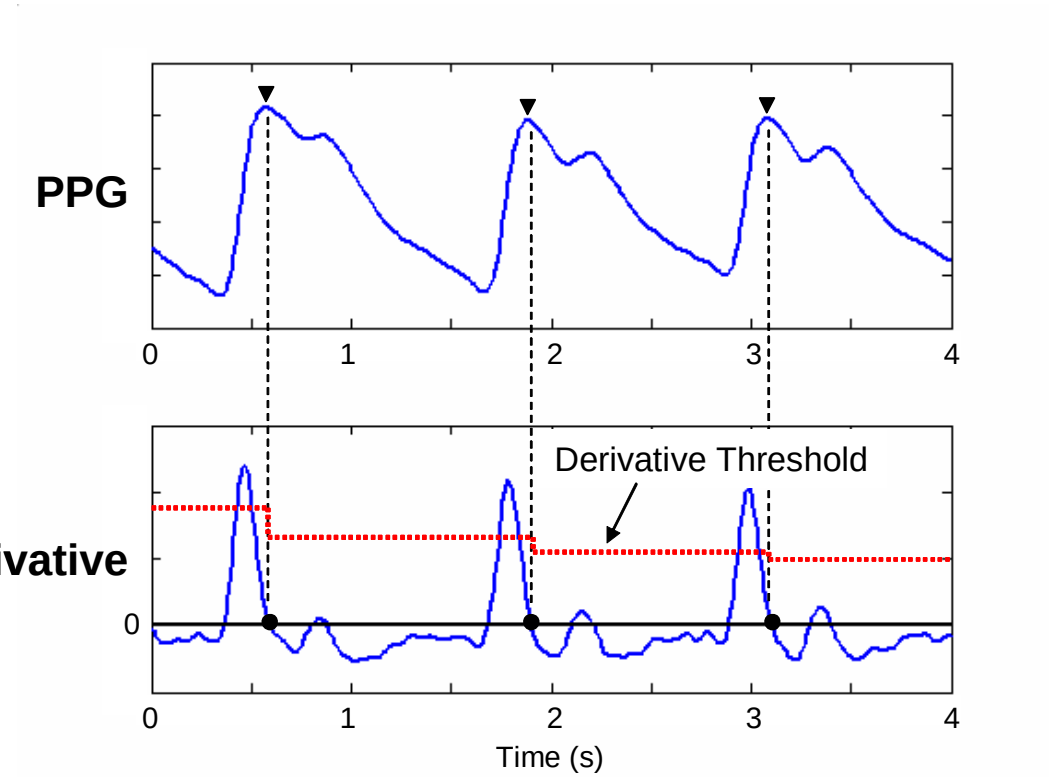

Figure 7.19. *The identification of pulse peaks using a PPG derivative and the adaptation of the derivative's threshold.*

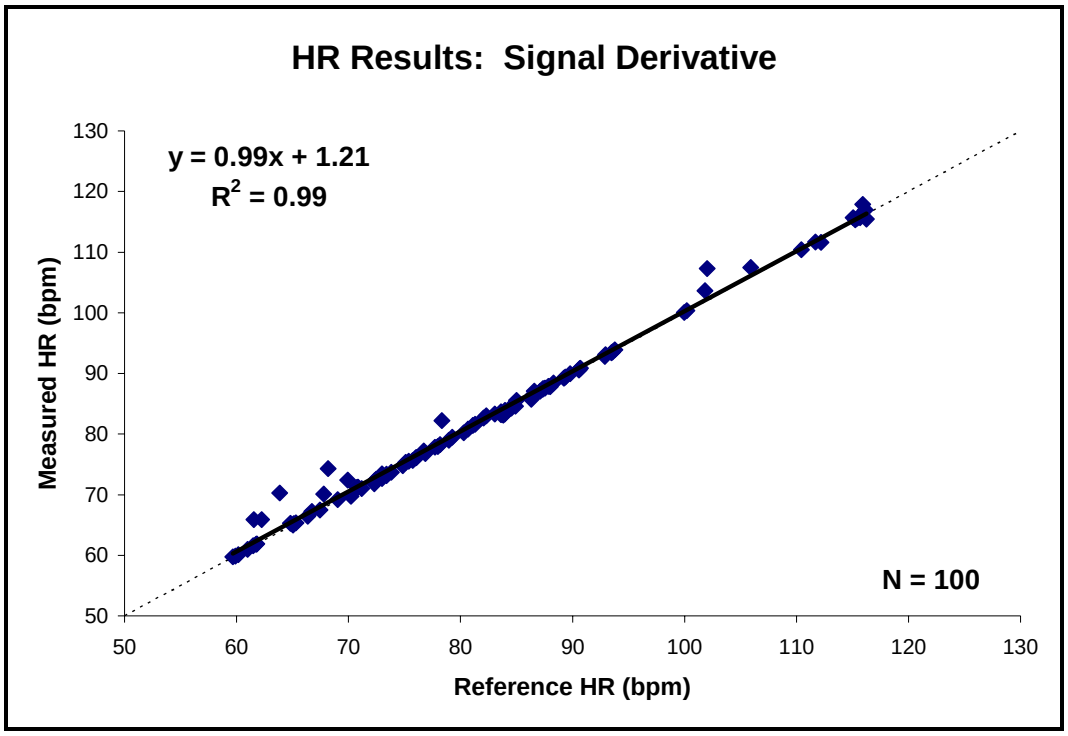

Figure 7.20. *HR measurements obtained using PPG derivatives with resulting regression line (—) and line of identity (---).*

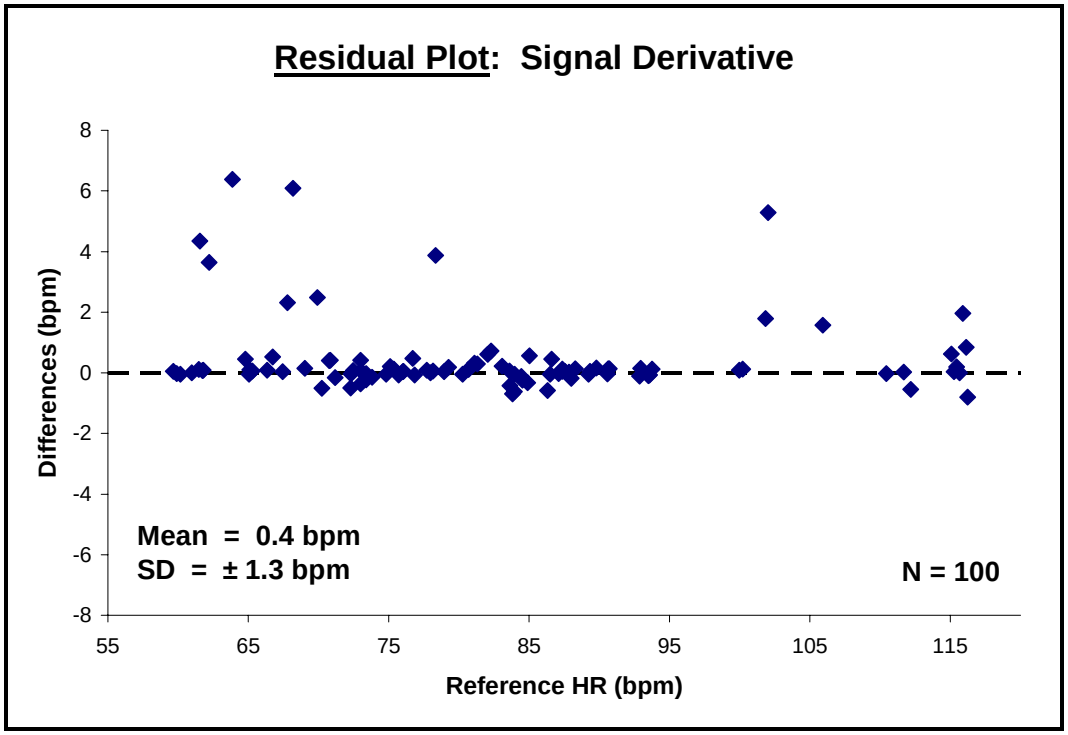

Figure 7.21. *Residual data plot from HR measurements based on PPG derivatives.*

7.3.3 Spectral Analysis:

Spectral analyses of the PPG signals were used to estimate cardiac frequencies. As shown in Figure 7.22, a 1-minute PPG segment (200 s/s) was transformed into the frequency domain using a 12,000-point FFT. The resolution of the transform was 0.0167 Hz, which allowed a HR measurement resolution of 1 bpm. The largest peak in the cardiac range of 0.5 – 5 Hz was located since it represented the predominant cardiac frequency for the 1-minute interval, and the frequency of the peak was multiplied by 60 to obtain a HR measurement in beats-per-minute. To assess method accuracy, HR measurements from each data set were plotted against reference HR values obtained through the BIOPAC, as shown in Figures 7.23 – 7.24.

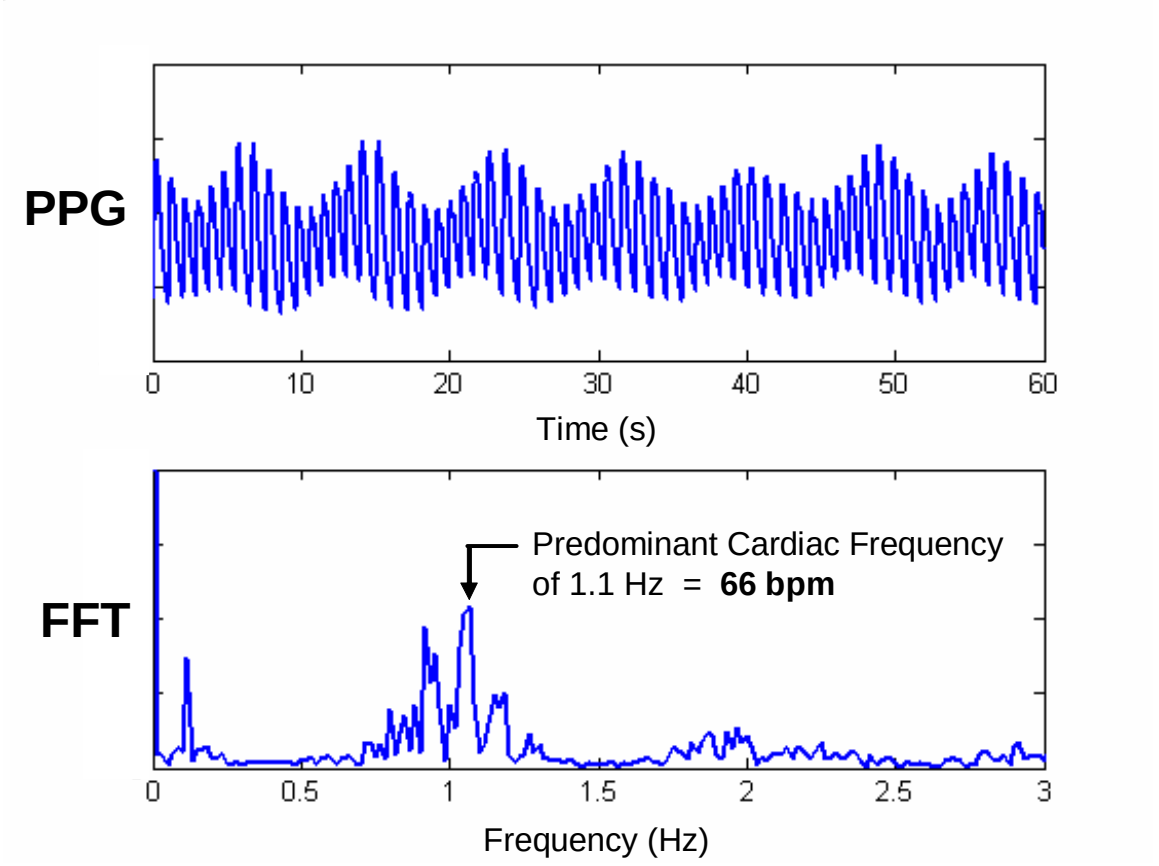

Figure 7.22. *PPG and corresponding FFT showing cardiac frequency component.*

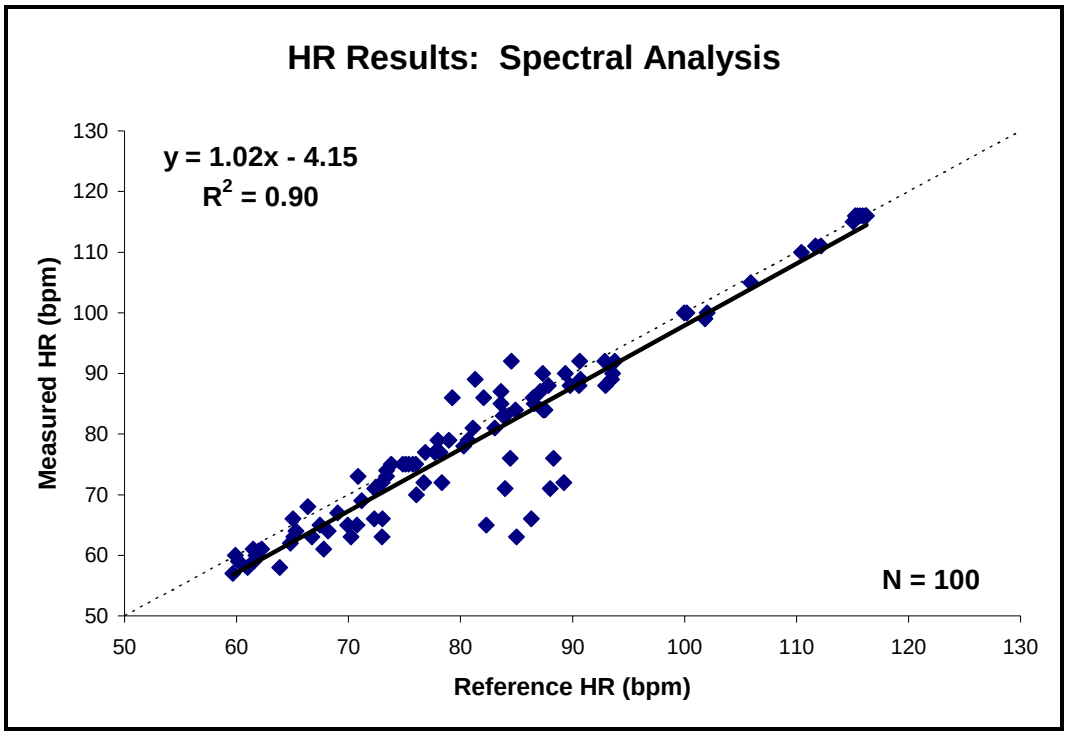

Figure 7.23. *HR measurements obtained using spectral analysis with resulting regression line (—) and line of identity (---).*

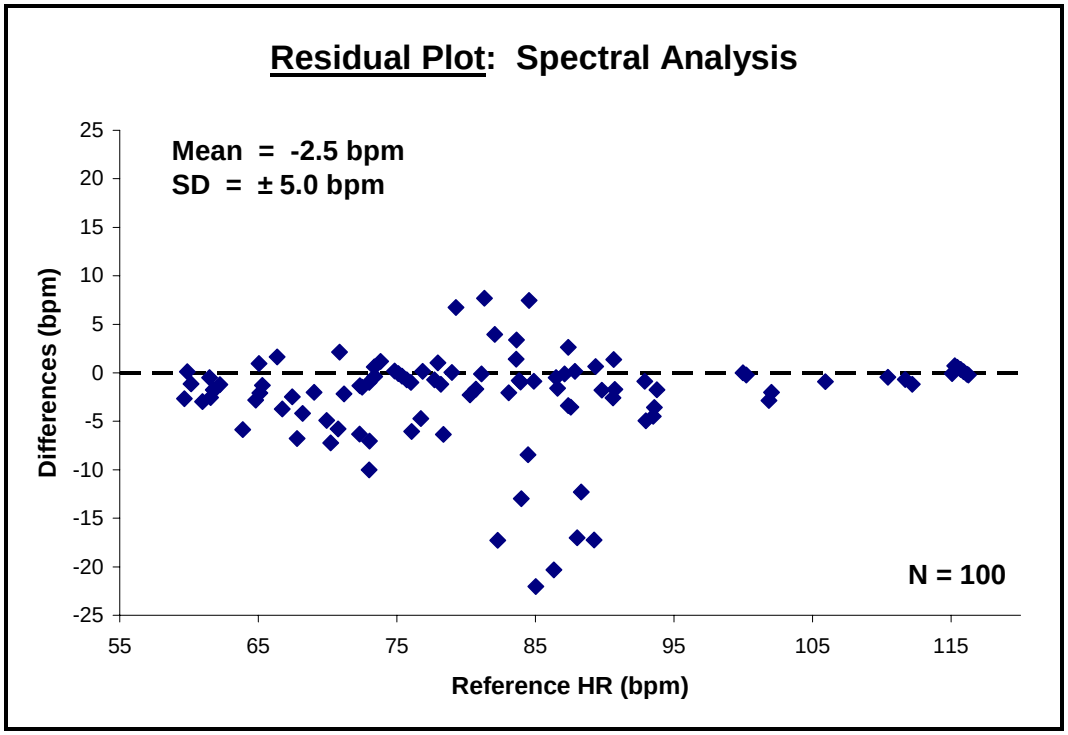

Figure 7.24. *Residual data plot from HR measurements based on spectral analysis.*

Table 7.4. *Assessment results for HR processing methods.*

Processing Methods	R^2 Value	Bias (bpm)	SEE (bpm)
Moving Window	0.64	6.62	15.48
Signal Derivative	0.99	0.43	1.27
Spectral Analysis	0.90	-2.45	4.98

7.4 HRV Processing Methods

Of the HRV indices described in section 3.4, only those capable of providing short-term assessments (using less than 5 minutes of data) were selected for testing. Since field-based monitoring applications are centered on detecting physiological deterioration and potentially detrimental conditions in a fast and efficient manner, long-term assessments requiring hours of monitoring (as normally practiced in a clinical environment) are not feasible in field triage situations.

The short-term HRV indices selected for evaluation were all based on NN intervals measurements. As such, the IR PPG signals recorded during the HRV experiments were pre-processed prior to testing the individual measurement methods. NN intervals, measured in milliseconds, were extracted from every PPG signal. The NN data sets were then processed to obtain SDNN and COV index values. The remaining 4 indices were based on the differences between successive NN intervals, so each set of NN intervals were processed further to obtain these values. The sets of NN differences were assessed to provide SDSD, RMSSD, NN50, and pNN50 index values for all data sets. Table 7.5 lists the HRV indices and their calculation methods. Individual index results are shown in Figures 7.25 – 7.36, plotted against reference values obtained through the BIOPAC, while the assessment results are summarized in Table 7.6.

Table 7.5. *List of HRV indices and their calculation methods.*

HRV Indices	Calculation Methods	Physiological Indications
SDNN [80, 81, 83, 85, 103]	Standard deviation of NN intervals	Measure of the overall variability in HR
COV [85]	Coefficient of variance (normalized SDNN = SDNN / mean NN interval)	Changes in overall variability independent of changes in mean NN interval.
SDSD [81]	Standard deviation of successive NN differences	Reflection of parasympathetic influence on the heart.
RMSSD [80, 85, 103]	Root-mean-square of successive NN differences	Reflection of parasympathetic influence on the heart.
NN50 [85]	Number of successive NN differences greater than 50 ms	Index of vagal tone.
pNN50 [80, 85, 103]	Proportion of successive NN differences greater than 50 ms (NN50 / # of NN differences)	Normalized version of NN50, independent of HR.

Table 7.6. *Assessment results for HRV indices.*

HRV Indices	R^2 Value	Normalized Bias	Normalized SEE
SDNN	0.97	0.09	0.72
COV	0.97	0.09	0.03
SDSD	0.68	0.44	2.75
RMSSD	0.68	0.44	2.75
NN50	0.71	0.78	4.08
pNN50	0.75	0.51	2.29

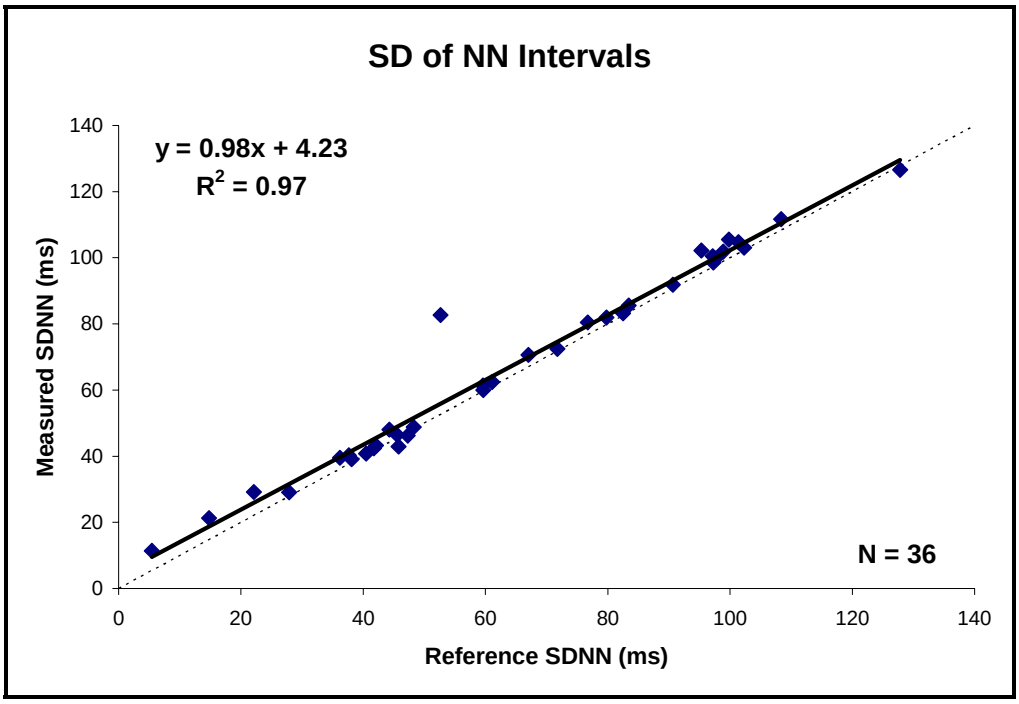

Figure 7.25. *SDNN index measurements with resulting regression line (—) and line of identity (---).*

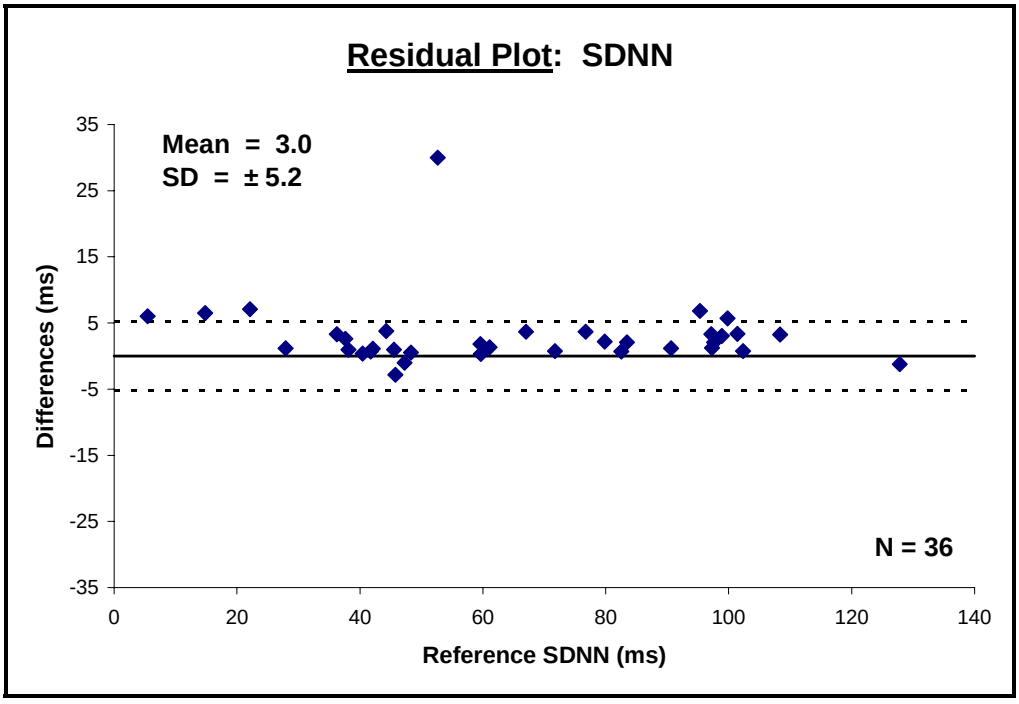

Figure 7.26. *Residual plot for SDNN measurements.*

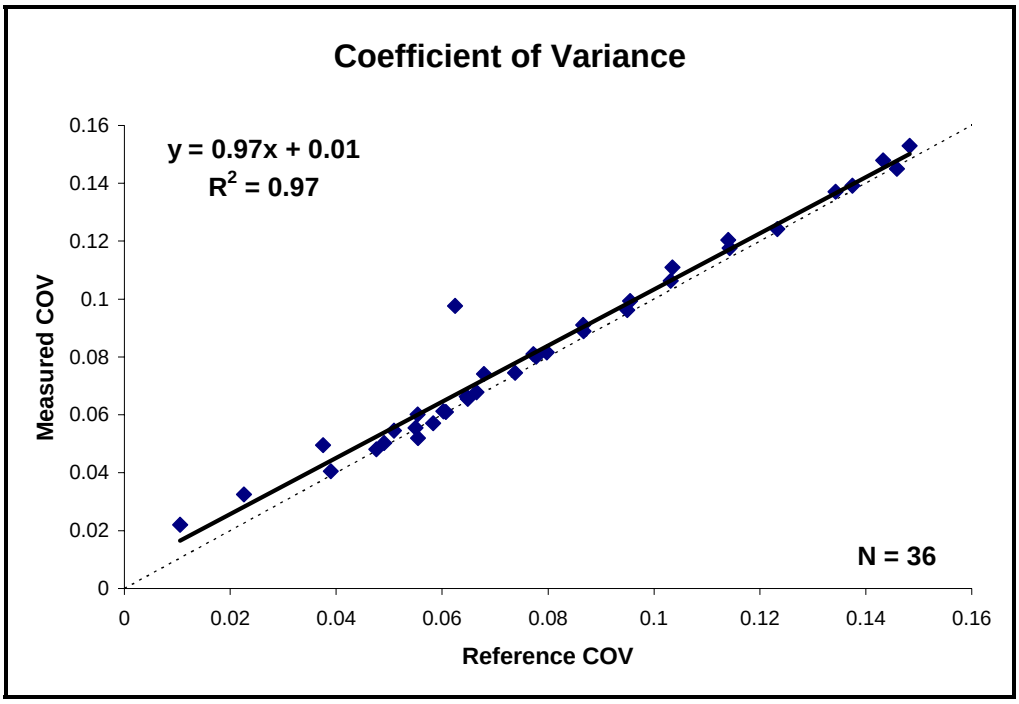

Figure 7.27. *COV index measurements with resulting regression line (—) and line of identity (---).*

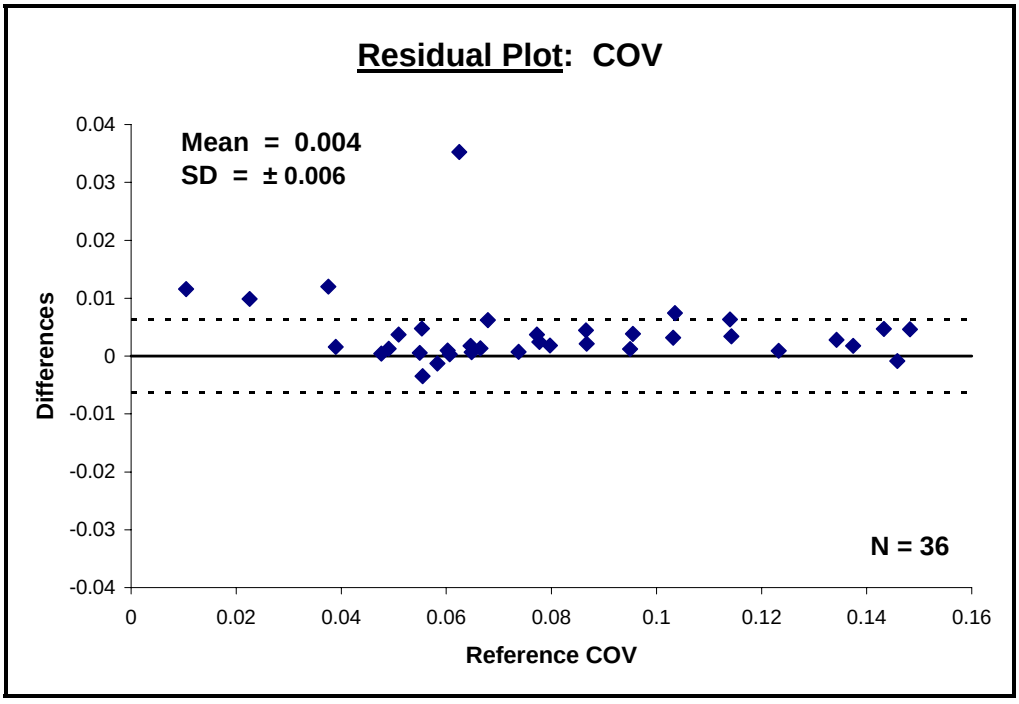

Figure 7.28. *Residual plot for COV measurements.*

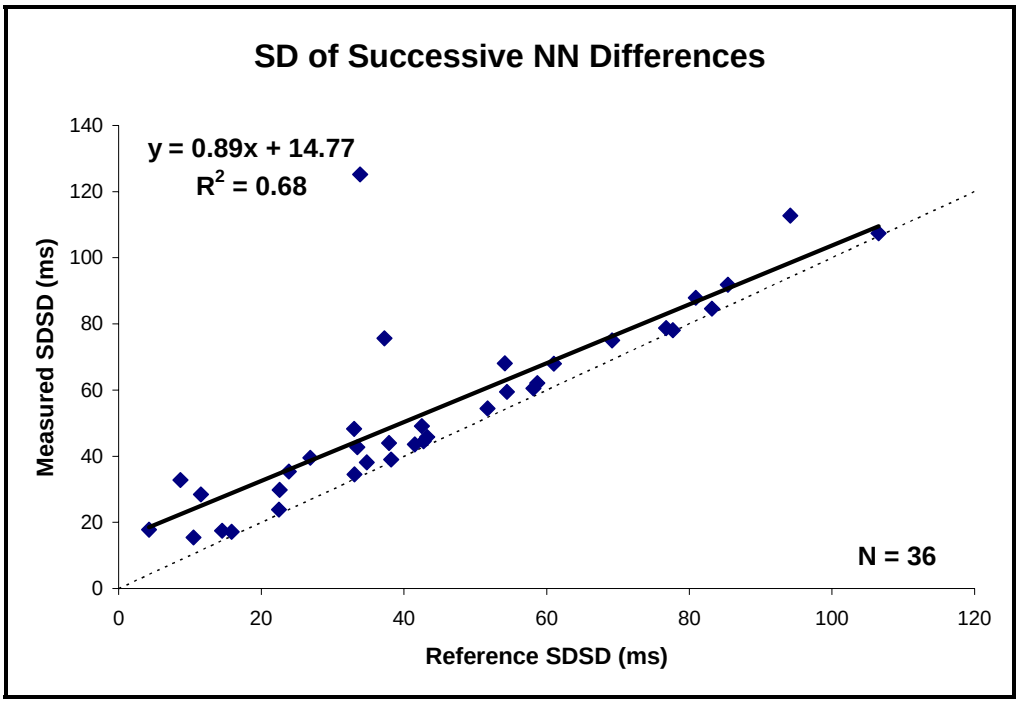

Figure 7.29. *SDSD index measurements with resulting regression line (—) and line of identity (---).*

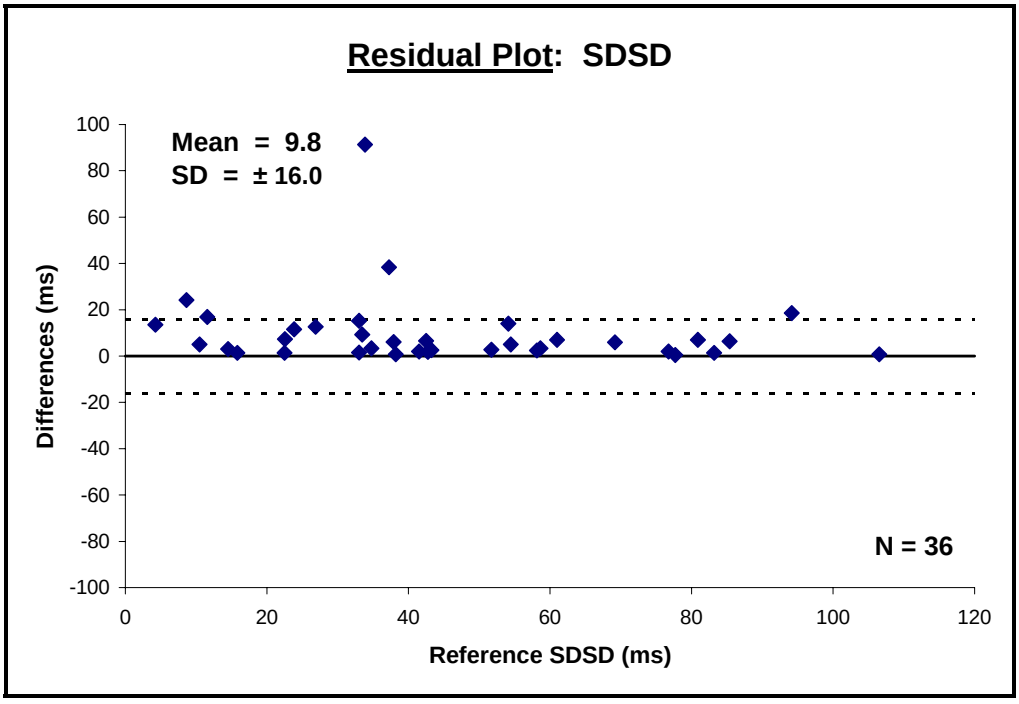

Figure 7.30. *Residual plot for SDSD measurements.*

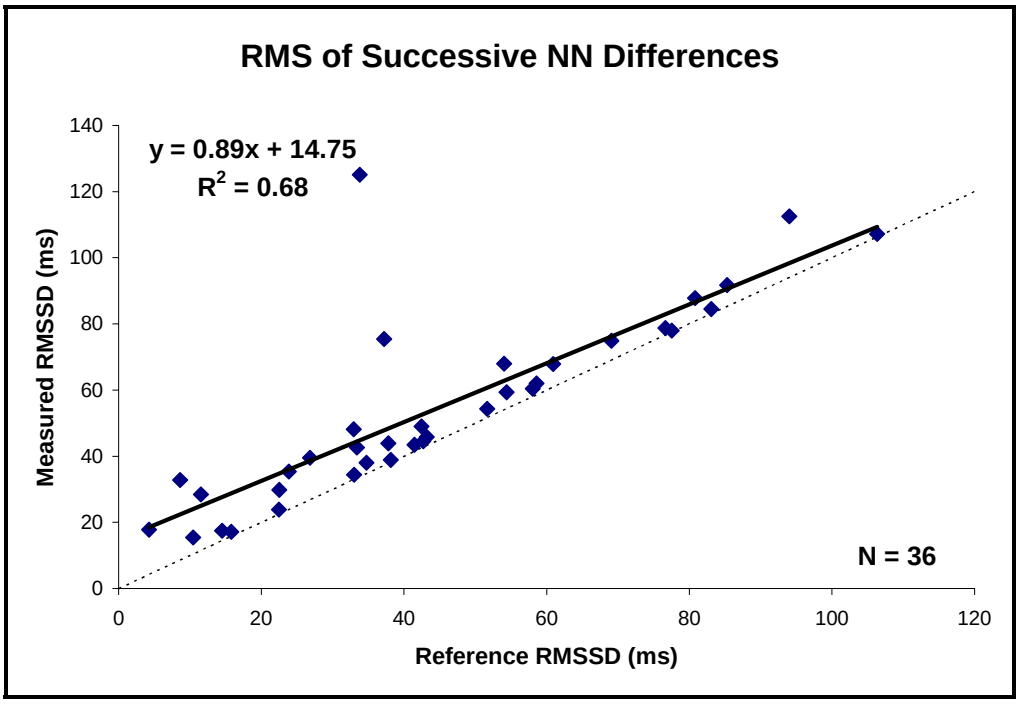

Figure 7.31. *RMSSD index measurements with resulting regression line (—) and line of identity (---).*

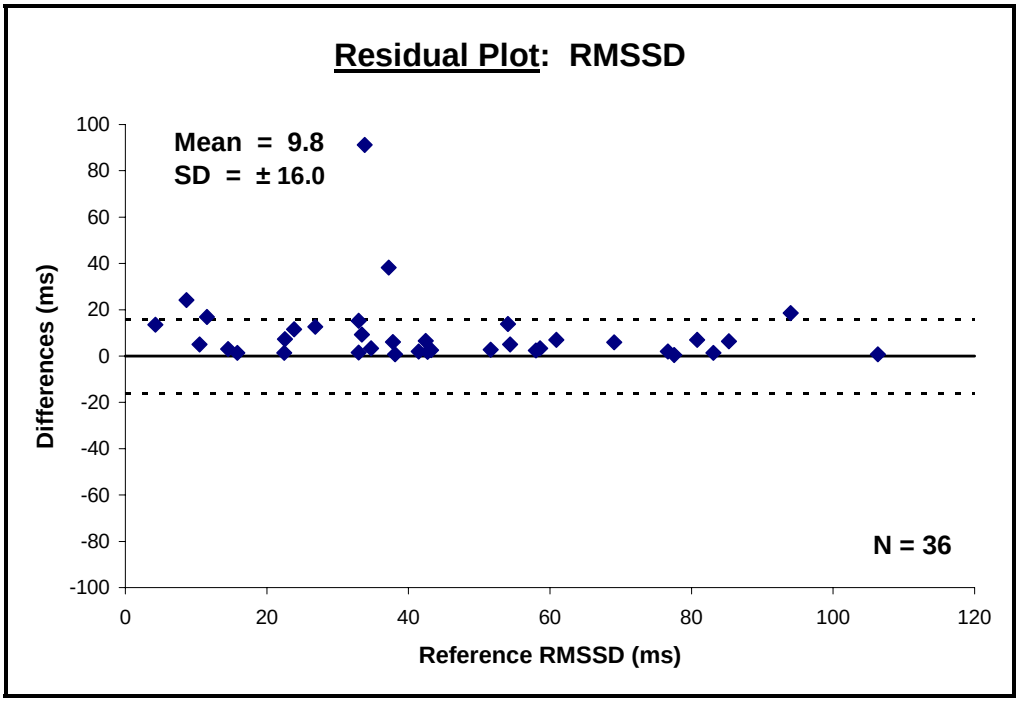

Figure 7.32. *Residual plot for RMSSD measurements.*

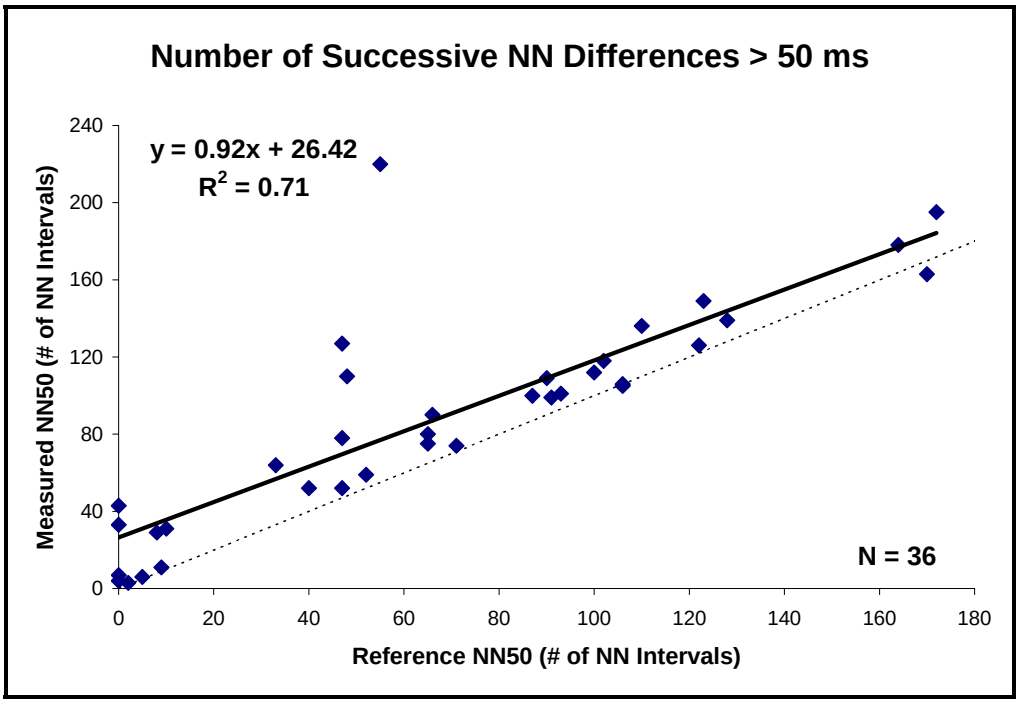

Figure 7.33. *NN50 index measurements with resulting regression line (—) and line of identity (---).*

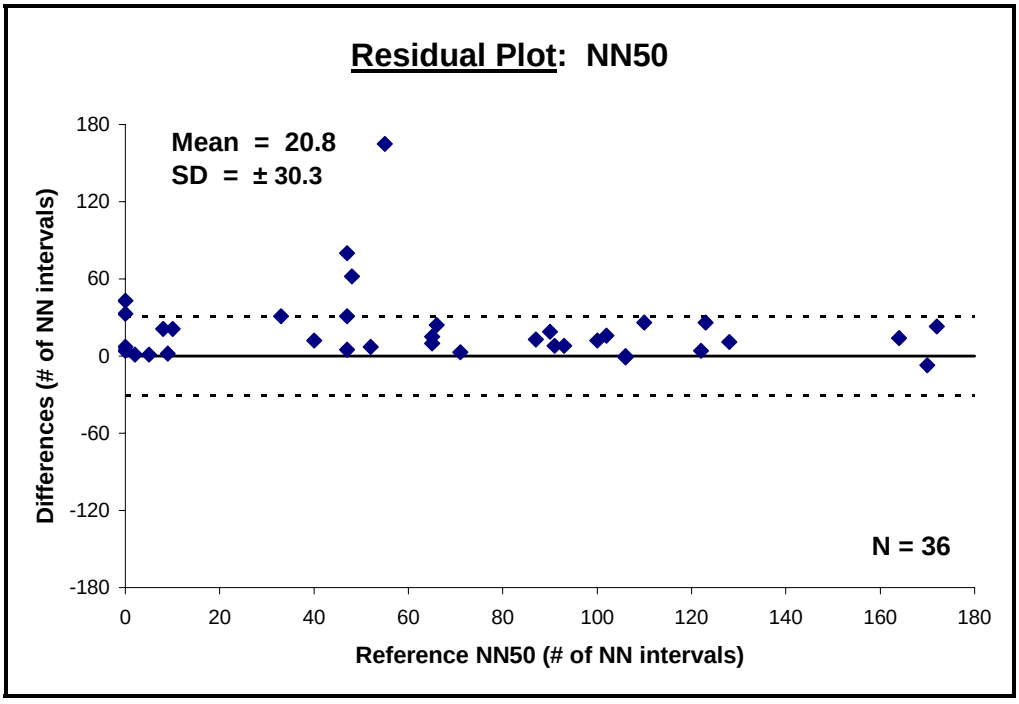

Figure 7.34. *Residual plot for NN50 measurements.*

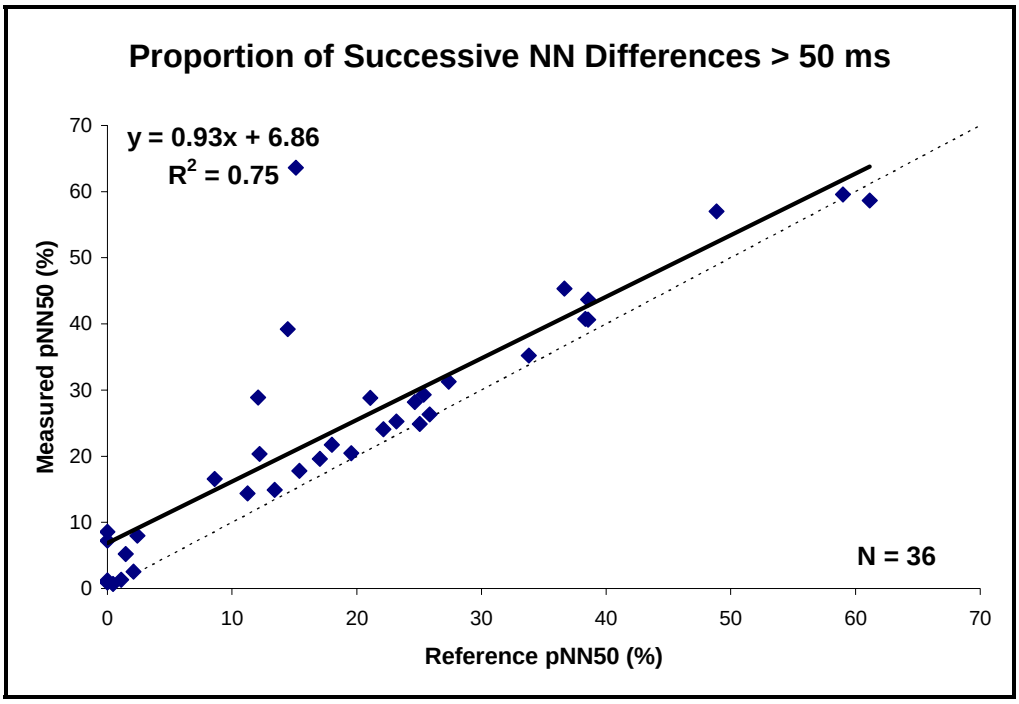

Figure 7.35. *pNN50 index measurements with resulting regression line (—) and line of identity (---).*

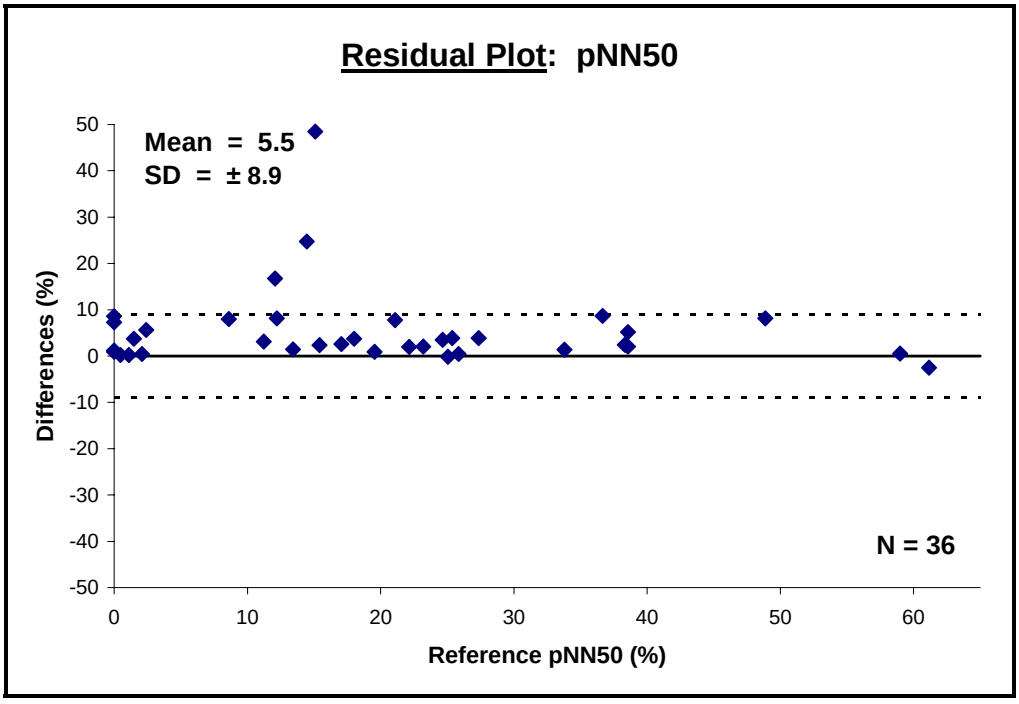

Figure 7.36. *Residual plot for pNN50 measurements.*

7.5 RR Processing Methods

As described in section 3.5, contributions from pulmonary activity can be observed in 3 prominent facets of the PPG signal: baseline modulations, pulse amplitude modulations, and pulse interval fluctuations. When isolated, all 3 waveforms could potentially provide sufficient information for estimating RR. In addition, both cycle length assessment and spectral analysis are capable of performing accurate measurements. As a result, the 6 unique processing methods listed in Table 7.7 were identified and selected for testing.

As with HR analysis, IR signals were selected for RR analysis due to their consistently larger amplitudes. The recordings acquired during the RR experiments were each 90 seconds in length. The 15 seconds of signal at the beginning and end of a recording were excluded during analysis because sensor transients and reactions from the subjects occasionally caused abnormal events in these portions of the recordings. Therefore, only the middle 60 seconds were processed. Table 7.8 summarizes the results of the method assessments.

7.5.1 Band-Pass Filtering:

All filtering performed during the RR method assessments employed a band-pass filter (BPF) that removed signal components outside of the respiratory frequency range. The filter was an IIR Butterworth which allowed for a reduced number of coefficients compared to FIR filters and had a smooth passband with no significant ripple. Cutoffs were set at 0.05 and 0.7 Hz and a 6^{th} order filter was required to maintain stability.

Table 7.7. *List of processing methods capable of providing RR measurements.*

Analysis Methods	General Description
Signal Source: Band-Pass Filtered PPG Signal [33, 101]	The waveform obtained by applying a BPF to a PPG signal.
Signal Source: PPG Pulse Envelope [94]	The waveform obtained by connecting the positive peaks of cardiac pulses using interpolation.
Signal Source: IHR Fluctuations [34, 102]	The waveform obtained by tracking changes in individual beat-to-beat intervals.
Analysis Method: Measuring Cycle Lengths [33]	A measure of the average length of the respiratory cycles in a waveform.
Analysis Method: Spectral Analysis [94, 101, 102]	Estimation of RR based on the predominant respiratory frequency.

7.5.2 Waveform Analysis:

RR measurements were obtained from respiratory waveforms in two ways. The first analysis method consisted of measuring the length of each full respiratory cycle in a waveform. As demonstrated in Figure 7.37a, respiratory cycles were measured between zero-crossings. The average of all cycle intervals in a 1-minute waveform was used to calculate a RR measurement in breaths-per-minute.

The second analysis method was an assessment of the waveform's frequency. A 4,500-point FFT was applied to the 60-second (75 s/s) respiratory waveform, as shown in Figure 7.37b. The resolution of the transform was 0.0167 Hz, which allowed a RR measurement resolution of 1 breath-per-minute. The largest peak in the respiratory range of 0.05 – 0.7 Hz was located since it represented the predominant respiratory frequency for the 1-minute interval. The frequency of the peak was multiplied by 60 to obtain a RR measurement in breaths-per-minute.

Every respiratory waveform extracted from the PPGs was assessed using both analysis methods.

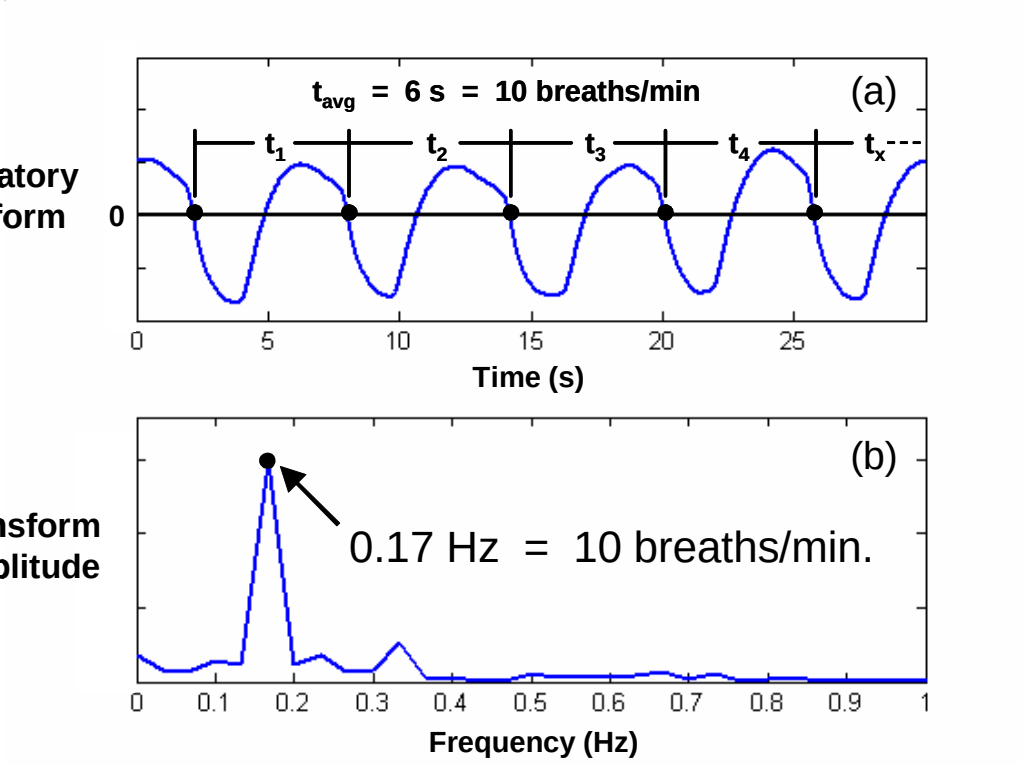

Figure 7.37. *Waveform analyses used to obtain RR values based on (a) cycle length measurements and (b) frequency transforms.*

7.5.3 PPG Baseline Modulations:

The PPGs recorded during the RR experiments were passed through the BPF described above to remove the DC component and isolate the respiratory-induced baseline modulations. The resulting respiratory waveforms were assessed using the two analysis methods described above. To evaluate accuracy, the RR measurements obtained from the PPGs were plotted against their reference values obtained through the BIOPAC, as shown in Figures 7.38 – 7.39.

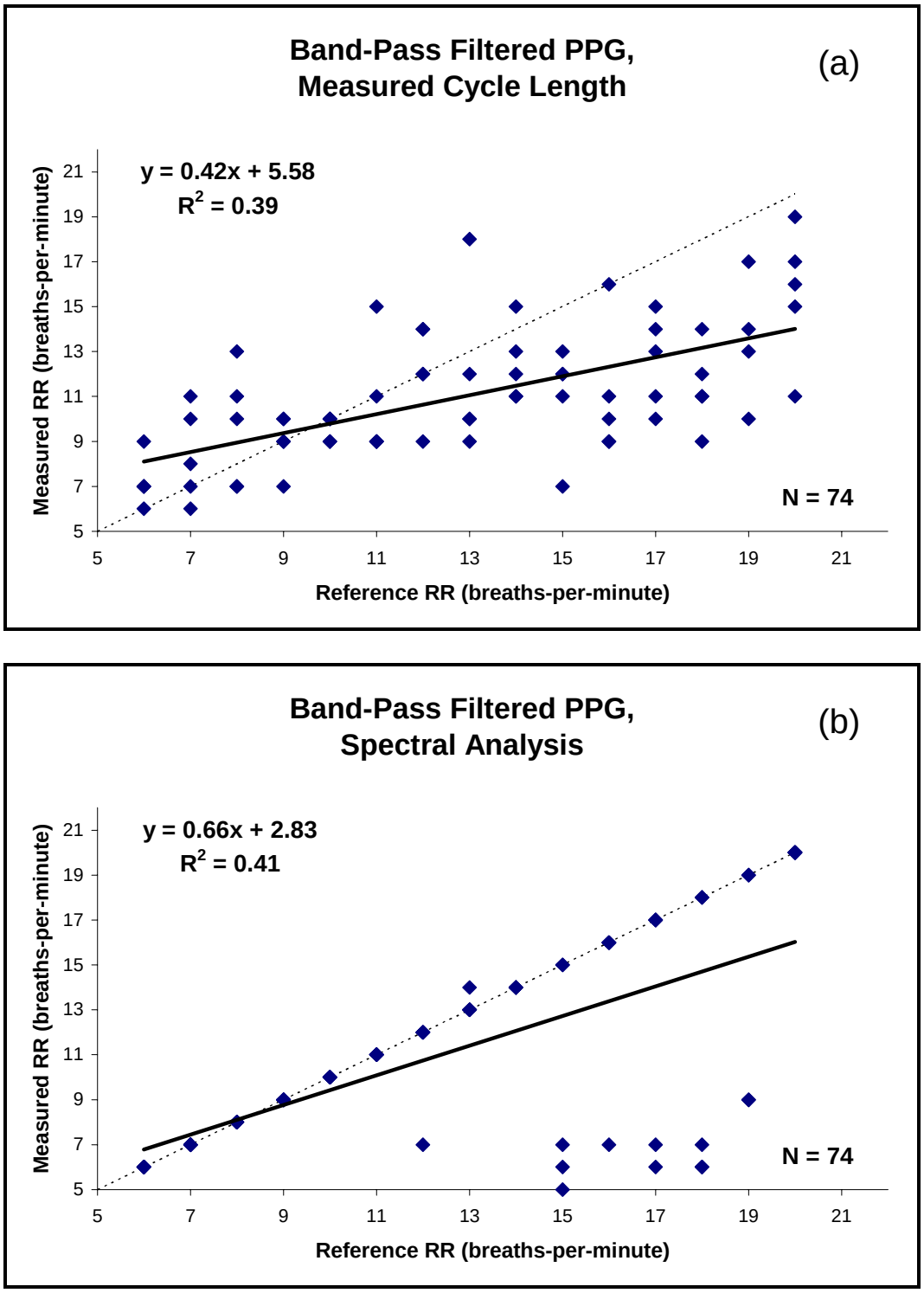

Figure 7.38. *RR measurements based on band-pass filtered PPG signals obtained using (a) measured cycle length and (b) spectral analysis, with resulting regression lines (—) and lines of identity (---).*

*Note: Due to discrete values, some data points are plotted on top of each other.

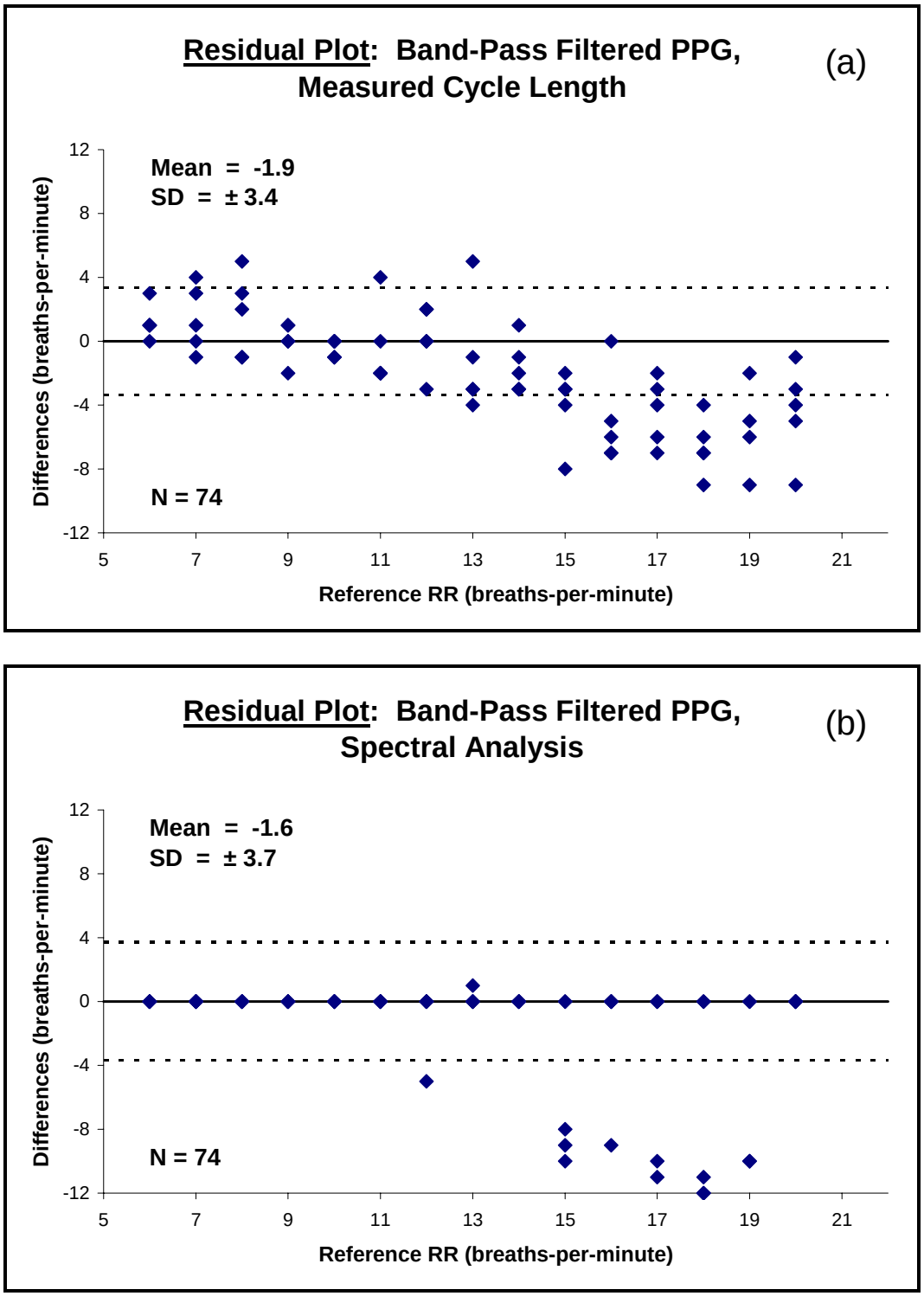

Figure 7.39. *Residual data plot from RR measurements based on band-pass filtered PPG signals obtained using (a) measured cycle length and (b) spectral analysis.*

*Note: Due to discrete values, some data points are plotted on top of each other.

7.5.4 PPG Pulse Envelope:

The positive peaks of the cardiac pulses in the PPGs were identified using derivatives. As shown in Figure 7.40, the tips of the peaks were connected using linear interpolation to produce signal envelopes based on the cardiac pulses. The envelopes were passed through the BPF to remove the offsets and smooth the waveforms. The resulting respiratory waveforms were assessed using the two analysis methods described above. To evaluate accuracy, the RR measurements obtained from the PPGs were plotted against their reference values obtained through the BIOPAC, as shown in Figures 7.41 – 7.42.

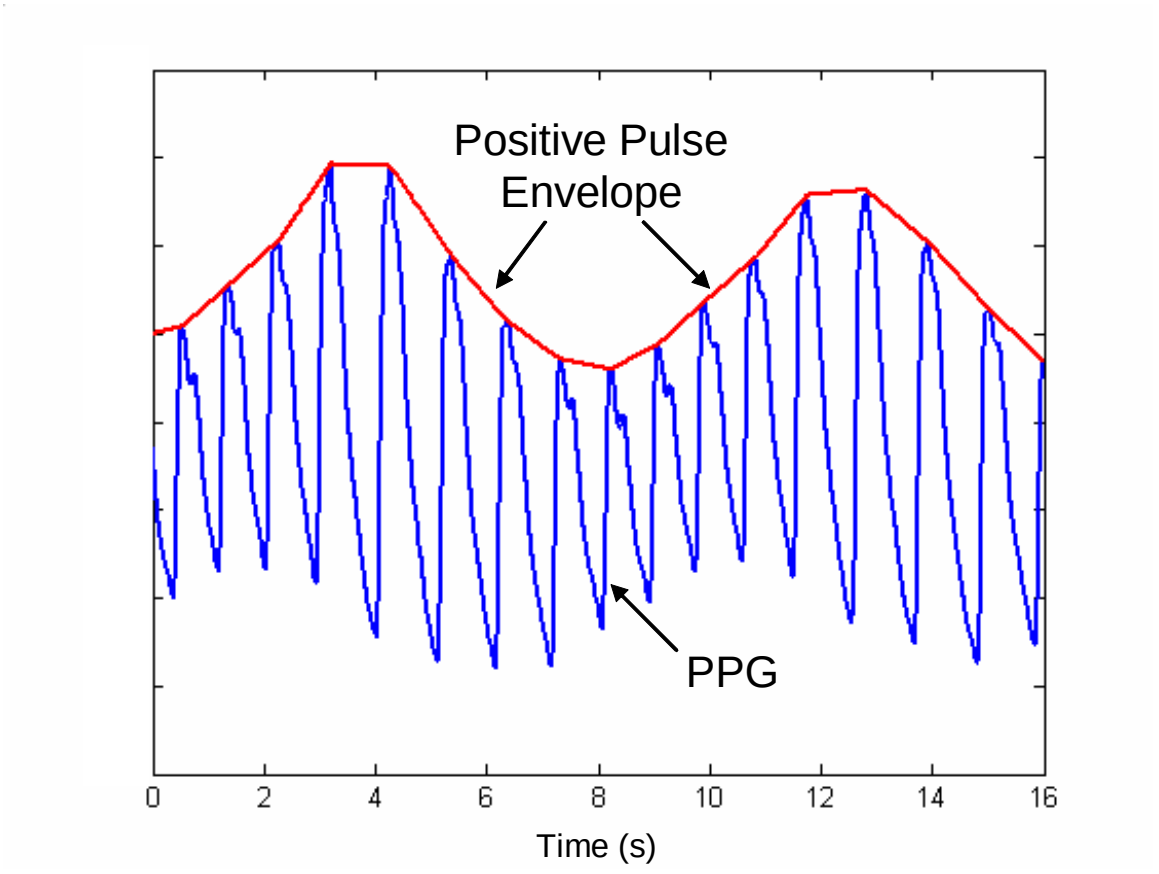

Figure 7.40. *PPG with positive pulse envelope derived from cardiac peaks.*

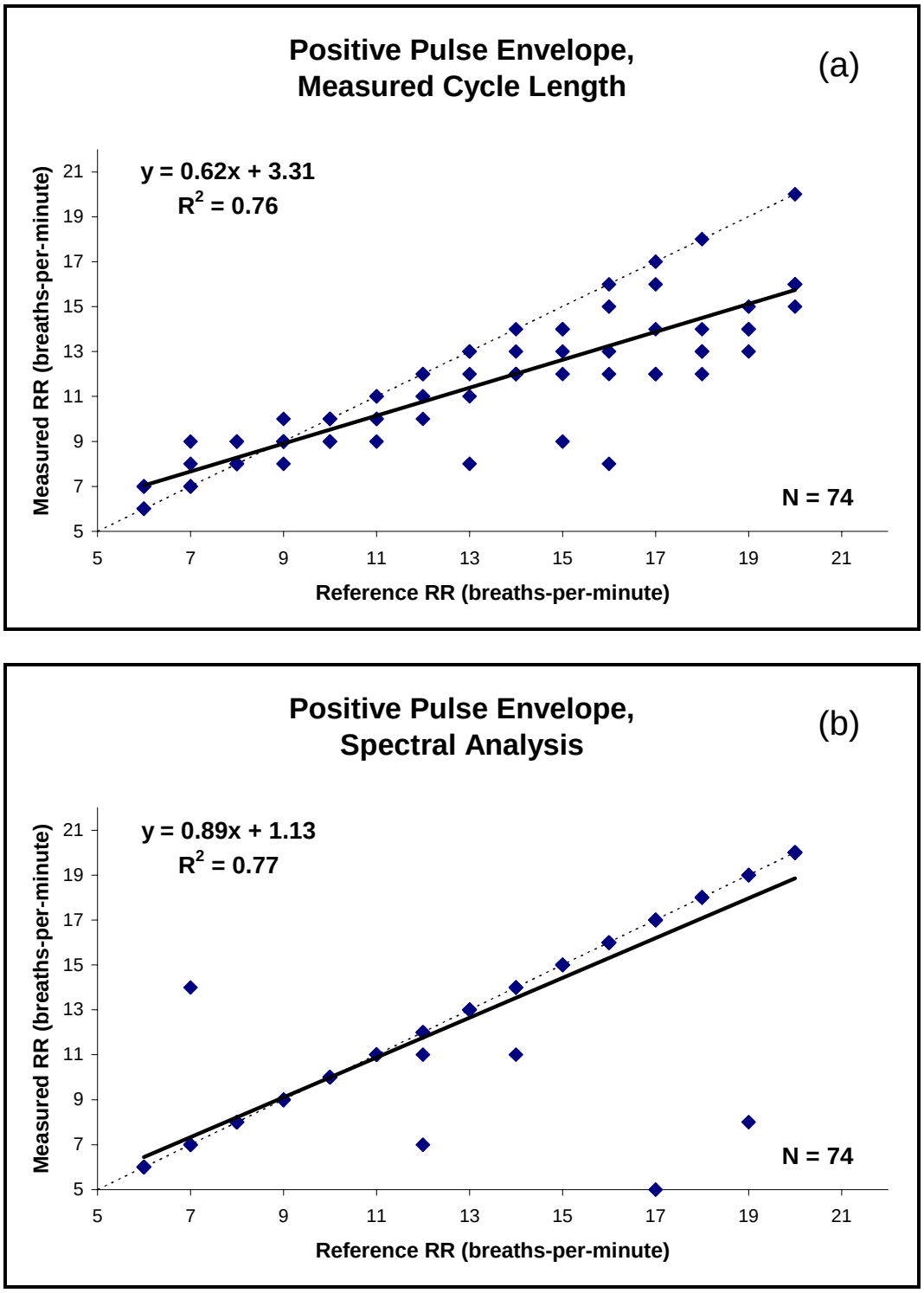

Figure 7.41. *RR measurements based on positive PPG pulse envelopes obtained using (a) measured cycle length and (b) spectral analysis, with resulting regression lines (—) and lines of identity (---).*

*Note: Due to discrete values, some data points are plotted on top of each other.

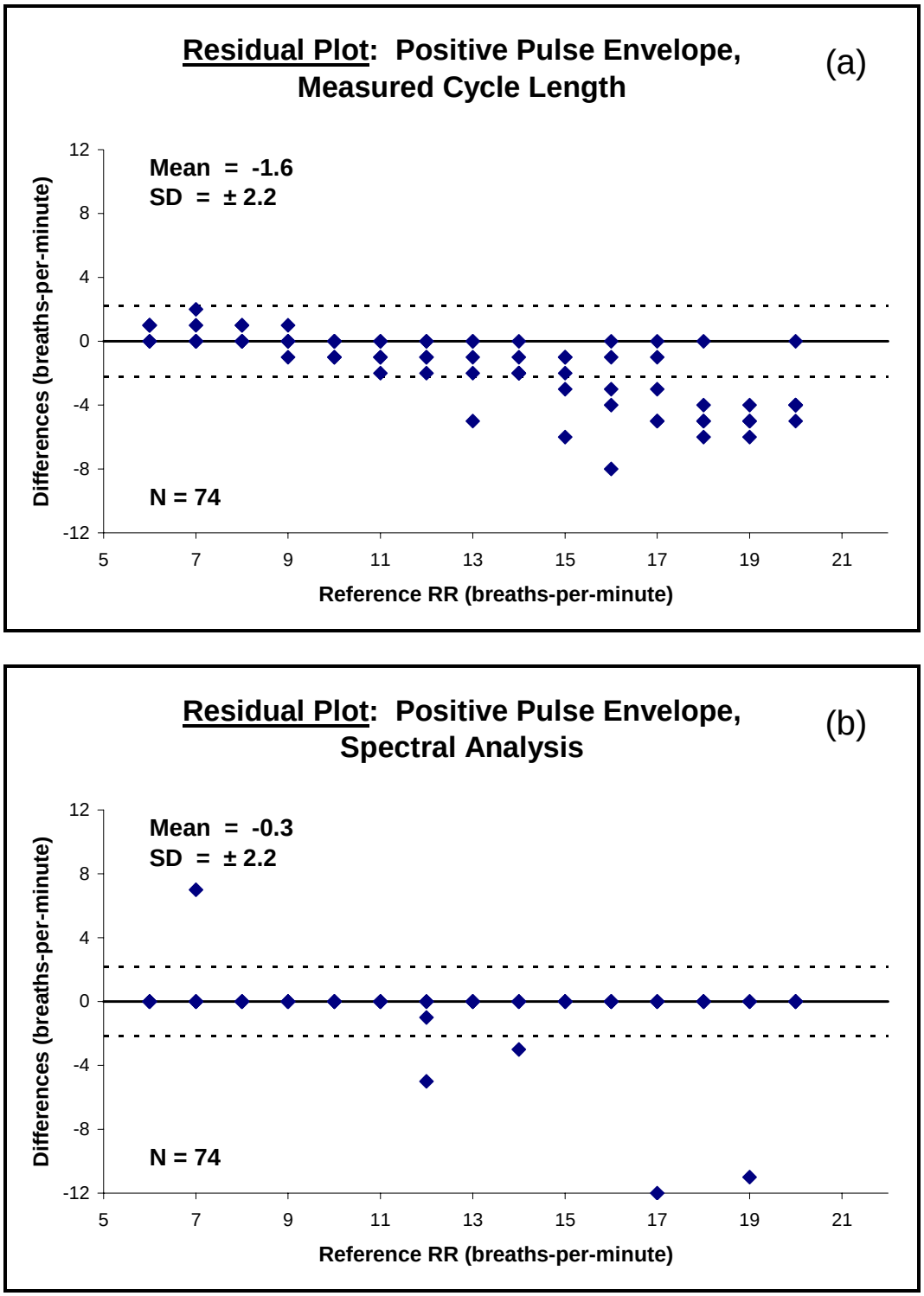

Figure 7.42. *Residual data plot from RR measurements based on positive PPG pulse envelopes obtained using (a) measured cycle length and (b) spectral analysis.*

*Note: Due to discrete values, some data points are plotted on top of each other.

7.5.5 Instantaneous Heart Rate (IHR) Fluctuations:

Signal derivatives were used to identify cardiac pulses in the PPGs, and IHR values were calculated for each pulse interval. The data points in each interval were assigned the interval's IHR value, producing a stepped waveform that fluctuated with HR, as shown in Figure 7.43. The stepped IHR waveform was passed through the BPF to remove its offset and smooth the sharp transitions. The resulting respiratory waveform was assessed using the two analysis methods described above. To evaluate accuracy, the RR measurements obtained from each data set were plotted against their reference values obtained through the BIOPAC, as shown in Figures 7.44 – 7.45.

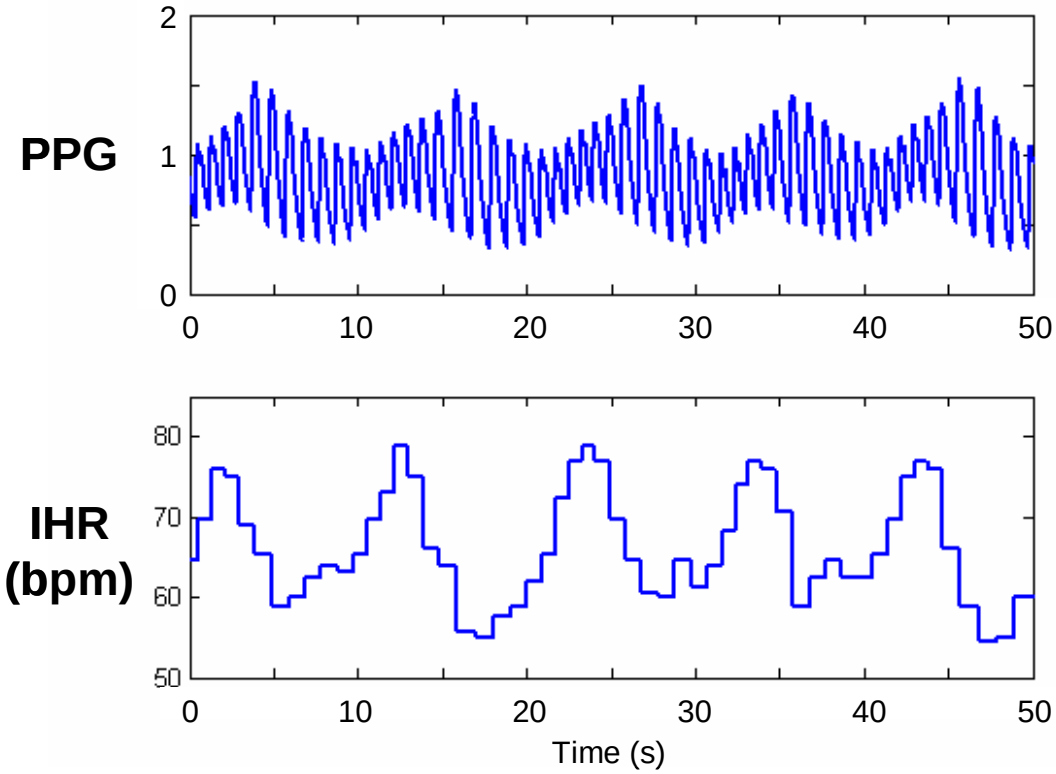

Figure 7.43. *PPG and corresponding IHR values.*

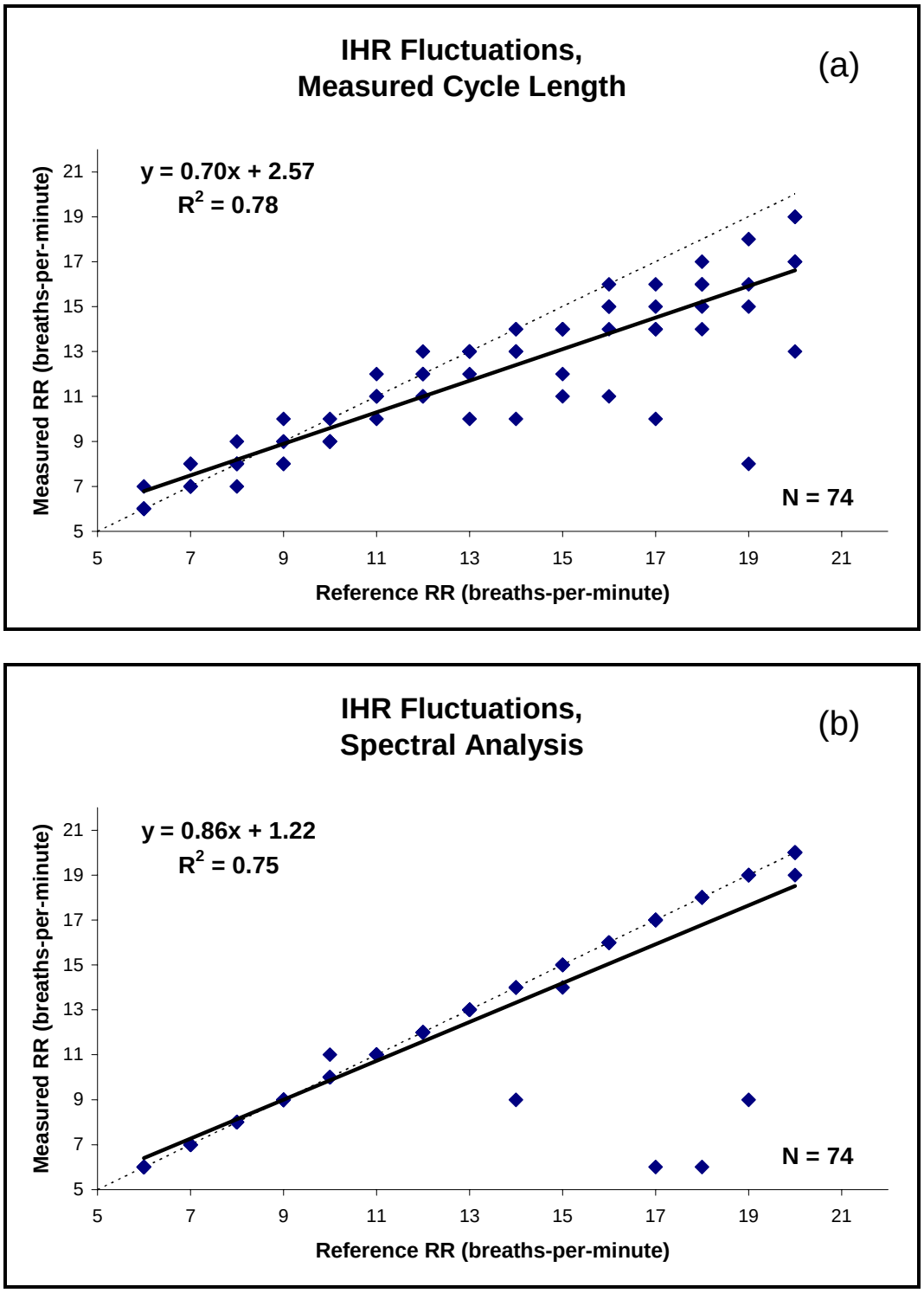

Figure 7.44. *RR measurements based on IHR fluctuations obtained using (a) measured cycle length and (b) spectral analysis, with resulting regression lines (—) and lines of identity (---).*

*Note: Due to discrete values, some data points are plotted on top of each other.

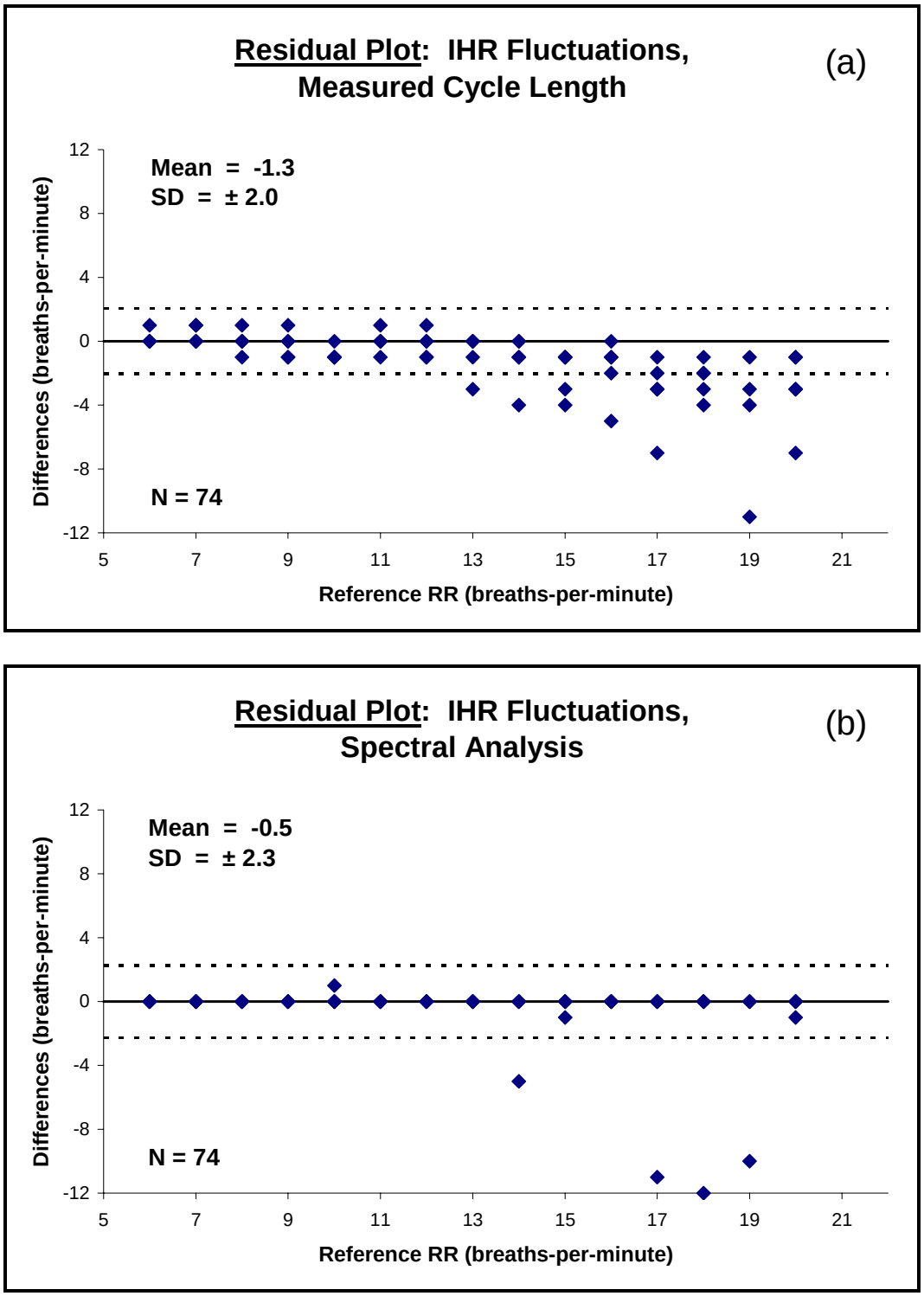

Figure 7.45. *Residual data plot from RR measurements based on IHR fluctuations obtained using (a) measured cycle length and (b) spectral analysis.*

*Note: Due to discrete values, some data points are plotted on top of each other.

Table 7.8. *Assessment results for RR processing methods.*

Signal Extraction	Analysis Method	R^2 Value	Bias (breaths-per-minute)	SEE (breaths-per-minute)
Band-Pass Filtered PPG	Cycle Length	0.39	-1.89	2.26
	Spectral Analysis	0.41	-1.57	3.37
PPG Pulse Envelope	Cycle Length	0.76	-1.58	1.50
	Spectral Analysis	0.77	-0.34	2.09
IHR Fluctuations	Cycle Length	0.78	-1.27	1.59
	Spectral Analysis	0.75	-0.53	2.17

8. DISCUSSION

8.1 SpO_2 Assessment

8.1.1 Measurement Response Times:

During assessment of the SpO_2 processing methods, a difference in the response times was noted when comparing the SpO_2 values provided by the processing methods to those obtained from the reference oximeter. As shown in Figure 8.1a, comparable drops in SpO_2 were registered between 5 and 20 seconds apart by the reference source and all the processing methods. This shift was attributed to two factors: differences in sensor locations and differences in processing technique.

Reference readings were obtained from a sensor attached to the finger while the processing methods assessed signals recorded from a sensor mounted on the forehead. Due to differences in the circulation between the heart and the two sensor sites, drops in SpO_2 occur earlier at the forehead compared to the fingertip due to differences in circulation transport.

Because of differences between software algorithms, the measurements produced by the reference source and the processing methods invariably responded at different rates to changes in SpO_2. An example of the differences in response times can be observed in Figure 8.1b around 150 seconds when the subject's SpO_2 levels returned to a normal level after a desaturation episode.

In order to accurately compare the SpO_2 measurements from the two sites, each pair of measurement sets were shifted to align the drops in SpO_2, as demonstrated in Figure 8.1b.

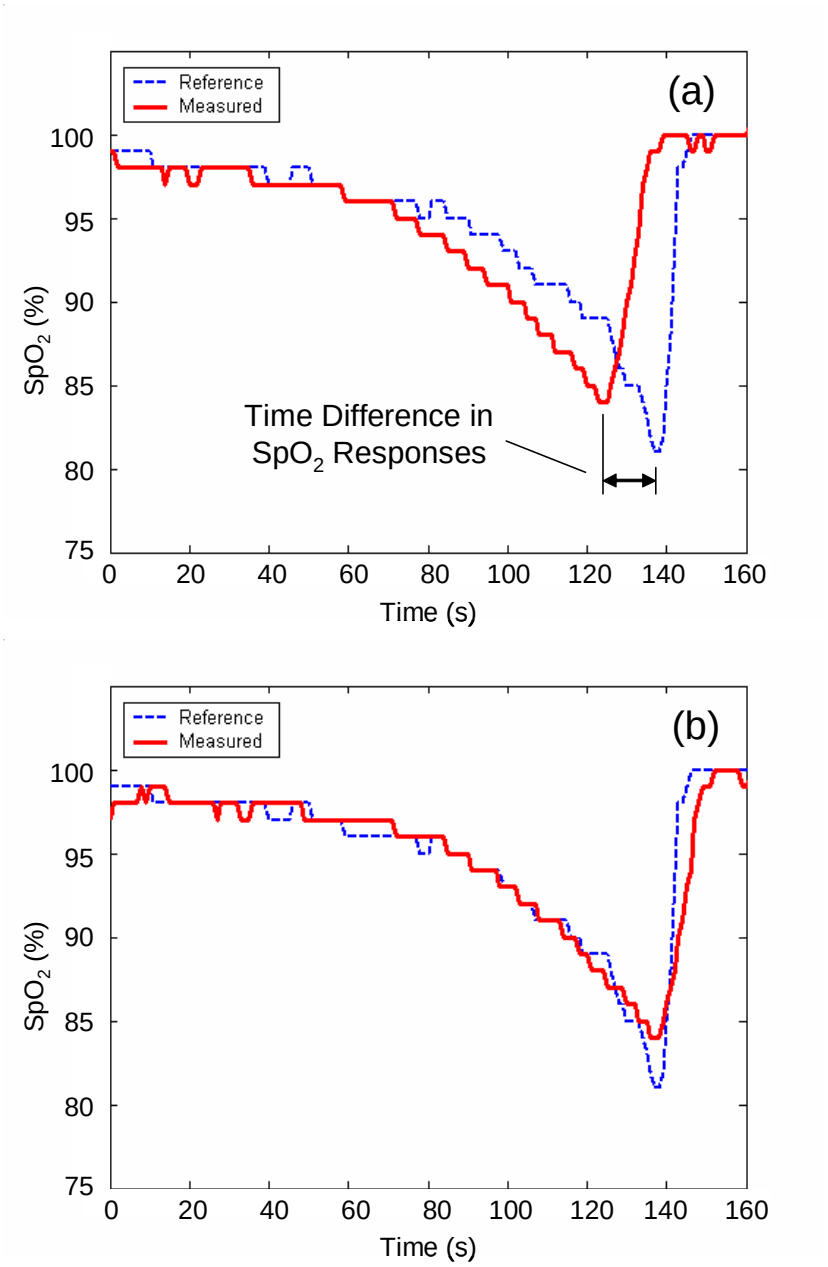

Figure 8.1. *Measured and reference SpO_2 values (a) as they are normally obtained in relation to each other and (b) after aligning the drops in SpO_2.*

Since dynamic changes in SpO_2 levels are difficult to match precisely between devices, accepted calibration procedures are based on comparing measurements obtained during steady-state conditions. A normal calibration setup consists of a subject monitored with the oximeter being calibrated, but also requires periodic arterial blood samples to be

analyzed simultaneously by a reference co-oximeter. To achieve hypoxemia, the percentage of inspired oxygen is controlled to induce a steady-state level change in SpO_2. Once the measurements from both devices are stable, the values are recorded and compared. By repeating this procedure, the measurements from two different devices can be accurately compared over a wide range of SpO_2 values without being affected by differences in sensor locations or measurement response times.

8.1.2 Reference Measurement Error:

For the preliminary SpO_2 experiments performed, the most appropriate reference source was a commercial pulse oximeter. It is important to note that the measurements obtained from the reference oximeter contained a certain error which is typically about ±2%. During analysis, the error introduced by the reference source and the error inherent in the specific algorithmic based measurements are not separable. This makes it difficult to precisely quantitate the accuracy of the SpO_2 processing methods that were tested. Future studies would need to consider the reference pulse oximeter inaccuracies in order to draw more definitive conclusions about the accuracy of each algorithm. In addition, steady-state, as opposed to transient, hypoxia studies should be conducted to better characterize the performance of each algorithm. As described in section *8.1.1*, these studies would consist of controlling inspired oxygen levels and obtaining periodic arterial blood samples, analyzed by a co-oximeter, to provide reference SpO_2 measurements.

8.1.3 Regression Analysis Index:

This processing method is somewhat unique in that it provides a measurement index instead of a typical ***R*** value [52-56]. Accordingly, as shown in Figure 3.7, a change in SpO_2 was correlated to a change in the slope of the regression line, where a steep slope

indicated high SpO_2 and vice versa. The slope can range from 0, when parallel with the x-axis, to an asymptote tending towards positive infinity, when parallel to the y-axis. Although neither of these extremes was possible, the relationship between the slope index and the SpO_2 values became very non-linear, making it difficult to derive a simple equation that would accurately approximate the relationship. Therefore, the slope was used to calculate the angle of the regression line from the x-axis. Using the regression angle, the index ranged between 0 and 90 degrees, allowing a simple equation to better approximate the relationship between the regression slope and SpO_2.

As demonstrated by this method, the calculation of an $\boldsymbol{R}$ value, derived using Equation 3.2, is not an absolute requirement when measuring SpO_2. Any index that changes proportionally with SpO_2 can potentially be employed when performing measurements.

8.2 HR Measurements

8.2.1 Window Instability:

The window-based processing method used in section 7.3 to identify the peaks of cardiac pulses produced some extremely high, exaggerated measurements. Upon closer examination of the PPG signals and the results in Figures 7.17 – 7.18, it was determined that the method was potentially unstable due to the adaptive property of the analysis window. The shape, frequency, and general form of cardiac pulses in PPGs can change over short periods of time. To account for these changes, specifically the frequency of the pulses, the width of the analysis window was adjusted after each identified peak to ensure that the next pulse could be better identified. Pronounced dicrotic notches, due to their shape, had the potential to be identified as pulse peaks, given the right conditions. Once a notch was detected as a peak, the adaptive window would shrink under the pretext of a faster HR. This, in turn, enhanced the sensitivity of the peak detection and increased the chances of identifying the following dicrotic notch as a pulse, perpetuating an unstable cycle. During periods of incorrect peak identification, as shown in Figure 8.2, the HR was estimated to be approximately twice its actual rate. As observed in the results, inaccurate measurements ranged as high as twice the reference values and were due almost exclusively to the detection of dicrotic notches.

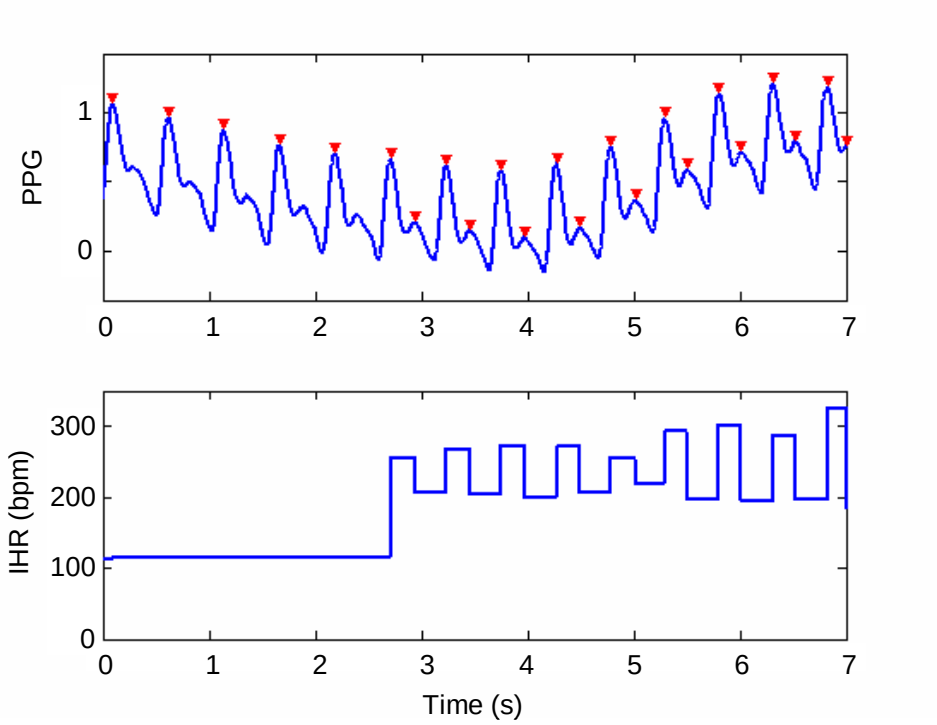

Figure 8.2. *A PPG signal (top) and its corresponding IHR values (bottom) as measured using the adaptive window method. Points identified as peaks are indicated by the arrows (▼). Note the point at 3 seconds when the dicrotic notch is first mistakenly identified as a pulse peak.*

8.2.2 Inaccuracy of Spectral Analysis:

The cardiac components in the PPG signals were very strong and prominent and were expected to generate an obvious peak in the FFT. Therefore, the unexpected inaccuracy of HR measurements provided through spectral analysis prompted further investigation. An individual's IHR naturally fluctuates over time, even between consecutive beat intervals. These IHR fluctuations can be generated by a variety of sources including pulmonary activity, physical exertion, or even mental stress. The constant fluctuations in IHR caused the power in the cardiac portions of the PPGs to spread across multiple frequencies, as seen in Figure 7.22 between 0.8 and 1.2 Hz. While identification of the most prominent cardiac peak in the FFT was relatively simple, the frequency did not

necessarily correspond to the average HR. As a result, the spectral-based measurements shown in Figures 7.23 – 7.24 did not provide acceptable accuracy when paired with their reference HR values.

However, the trend of the results supports a high correlation between measured HR and reference HR, despite the unexplained reduction in accuracy between 80 and 90 bpm. Further work on spectral-based analysis could potentially improve HR measurement accuracy and allow this method to provide more accurate results.

8.3 HRV Index Accuracy

It is easily observed that the PPG waveform is strongly influenced by cardiac activity and contains much information that is also present in ECG signals. As such, HR measurements and HRV indices can be extracted from the PPG waveform. However, the results in section 7.4 showed that some HRV indices measured from the PPGs contained significant errors. Typically, most inaccurate measurements based on the PPGs estimated higher values than the reference values provided by the ECGs. Since the cardiac pulses were correctly identified in all PPG signals, it was concluded that an additional source of variance was present in the waveforms and not the methods of measurement. This additional variance was attributed to the cardiovascular factors that shape the cardiac pulse in the PPG.

The QRS complexes in ECG signals contain very distinct R-waves. The sharp nature of the periodic R-waves provides a means of accurately measuring the duration of each beat interval. The shapes of the corresponding PPG pulses, however, are much more rounded as they are reflections of pressure waves and changing blood volumes. As

depicted in Figure 3.8, a delay occurs between the R-wave in an ECG and the corresponding pulse peak in a PPG. This delay is the combined result of two physiological events. First, immediately following depolarization, the heart contracts and ejects blood from the left ventricle into the arterial pathways. This mechanical contraction is not instantaneous and occurs over a short period of time. A further delay between R-wave and PPG pulse is incurred as the pressure wave from the ejected bolus of blood traverses the systemic vasculature. It is the physiological state of the cardiovascular pathways that is most likely to induce additional fluctuations in the beat-to-beat intervals of a PPG waveform. Factors such as arterial compliance, vasoconstriction, and vasodilation affect the speed at which the cardiac pressure wave moves through the systemic vasculature. Changes in the speed of the pressure wave in turn vary the delay between the R-wave and the corresponding PPG pulse. The end result is an additional source of variation that can be observed in PPG pulse intervals but is not present in ECG R-R intervals.

The nature of the above variance was reflected in the results of the HRV index measurements graphed in Figures 7.29 – 7.36. The HRV indices that were based on NN intervals (SDNN, COV) provided relatively accurate results, illustrating that the additional source of variation did not significantly affect the range of the NN intervals, as portrayed in Figure 8.3. Assessing the differences between successive NN intervals, which are also depicted in Figure 8.3, magnified the effects of the additional fluctuations. The indices based on these differences (SDSD, RMSSD, NN50, pNN50) repeatedly provided results that were higher than the corresponding reference indices that were based on ECGs.

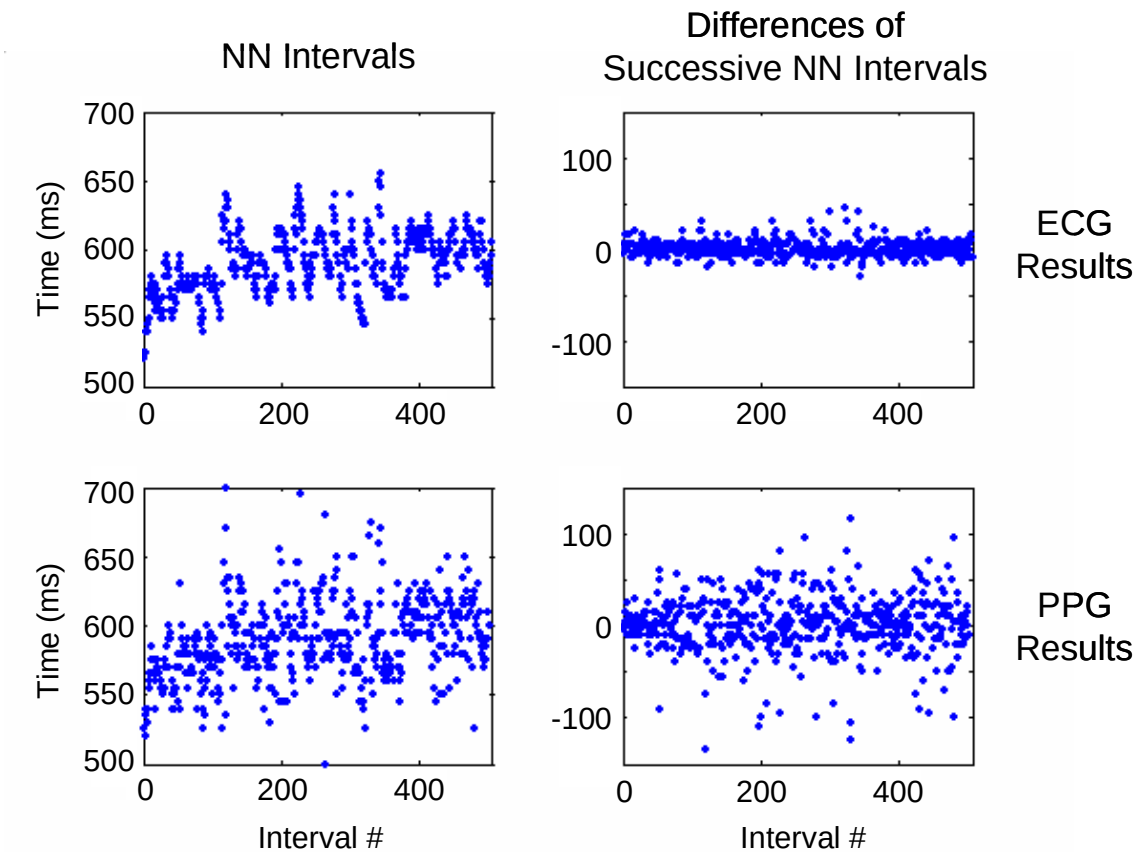

Figure 8.3. *A visual comparison between ECG and PPG measurements of NN intervals and successive differences of NN intervals. Note the increased variance present in the PPG measurements, especially in the successive differences.*

8.4 RR Measurement Degradation

In general, it was found that measurements at low RR values from about 6 to 12 breaths-per-minute were relatively accurate for all processing methods in section 7.5. Many results above 13 breaths-per-minute, however, were either inaccurate or showed significant variation between measurements. After closer examination of the respiratory and PPG waveforms, it was determined that the drop in measurement accuracy at higher RRs was most likely due to the voluntary increase in breathing rate performed during the experiments.

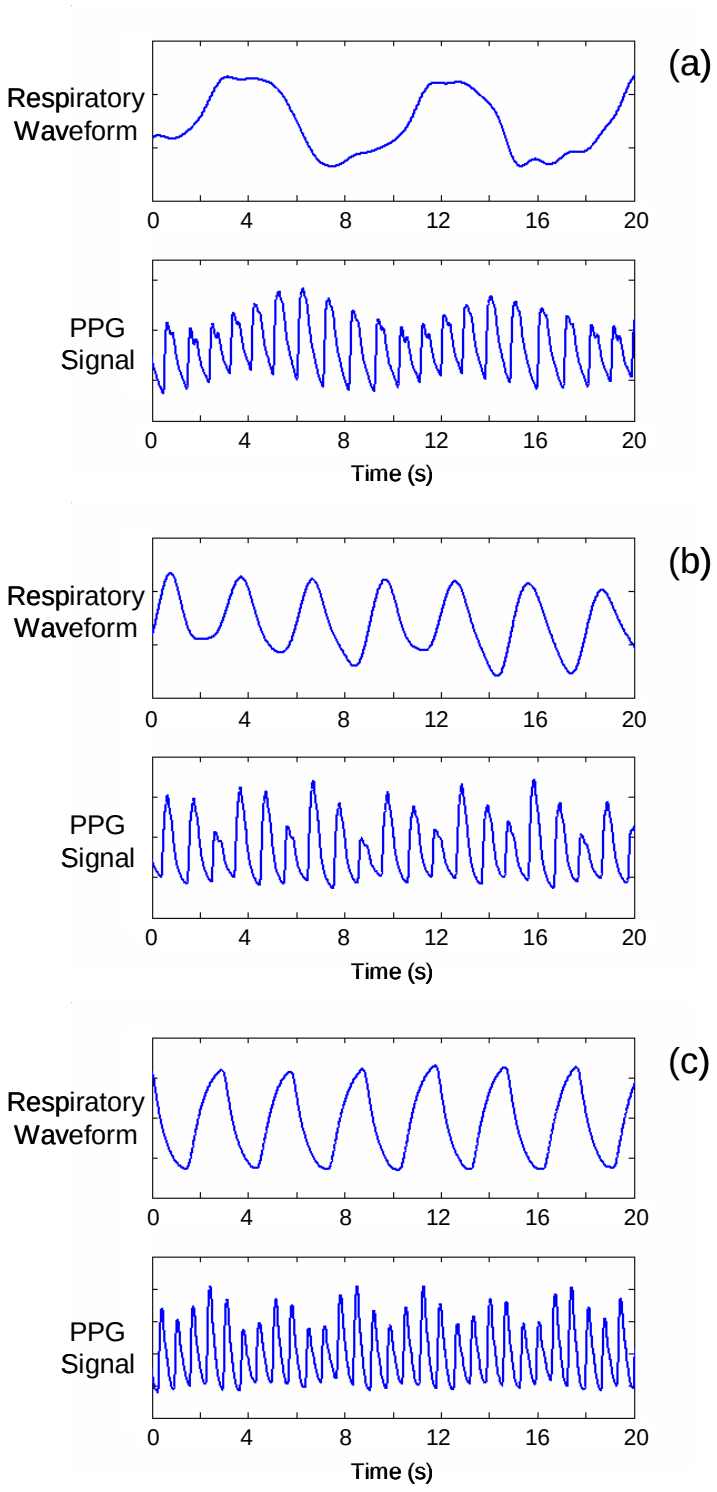

Figure 8.4. *Respiratory waveforms and corresponding PPG signals. (a) A low-frequency RR of 7 breaths-per-minute is easily observed in a PPG signal with a HR of 60 bpm. (b) A voluntary increase in RR to 20 breaths-per-minute is difficult to observe in a PPG with a HR of 60 bpm. (c) An increase in HR to 90 bpm due to physical exertion allows a RR of 20 breaths-per-minute to be more easily observed in the PPG.*

A natural increase in RR, through physical exertion for example, is often accompanied by a relatively proportional increase in HR [33], as demonstrated in Figure 8.4c. Since the form of the PPG is a product of cardiovascular activity, an increase in cardiac output allows respiratory influences to propagate through the vasculature more efficiently. A voluntary increase in RR, as performed in the data recording experiments and shown in Figure 8.4b, did not necessarily demand a similar increase in HR. The comparably lower degree of cardiac activity transferred the respiratory influences less efficiently through the vasculature. The result was a reduction in the observable effects of pulmonary activity on the PPG and a corresponding drop in RR measurement accuracy.

8.5 Regression Analyses

It was originally anticipated that the reference values and the measurements from the processing methods would have linear relationships for all 4 types of physiological measurements. However, data trends were observed in several results plots that suggested non-linear relationships could be present. Therefore, results from alternative regression analyses were examined to determine if different equations could better describe the relationships observed in the data.

In addition to the linear analyses, exponential, logarithmic, power, and polynomial regression curves were fitted to the data sets from chapter 7. The results are summarized in Tables 8.1 – 8.4.

8.5.1 SpO2 Regression Results:

Although a number of the measurement sets appeared to be non-linear to the extent of requiring a 4^{th}-order equation, the SpO_2 regression results in Table 8.1 did not show

many significant differences between the linear analyses and the alternative analyses. The data sets from the window-based measurements did demonstrate slightly better regression approximations using 4th-order polynomial equations. However, as the order of a polynomial equation increases, there is a greater chance of inadvertently justifying inaccurate or incorrect measurements. In addition, without performing proper calibration procedures as outlined in section *8.1.1*, hysteresis can potentially cause abnormal relationships to be observed between the reference values and measured values in a data set. Considering these factors, the regression equations used to approximate the SpO_2 results should be limited to lower-order (1st or 2nd) polynomials following a proper calibration procedure.

Table 8.1. *R^2 values from regression analyses of SpO_2 measurement results.*

AC	DC	Exponential	Logarithmic	Power	Polynomial			
					Linear	Order 2	Order 3	Order 4
Diff.	Avg.	0.96	0.96	0.96	0.96	0.96	0.96	0.97
	LPF	0.97	0.97	0.97	0.97	0.97	0.97	0.97
	Wind.	0.96	0.96	0.96	0.96	0.96	0.96	0.97
Pulses	Avg.	0.97	0.97	0.97	0.97	0.97	0.97	0.97
	LPF	0.97	0.97	0.97	0.97	0.97	0.97	0.97
	Wind.	0.97	0.97	0.97	0.97	0.97	0.97	0.97
Regr.	Avg.	0.93	0.92	0.92	0.92	0.94	0.95	0.95
	LPF	0.96	0.95	0.96	0.96	0.96	0.96	0.96
	Wind.	0.96	0.95	0.96	0.95	0.96	0.96	0.96
Wind.	Avg.	0.89	0.89	0.89	0.90	0.91	0.93	0.94
	LPF	0.90	0.90	0.89	0.90	0.91	0.93	0.94
	Wind.	0.89	0.89	0.89	0.89	0.90	0.93	0.94
Spec.	Spec.	0.96	0.96	0.96	0.96	0.96	0.96	0.97

8.5.2 HR Regression Results:

The HR regression results in Table 8.2 also showed very few significant differences between the linear analyses and the alternative analyses. The results for the window-

based processing method did show a supposed exponential or power relationship between the measured and reference values. However, based on the examinations in section *8.2.1*, these two forms of regression were most likely influenced by the method's instability issues that appeared at elevated HRs.

Table 8.2. *R^2 values from regression analyses of HR measurement results.*

Methods	Exponential	Logarithmic	Power	Polynomial		
				Linear	Order 2	Order 3
Window	0.74	0.64	0.75	0.64	0.64	0.66
Derivative	0.98	0.98	0.99	0.99	0.99	0.99
Spectral	0.89	0.88	0.89	0.90	0.91	0.91

8.5.3 HRV Regression Results:

The HRV regression results in Table 8.3 showed some mixed results. First, regression estimations for the SDNN and COV index measurements did not improve beyond that of the linear equations. Second, the results for the SDSD and RMSSD indices appeared to be better approximated with a power-based equation. Third, a slight improvement in regression estimation was observed with 3rd-order polynomial equations for the NN50 and pNN50 indices. It should be noted that due to a number of values occurring at zero, the regression equations for these final two indices could not be approximated using logarithmic- or power-based equations.

Table 8.3. *R^2 values from regression analyses of HRV measurement results.*

Indices	Exponential	Logarithmic	Power	Polynomial		
				Linear	Order 2	Order 3
SDNN	0.90	0.81	0.96	0.97	0.97	0.97
COV	0.92	0.81	0.94	0.97	0.97	0.97
SDSD	0.72	0.59	0.73	0.68	0.68	0.69
RMSSD	0.72	0.59	0.73	0.68	0.68	0.69
NN50	0.59	---	---	0.71	0.72	0.74
pNN50	0.58	---	---	0.75	0.76	0.77

8.5.4 RR Regression Results:

The RR regression results in Table 8.4 also showed variations in its assessments. The 3 measurement sets analyzed in the time domain appeared to be best characterized using power regression equations, while the 3 measurement sets analyzed in the frequency domain were best estimated with their original linear equations.

Table 8.4. *R^2 values from regression analyses of RR measurement results.*

Waveform	Analysis Method	Exponential	Logarithmic	Power	Polynomial		
					Linear	Order 2	Order 3
BPF	Time	0.41	0.39	0.43	0.39	0.39	0.43
	Freq	0.34	0.41	0.36	0.41	0.41	0.47
Envelope	Time	0.77	0.75	0.80	0.76	0.76	0.76
	Freq	0.70	0.74	0.72	0.77	0.77	0.77
IHRs	Time	0.78	0.79	0.82	0.78	0.79	0.79
	Freq	0.69	0.74	0.73	0.75	0.75	0.75

8.6 Comparisons to Clinical Standards

8.6.1 Clinical Standards:

In order to be considered for implementation in a medical device, the accuracy of a processing method first had to be acceptable from a clinical standpoint. Since the SEE reflected the standard amount of error present in a set of results, it was compared to the measurement's clinically acceptable error to determine whether a given processing method was a viable option for use in a wearable pulse oximeter.

The clinically acceptable accuracies for the physiological measurements are typically ±2% for SpO_2 [28, 42, 44], ±4 bpm for HR [33, 43], and ±4 breaths-per-minute for RR [33, 43]. Since there is currently no universally employed index for measuring

HRV [79], no specific measurement accuracy is considered the standard for clinical acceptance. Therefore, the results from Student's t-tests were examined to assure that the HRV indices based on the PPGs demonstrated a high degree of correlation with the reference values. Table 8.5 summarizes the evaluation results that determined which processing methods provided clinically acceptable measurements.

8.6.2 SpO_2 Reference Accuracy:

Since invasive clinical experiments and calibration procedures were not feasible during preliminary testing, a standard commercial pulse oximeter (Nonin Xpod®) was employed as a reference source to characterize the SpO_2 measurement methods being examined. However, as mentioned previously, measurements provided by the reference oximeter contained a certain degree of error and were only accurate to ±2%. For a given SpO_2 value, the maximum difference between clinically viable measurements from the reference source and the processing method would therefore occur if one source estimated high by 2% while the other estimated low by 2%. As a result, clinically valid processing methods could potentially produce as much as a 4% difference from the reference measurements. Therefore, all methods with an accuracy of less than 4% were considered potentially viable options and were included in the compiled software library.

8.6.3 Comparison Results:

The 13 methods evaluated for measuring SpO_2 all provided accuracies of less than ±4%, indicating that they were all potentially viable options for implementation. However, measurements based on signal differentials and pulse amplitudes showed the best accuracy under laboratory conditions.

Table 8.5. *Evaluation of processing methods for clinical acceptability.*

Measurement Methods		Minimum Clinical Accuracy	Method Accuracy	Viable Measurement Technique?
SpO_2				
Differentials	Averaging	± 2 % (± 4 %)*	0.84	Yes
	LPF		0.82	Yes
	Window Min.		0.91	Yes
Pulse Amplitudes	Averaging		0.82	Yes
	LPF		0.91	Yes
	Window Min.		0.81	Yes
Regression Analysis	Averaging		1.37	Yes
	LPF		1.11	Yes
	Window Min.		0.96	Yes
Windowed Analysis	Averaging		1.38	Yes
	LPF		1.41	Yes
	Window Min.		1.44	Yes
Spectral Analysis	Spectral Analysis		0.84	Yes
HR				
Moving Window		± 4 bpm	15.48	No
Signal Derivative			1.27	Yes
Spectral Analysis			4.98	No
HRV				
SDNN		$p > 0.05$	$p > 0.05$	Yes
COV			$p > 0.05$	Yes
SDSD			$p > 0.05$	Yes
RMSSD			$p > 0.05$	Yes
NN50			$p > 0.05$	Yes
pNN50			$p > 0.05$	Yes
RR				
Band-Pass Filtered PPG	Cycle Length	± 4 breaths-per-minute	2.26	No ($p < 0.05$)
	Spectral		3.37	No ($p < 0.05$)
Positive PPG Pulse Envelope	Cycle Length		1.50	Yes
	Spectral		2.09	Yes
IHR Fluctuations	Cycle Length		1.59	Yes
	Spectral		2.17	Yes

* The measurement accuracy of the reference oximeter was ±2%. Valid measurement methods could therefore potentially show a 4% difference from the reference measurements and still provide acceptable accuracy from a clinical standpoint.

The results from the evaluations of the HR processing methods revealed that the moving window and spectral analysis methods produced significant amounts of error that resulted in unacceptable accuracies. SEE values of 15.5 and 5.0 for the window and spectral methods, respectively, were above the clinically desirable accuracy of 4 bpm. As a result, these methods were deemed inappropriate for clinical use and were not considered viable options for performing HR measurements in a pulse oximeter. Only the method based on signal derivatives provided acceptable measurement accuracy.

The 6 HRV indices extracted from the PPG waveforms all provided results that correlated significantly with the reference measurements.

Of the 3 respiratory waveforms extracted from the PPGs, the baseline modulations obtained using the BPF produced very low degrees of accuracy. Although the average measurement accuracy was within acceptable limits, the measured RR values were found to be significantly different from the reference RR values ($p < 0.05$). As a result, baseline modulations obtained from a BPF were deemed inappropriate for accurately assessing respiratory activity and were not considered viable options for performing RR measurements in a pulse oximeter. Conversely, the positive pulse envelopes and IHR fluctuations provided relatively high degrees of accuracy that were within the clinically acceptable margin of error and showed no significant differences from the reference values.

8.7 Expanding Upon the Research Results

8.7.1 Results Limitations:

The results derived from this research fulfilled a crucial step in the development of a wearable pulse oximeter platform. However, these results cover a limited amount of knowledge which further studies must expand upon. Specifically, this work characterized the accuracies of different processing methods in a controlled laboratory setting from healthy subjects mostly during resting conditions.

The study has characterized signal processing methods across a limited range of physiological conditions. Specifically, SpO_2 measurements were examined over the range of 85% – 100%, HR was assessed from approximately 60 – 115 bpm, and RR was evaluated between 6 – 20 breaths-per-minute. These ranges are typically observed in normal, healthy individuals at rest or during light physical activity. However, measurements can fall outside of these ranges as a result of injury, abnormal health conditions, or more intense physical activities.

The conditions in which experiments were performed were limited in scope. All activities took place in a controlled laboratory setting which was optimal for acquiring strong, stable PPG signals that allowed for the most accurate measurements to be attained. Although these conditions are satisfactory for the initial evaluations of different signal processing algorithms, they are not sufficient for evaluating each method during conditions that would normally be encountered during field-based applications. Low signal-to-noise ratios (SNR) or signal artifacts created by excessive motion or improper sensor attachment, for example, can degrade measurement accuracy during field testing.

Lastly, the diversity and number of subjects tested were also limited. Since subjects were healthy and provided strong, clean PPG signals, the results observed did not accurately reflect the potential differences between individuals of a larger group. For example, low blood pressure or a significant reduction in peripheral perfusion during shock can reduce the strength, and subsequently the SNR, of the PPG signals. Consequently, a reduction in signal quality can affect measurement accuracy.

8.7.2 Further Experiments:

Further experiments will be required to characterize the limits of the processing methods. Firstly, evaluations in a controlled setting should be performed so that each method can be evaluated over a wider range of physiological values that might be encountered on the battlefield or during other relevant applications. For example, low SpO_2 values around 60%, HRs ranging between 30 – 300 bpm, and RRs between 3 and 40 braths-per-minute should be considered.

Secondly, each algorithm must be evaluated when PPG signal quality has deteriorated. For example, experiments should be conducted to investigate the effects of various degrees of motion artifacts generated during walking, crawling, climbing, jogging, or running.

8.8 Considerations for Future Method Selections

During normal monitoring situations, the software algorithms in a wearable pulse oximeter are likely to encounter signals that have been corrupted by motion artifacts or degraded due to poor physiological conditions. While methods should be employed to minimize the effects of motion disturbances prior to analysis, algorithms that are capable

of providing accurate measurements during unfavorable conditions could extend the usefulness of a wearable device, allowing it to provide relevant physiological information over a more diverse range of monitoring situations. A number of processing methods evaluated in this research are known to be robust and can potentially provide adequate accuracy in the presence of degraded or corrupted PPG signals.

Signal differentials, pulse amplitudes, and window-based analyses perform measurements based on amplitude differences. Therefore, these methods are potentially more susceptible to signal corruptions that induce amplitude variations in the PPG signals. The regression [53, 54] and spectral [42] analyses, on the other hand, have been shown to be inherently insensitive to certain degrees of signal degradation such as short duration motion artifacts.

Although the analysis of signal derivatives was the only processing method to provide clinically acceptable results for HR measurements, the technique is highly susceptible to motion artifacts and sudden shifts in signal level. Conversely, the accuracy of spectral analysis was not quite within clinically acceptable standards, but its processing technique can potentially provide stable measurements in the presence of short-term artifacts and disruptive events [44]. Further work on improving the accuracy of this frequency-based method could allow a more robust algorithm to be implemented for measuring HR in a wearable pulse oximeter.

The SDNN and COV indices appeared to produce more accurate, stable HRV measurements than other indices, most likely due to their relative insensitivity to additional fluctuations introduced by the cardiovascular system, as discussed in section 8.3. In addition, these indices are some of the more common short-term HRV

assessments used in clinical settings [71, 85] as they provide a general measure of variability in cardiac function as opposed to specifically reflecting parasympathetic activity or vagal tone.

Spectral analysis can potentially provide improved RR measurement stability in the presence of partially corrupted PPG waveforms. Although frequency-based analyses were less accurate than time-based analyses, we found that measurement inaccuracies were still clinically acceptable, and stable results over a wider range of monitoring conditions could prove to be a greater benefit since the measurements remain accurate. The assessment of IHR fluctuations is also recommended over the extraction of positive pulse envelopes, since the latter method is much more susceptible to PPG amplitude changes.

9. CONCLUSIONS AND RECOMMENDATIONS

Acquiring accurate physiological measurements from patients is vital to providing effective triage and medical care in the field. As a result, the proper selection of a set of accurate processing methods is paramount in the development of a wearable medical device designed for field-based applications. This research evaluated different processing methods as a means of performing multiple physiological measurements based on a single set of photoplethysmograms acquired by a non-invasive wearable pulse oximeter.

Arterial oxygen saturation, heart rate, heart rate variability, and respiration rate were assessed in this research since these measurements provide vital physiological information to caregivers during medical evaluations. A series of *in vivo* experiments were conducted to record photoplethysmographic waveforms and corresponding reference values for these 4 types of physiological measurements. The data were then used to characterize the accuracies of the processing methods evaluated during the study.

Since a number of resulting data trends between sets of measured and reference values did not always appear to be linear, alternative regression equations were applied to the data sets to determine what form of equation best estimated the data's relationship. It was found that arterial oxygen saturation measurements were best approximated with 1st (linear) and 2nd order polynomial regression equations, although proper calibration procedures must be performed prior to finalizing the equations. Derivative and spectral analysis methods employed to measure heart rate were best described with their original linear equations, while window-based analyses appeared to provide measurements that displayed a power relationship. For heart rate variability index measurements, most data

sets (SDNN, COV, NN50, pNN50) retained the use of linear equations for describing their regression curves. The data from the SDSD and RMSSD indices, however, appeared to be better described with power equations. Respiration rate measurement sets produced two distinct results. Time-based measurements were better approximated with power equations, while frequency-based measurements were described most accurately with linear equations.

Processing methods that provided clinically acceptable accuracies during controlled conditions were identified as techniques that could potentially be implemented in a wearable pulse oximeter. A low degree of accuracy or correlation with reference measurements indicated that a particular method was not suitable for clinical use. Thirteen processing methods based on signal differentials, pulse amplitudes, regression slopes, windowed analysis, and spectral analysis achieved potentially acceptable levels of accuracy when measuring arterial oxygen saturation (standard clinical accuracy: ±2%). Due to measurement inaccuracies, 2 of the 3 methods examined for performing heart rate measurements were clinically unacceptable. The remaining method, based on signal derivatives, provided clinically acceptable heart rate measurements extracted from the photoplethysmographic waveforms (standard clinical accuracy: ±4 bpm). However, further work regarding spectral-based heart rate analysis could improve the algorithm's accuracy and provide stable measurements in the presence of corrupted signals. Based on assessments using Student's t-test ($p < 0.05$ was considered significant), 6 heart rate variability indices, 2 based on the lengths of beat intervals and 4 based on differences between successive beat intervals, were accurately extracted from the PPG signals for the purpose of characterizing heart rate variability. Lastly, respiration rate measurements

obtained from photoplethysmogram baseline modulations did not produce a significant correlation with reference values, so were not considered suitable for providing measurements during clinical applications. The remaining 4 processing methods, based on positive pulse envelopes and instantaneous heart rate fluctuations, did provide acceptable clinical accuracy for respiration rate measurements (standard clinical accuracy: ±4 breaths-per-minute).

Since the primary goal of the wearable pulse oximeter being developed at WPI is deployment in field applications, a broad range of monitoring conditions will be common during use. Therefore, it is recommended that additional evaluations be performed to further characterize the measurement accuracies of the processing methods in non-laboratory conditions, including situations where distorted or noisy PPG signals are acquired. Motion artifacts, for example, can cause measurement accuracies to become clinically unacceptable, and their effects on the robustness of processing methods must be examined. Methods should then be developed to prevent or minimize these detrimental effects before they cause the results of the physiological measurements to deteriorate to unacceptable levels. Improved sensor attachment techniques or adaptive filtering, for example, can potentially be used to improve physiological measurement accuracy in field-based applications.

Although the miniaturized wearable pulse oximeter developed in our lab has been optimized for physical size and power, further evaluations must be conducted to understand the limitations of each signal processing method in terms of suitability for implementation in a microcontroller environment. Preliminary assessments of processing requirements suggest that the measurement algorithms will require a minimum amount of

resources. Program memory does not appear to be the limiting factor, since, on average, each method will require approximately 2KB of space. However, extensive data memory may be required. First, about 2KB of RAM will be necessary for retaining raw PPG data during analysis. Additionally, each implemented algorithm will require approximately 100 bytes for basic processing procedures. If a Fast Fourier Transform is implemented to perform spectral analysis, additional data memory will be required. For example, a 64-point FFT will require about 1280 bytes of RAM. Larger transforms will require proportionately greater amounts of memory. FFT routines will also be the only functions that will potentially require a custom data structure consisting of a pair of 32-bit floating-point variables for the real and imaginary components of a single complex value.

It is estimated that the number of instructions executed per processing method will be about 30,000, while spectral analysis using a 64-point FFT is estimated to be about 300,000. Based on a clock speed of 10 MHz, basic algorithms would require 3 ms to execute while additional spectral analysis would require about 30 ms. Speeds lower than 10 MHz, such as the 4 MHz commonly used in miniaturized systems, could potentially cause a backlog of processing functions. Speeds at or above 10 MHz, such as the standard speeds of 20 and 40 MHz, are recommended to guarantee adequate processing time.

Based on these preliminary assessments, any moderate or high-end microcontroller providing 10KB of program memory, 5KB of data memory, and a clock speed of at least 10 MHz should be capable of implementing the software functions required to perform the desired physiological measurements. It should be noted, however,

that performing additional peripheral functions could increase the memory or speed requirements of the embedded microcontroller.

APPENDIX A – FLOWCHARTS FOR PROCESSING METHODS

A.1 SpO_2 Processing Methods

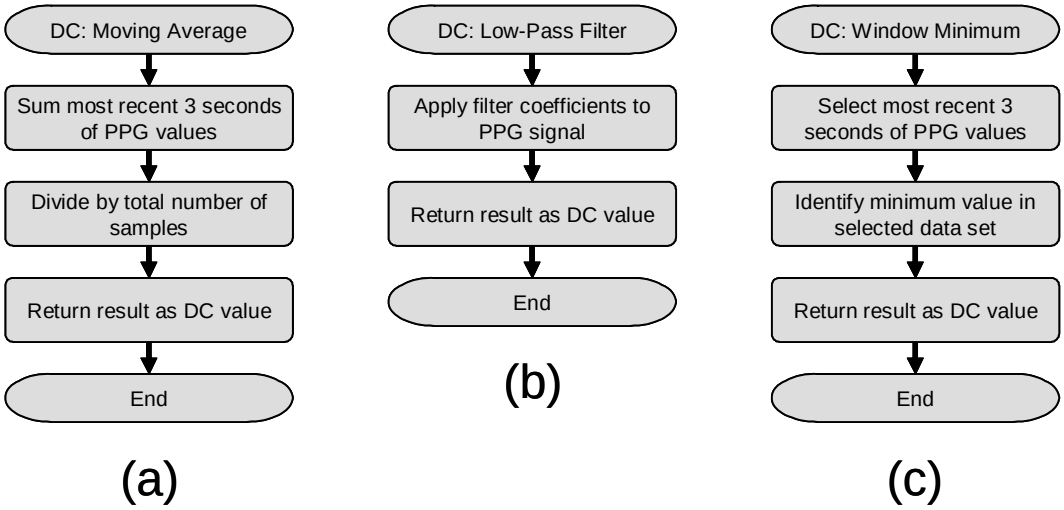

Figure A.1. *DC measurement methods for SpO_2 calculations: (a) Moving Average, (b) LPF, (c) Window Minimum.*

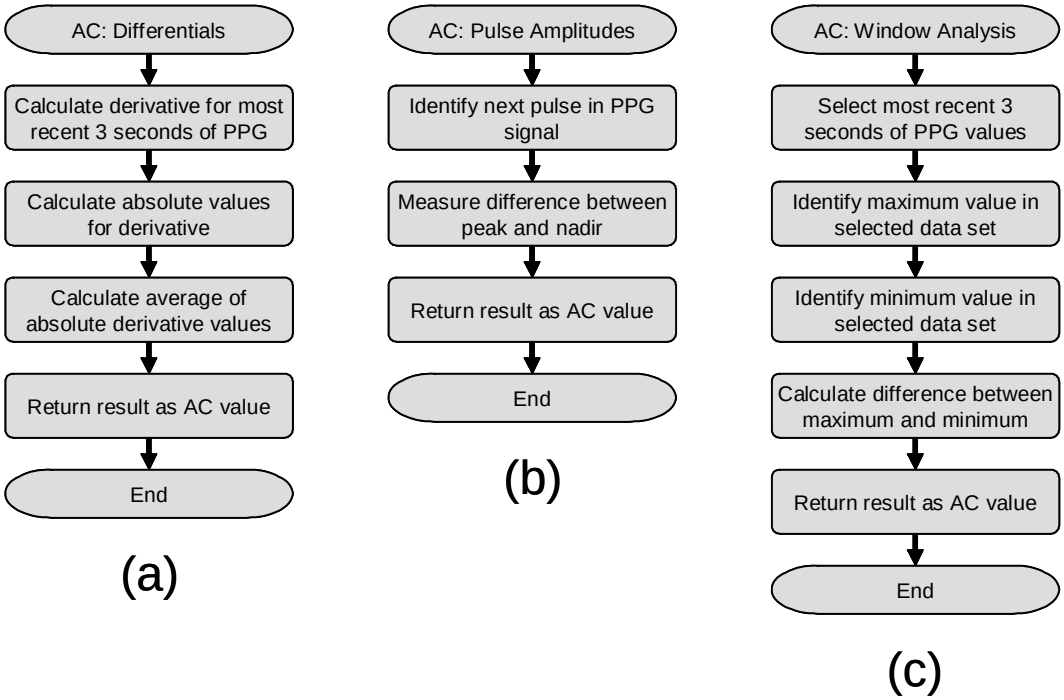

Figure A.2. *AC measurement methods for SpO_2 calculations: (a) Average Differentials, (b) Pulse Amplitudes, (c) Window Analysis.*

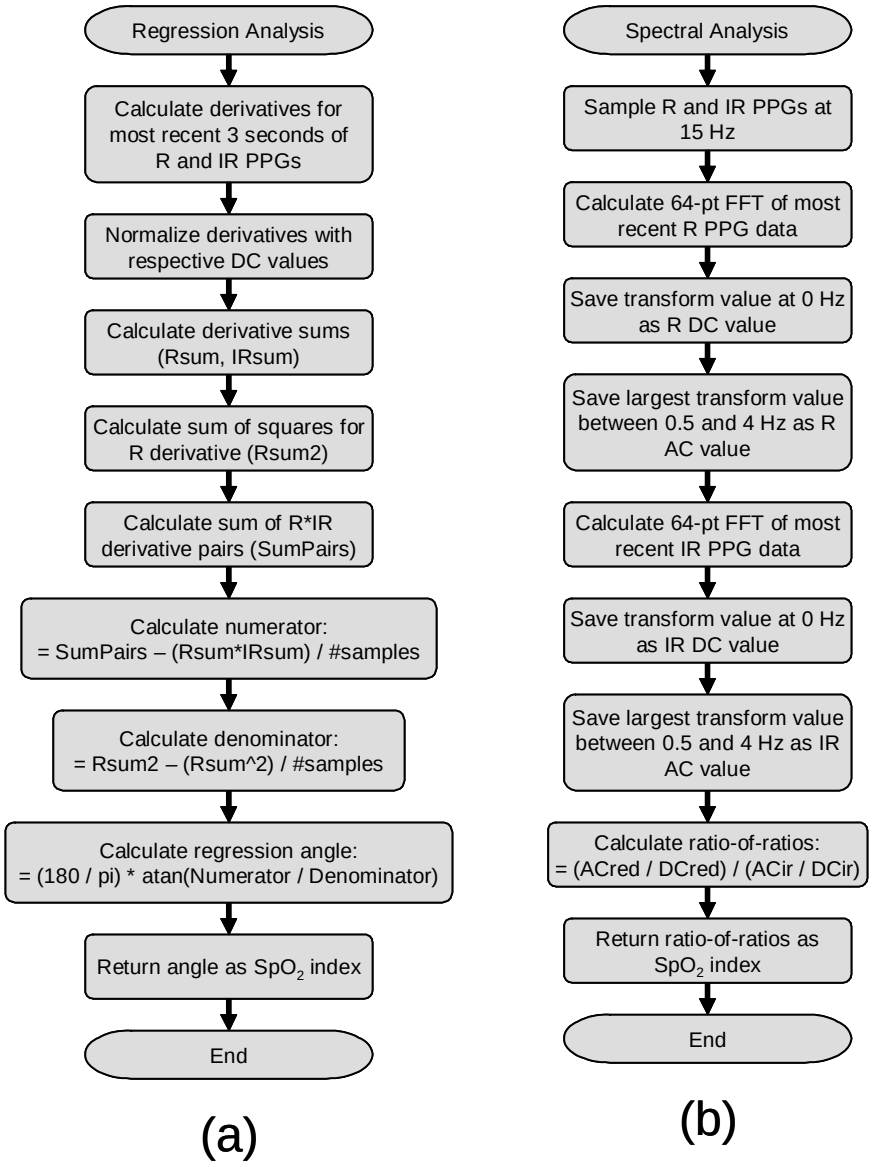

Figure A.3. *AC measurement methods for SpO_2 calculations: (a) Regression Analysis, (b) Spectral Analysis.*

A.2 HR Processing Methods

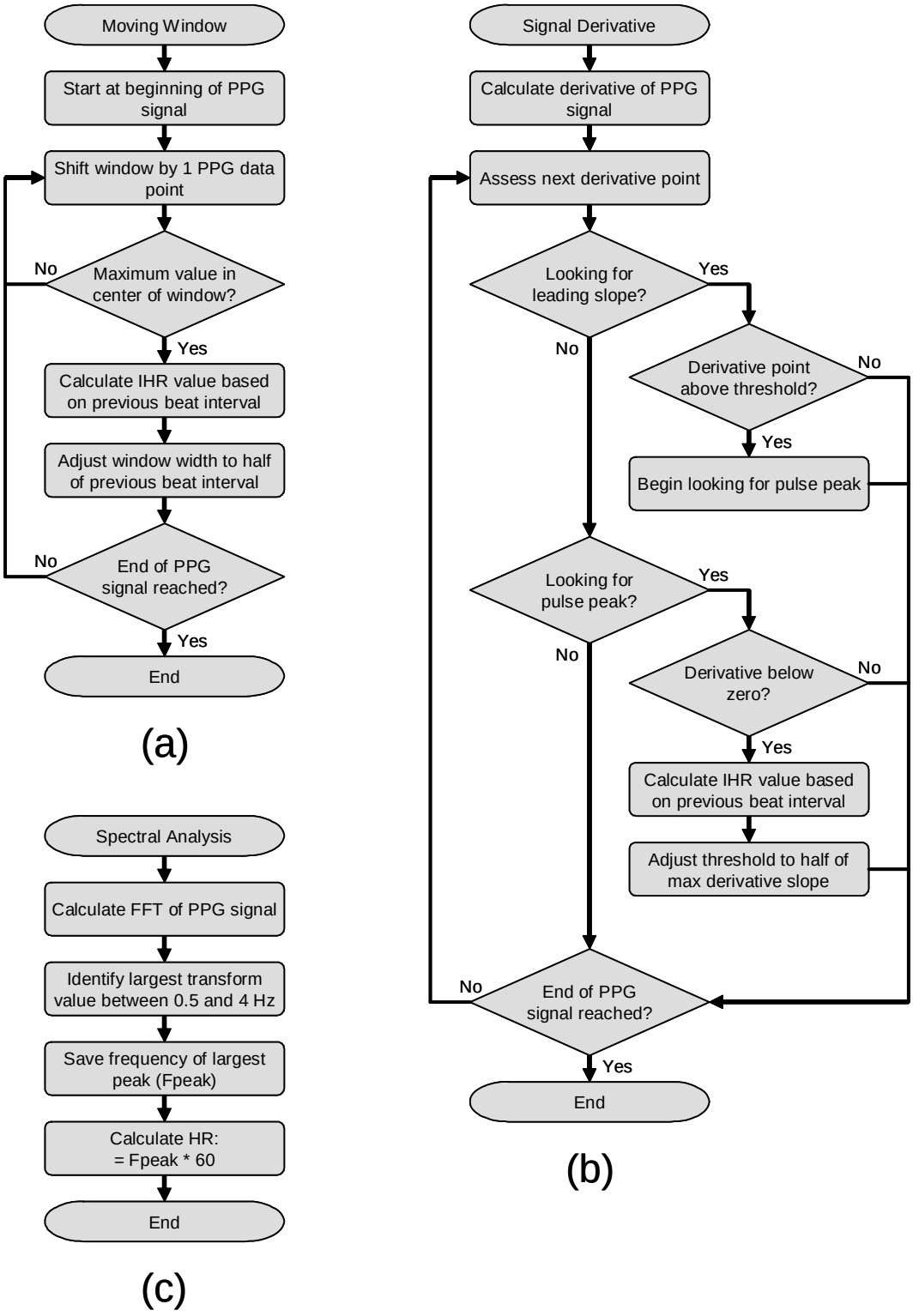

Figure A.4. *Processing methods for HR calculation: (a) Adaptive Moving Window, (b) Signal Derivative, (c) Spectral Analysis.*

A.3 HRV Processing Methods

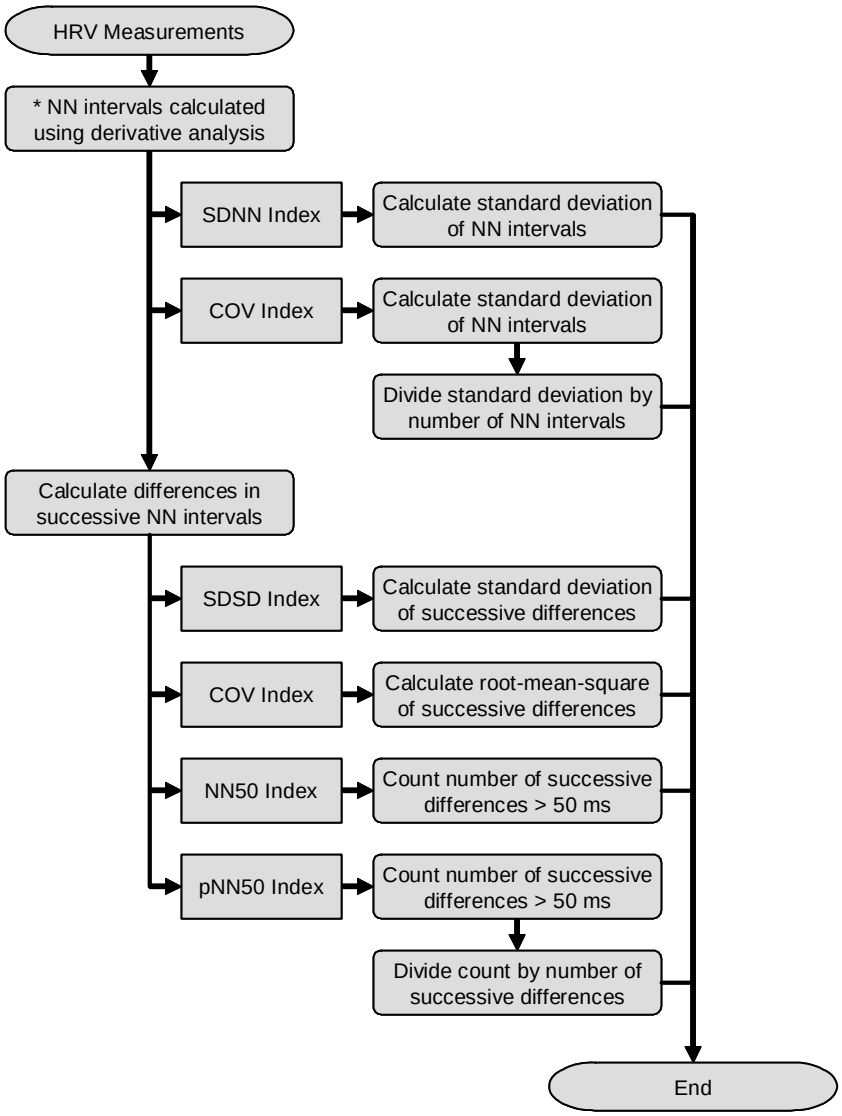

Figure A.5. *Processing methods for HRV index calculations.*

A.4 RR Processing Methods

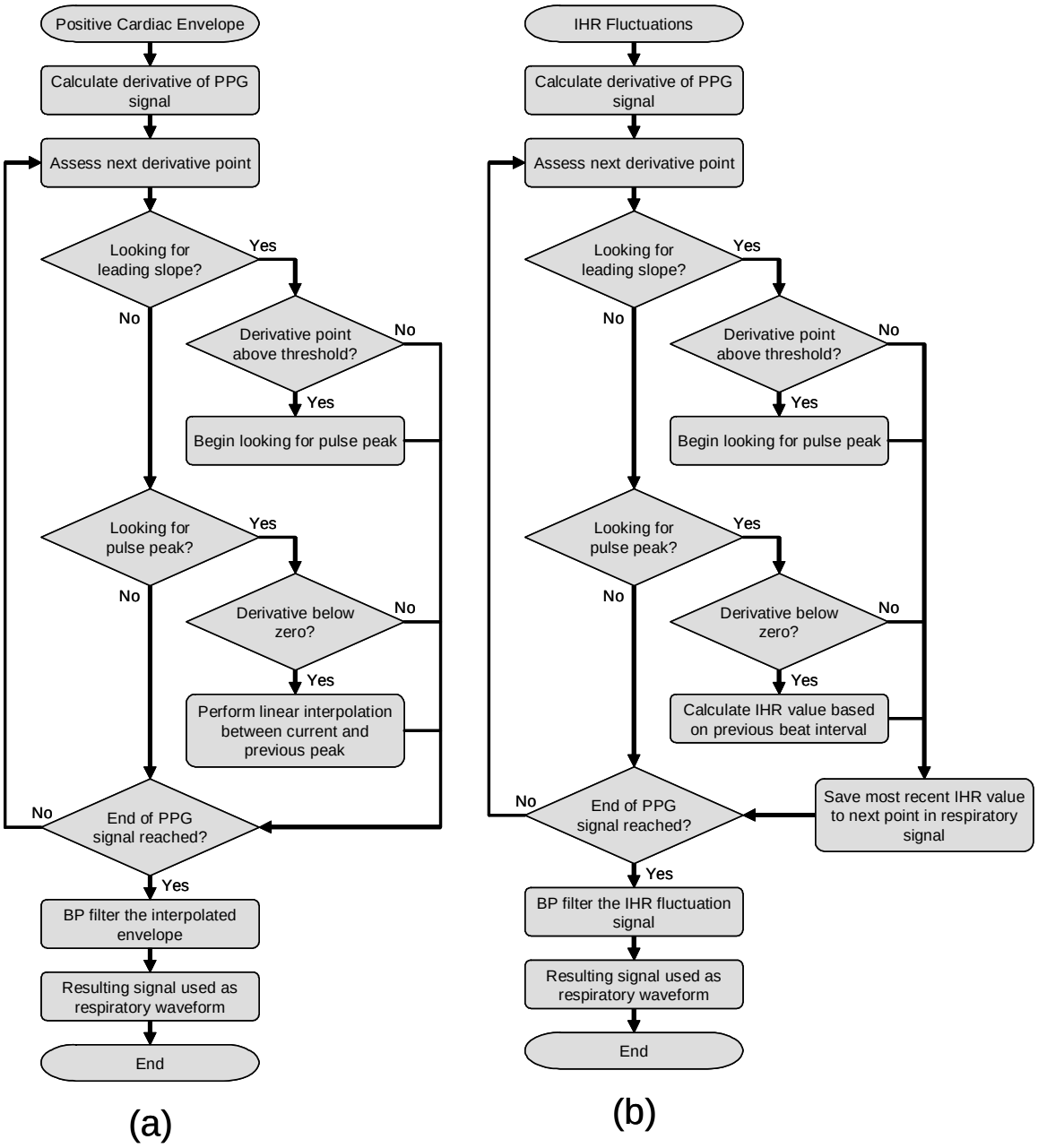

Figure A.6. *Waveform extraction for RR calculation: (a) Positive Cardiac Envelope, (b) IHR Fluctuations.*

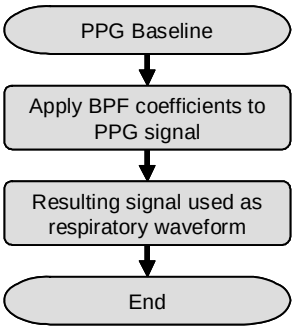

Figure A.7. *Waveform extraction for RR calculation: Baseline Modulations.*

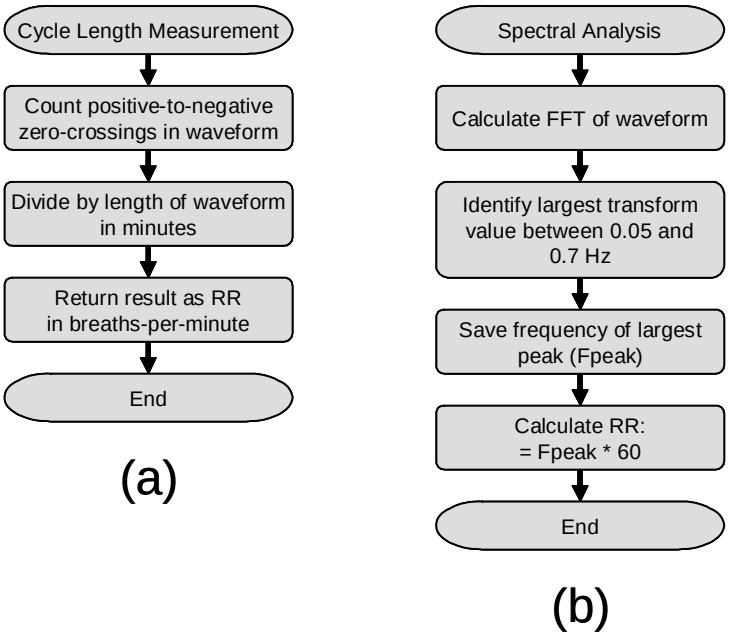

Figure A.8. *Waveform analysis for RR calculation: (a) Cycle Length Measurement, (b) Spectral Analysis.*

REFERENCES

[1] C. J. Obusek, "Warfighter Physiological Status Monitoing (WPSM)," in *The Warrior*, 2001, pp. 6 - 8.

[2] G. S. F. Ling, B. K. Day, P. Rhee, and J. M. Ecklund, "In Search of Technological Solutions to Battlefield Management of Combat Casualties," presented at SPIE Conference on Battlefield Biomedical Technologies, 1999.

[3] "Notes from TATRC Off-Site Meeting," Worcester Polytechnic Institute, Worcester, MA Aug. 2003.

[4] S. P. McGrath, E. Grigg, S. Wendelden, G. Blike, M. DeRosa, A. Fiske, and R. Gray, "ARTEMIS: A Vision for Remote Triage and Emergency Management Information Integration," Dartmouth College, Hanover, NH Nov. 2003.

[5] S. P. McGrath, E. Grigg, S. Wendelden, G. Blike, M. DeRosa, and R. Gray, "Agent Based Casualty Care (ABC Care)," Dartmouth College, Hanover, NH.

[6] S. M. Wendelken, S. P. McGrath, and G. T. Blike, "A Medical Assessment Algorithm for Automated Remote Triage," presented at 25th Annual International Conference of the IEEE EMBS, 2003.

[7] S. Wendelken, S. McGrath, G. Blike, and M. Akay, "The Feasibility of Using a Forehead Reflectance Pulse Oximeter for Automated Remote Triage," presented at IEEE 30th Annual Northeast Conference, 2004.

[8] J. W. Lebak, J. Yao, and S. Warren, "Implementation of a Standards-Based Pulse Oximeter on a Wearable, Embedded Platform," presented at EMBC, 2003.

[9] J. Yao, R. Schmits, and S. Warren, "A Wearable Standards-Based Point-of-Care System for Home Use," presented at EMBC, 2003.

[10] J. Yao and S. Warren, "Design of a Plug-and-Play Pulse Oximeter," presented at Second Joint EMBS/BMES Conference, 2002.

[11] S. Warren, J. Yao, R. Schmitz, and L. Nagl, "Wearable Telemonitoring Systems Designed with Interoperability in Mind," presented at 25th Annual International Conference of the IEEE EMBS, 2003.

[12] J. Muhlsteff, O. Such, R. Schmidt, M. Perkuhn, H. Reiter, J. Lauter, J. Thijs, G. Musch, and M. Harris, "Wearable Approach for Continuous ECG - and Activity Patient-Monitoring," presented at 26th Annual International Conference of the IEEE EMBS, 2004.

[13] J. Y. Hwang, J. M. Kang, Y. W. Jang, and H. C. Kim, "Development of Novel Algorithm and Real-Time Monitoring Ambulatory System Using Bluetooth

Module for Fall Detection in the Elderly," presented at 26th Annual International Conference of the IEEE EMBS, 2004.

[14] A. Tura, M. Badanai, D. Longo, and L. Quareni, "A Medical Wearable Device with Wireless Bluetooth-Based Data Transmission," *Measurement Science Review*, vol. 3, pp. 1 - 4, 2003.

[15] V. Kremin, "Remote Health-Monitoring System," in *Circuit Cellar*, 2003, pp. 10 - 17.

[16] M. V. Scanlon, "Acoustic Sensor for Health Status Monitoring," presented at IRIS Acoustic and Seismic Sensing, 1998.

[17] M. V. Scanlon, "Acoustic Sensor Pad for Physiological Monitoring," presented at 19th Annual International Conference of the IEEE EMBS, 1997.

[18] H. H. Asada, P. Shaltis, A. Reisner, S. Rhee, and R. C. Hutchinson, "Mobile Monitoring with Wearable Photoplethysmographic Biosensors," in *IEEE Engineering in Medicine and Biology Magazine*, 2003, pp. 28 - 39.

[19] N. Aydin, A. Astaras, L. Wang, T. Arslan, A. F. Murray, S. P. Beamont, and D. R. S. Cumming, "Design and Implementation Considerations for an Advanced Wireless Interface in Miniaturized Sensor Microsystems," presented at 25th Annual International Conference of the IEEE EMBS, 2003.

[20] P. Lukowicz, U. Anliker, J. Ward, G. Troster, E. Hirt, and C. Neufelt, "AMON: A Wearable Medical Computer for High Risk Patients," presented at Proceedings of the 6th International Symposium on Wearable Computers, 2002.

[21] U. Anliker, J. A. Ward, P. Lukowicz, G. Troster, F. Dolveck, M. Baer, F. Keita, E. B. Schenker, F. Catarsi, L. Coluccini, A. Belardinelli, D. Shklarski, M. Alon, E. Hirt, R. Schmid, and M. Vuskovic, "AMON: A Wearable Multiparameter Medical Monitoring and Alert System," *IEEE Transactions on Information Technology in Biomedicine*, vol. 8, pp. 415 - 427, 2004.

[22] "Nonin WristOx 3100," Nonin, 2006.

[23] P. O. Isaacson, D. W. Gadtke, and T. L. Johnson, "Finger Clip Pulse Oximeter." USA: Nonin Medical Inc., 1998.

[24] S. P. Athan and J. E. Scharf, "Portable Pulse Oximeter." USA: University of South Florida, 1996.

[25] R. S. Potratz, "Condensed Oximeter System and Method with Noise Reduction Software." USA: Nellcor Puritan Bennett Inc., 1998.

[26] A. A. Ali, D. Carothers, D. Dalke, M. K. Diab, J. Goldman, M. E. Kiani, M. Lee, J. Novak, R. Smith, and V. E. Vaden, "Dual-Mode Pulse Oximeter." USA: Masimo Corporation, 2004.

[27] A. V. J. Challoner, "Photoelectric Plethysmography for Estimating Cutaneous Blood Flow," in *Non-Invasive Physiological Measurements*, vol. 1, P. Rolfe, Ed., pp. 125 - 151.

[28] Y. Mendelson, "Pulse Oximetry: Theory and Applications for Noninvasive Monitoring," *Clin. Chem.*, vol. 38, pp. 1601 - 1607, 1992.

[29] I. Yoshiya, Y. Shimada, and K. Tanaka, "Spectrophotometric Monitoring of Arterial Oxygen Saturation in the Fingertip," *Med. & Biol. Eng. & Comput.*, vol. 18, pp. 27 - 32, 1980.

[30] T. K. Aldrich, M. Moosikasuwan, S. D. Shah, and K. S. Deshpande, "Length-Normalized Pulse Photoplethysmography: A Noninvasive Method to Measure Blood Hemoglobin," *Annals of Biomedical Engineering*, vol. 30, pp. 1291 - 1298, 2002.

[31] W. B. Murray and P. A. Foster, "The Peripheral Pulse Wave: Information Overlooked," *Journal of Clinical Monitoring*, vol. 12, pp. 365 - 377, 1996.

[32] I. Hlimonenko, K. Meigas, and R. Vahisalu, "Waveform Analysis of Peripheral Pulse Wave Detected in the Fingertip with Photoplethysmograph," *Measurement Science Review*, vol. 3, pp. 49 - 52, 2003.

[33] K. Nakajima, T. Tamura, and H. Miike, "Monitoring of Heart and Respiratory Rates by Photoplethysmography Using a Digital Filtering Technique," *Med. Eng. Phys.*, vol. 18, pp. 365 - 372, 1996.

[34] M. Nitzan, H. de Boer, S. Turivnenko, A. Babchenko, and D. Sapoznikov, "Power Spectrum Analysis of Spontaneous Fluctuations in the Photoplethysmographic Signal," *Journal of Basic & Clinical Physiology & Pharmacology*, vol. 5, pp. 269 - 276, 1994.

[35] A. Johansson and T. Stromberg, "Influence of Tidal Volume and Thoraco-Abdominal Separation on the Respiratory Induced Variation of the Photoplethysmogram," *Journal of Clinical Monitoring and Computing*, vol. 16, pp. 575 - 581, 2000.

[36] P. D. Mannheimer, J. R. Casciani, M. E. Fein, and S. L. Nierlich, "Wavelength Selection for Low-Saturation Pulse Oximetry," *IEEE Transactions on Biomedical Engineering*, vol. 44, pp. 148 - 158, 1997.

[37] T. L. Ferrell, P. B. Crilly, S. F. Smith, A. L. Wintenberg, C. L. Britton, G. W. Morrison, M. N. Ericson, D. Hedden, D. Bouldin, A. Passian, T. Downey, A.

Wig, and F. Meriaudeau, "Medical Telesensors," *SPIE*, vol. 3253, pp. 193 - 198, 1998.

[38] J. Webster, *Design of Pulse Oximeters*: IOP Publishing Ltd, 1997.

[39] R. Chin, P. Mannheimer, and R. Flewelling, "Motion Compatible Sensor for Non-Invasive Optical Blood Analysis." USA: Nellcor Puritan Bennett Inc., 2000.

[40] T. K. Aldrich, "Non-Invasive Blood Component Analyzer." USA: Essential Medical Devices, 2000.

[41] T. L. Rusch, J. E. Scharf, and R. Sankar, "Alternate Pulse Oximetry Algorithms for SpO_2 Computation," presented at 16th Annual International Conference of the IEEE EMBS, 1994.

[42] J. E. Scharf, S. Athan, and D. Cain, "Pulse Oximetry Through Spectral Analysis," presented at 12th Southern Biomedical Engineering Conference, 1993.

[43] J. E. Scharf and T. L. Rusch, "Optimization of Portable Pulse Oximetry Through Fourier Analysis," presented at 12th Southern Biomedical Engineering Conference, 1993.

[44] T. L. Rusch, R. Sankar, and J. E. Scharf, "Signal Processing Methods for Pulse Oximetry," *Comput. Biol. Med.*, vol. 26, pp. 143 - 159, 1996.

[45] J. M. Kim, S. H. Kim, D. J. Lee, and H. S. Lim, "Signal Processing Using Fourier and Wavelet Transform for Pulse Oximetry," presented at 4th Pacific Rim Conference on Lasers and Electro-Optics, 2001.

[46] A. M. Terry, "Cepstral Domain Pulse Oximetry." USA: Datex-Ohmeda, Inc., 2003.

[47] T. J. Yorkey and P. D. Mannheimer, "Methods and Apparatus for Estimating a Physiological Parameter Using Transforms." USA: Nellcor Puritan Bennett, Inc., 2000.

[48] M. K. Diab, W. M. Weber, and A. Al-Ali, "Method and Apparatus for Demodulating Signals in a Pulse Oximetry System." USA: Masimo Corporation, 2003.

[49] A. Al-Ali, M. K. Diab, M. E. Kiani, R. J. Kopotic, and D. Tobler, "Stereo Pulse Oximeter." USA: Masimo Corporation, 2005.

[50] K. H. Jarman, "Method and Apparatus for Improved Photoplethysmographic Monitoring of Oxyhemoglobin, Deoxyhemoglobin and Methemoglobin." USA: Ohmeda Inc., 1998.

[51] M. S. Mortz, "System for Pulse Oximetry SPO2 Determination." USA: Datex-Ohmeda, Inc., 1999.

[52] M. S. Mortz, "System for Pulse Oximetry SPO2 Determination." USA: Datex-Ohmeda, Inc., 2002.

[53] D. W. Heckel, "Pulse Oximetry Method and System with Improved Motion Correction." USA: Datex-Ohmeda, Inc., 2002.

[54] M. A. Norris, "Method and Apparatus for Determining Pulse Oximetry Differential Values." USA: Datex-Ohmeda, Inc., 2003.

[55] F. U. Dowla, P. G. Skokowski, and R. R. Leach Jr., "Neural Networks and Wavelet Analysis in the Computer Interpretation of Pulse Oximetry Data," presented at IEEE Signal Processing Society Workshop, 1996.

[56] X. Wang, H. H. Sun, and J. M. van de Water, "Time-Frequency Distribution Technique in Biological Signal Processing," *Biomedical Instrumentation & Technology*, pp. 203 - 212, 1995.

[57] M. K. Diab, E. Kiani-Azarbayjany, I. M. Elfadel, J. McCarthy, W. M. Weber, and R. A. Smith, "Signal Processing Apparatus." USA: Masimo Corporation, 2003.

[58] M. K. Diab and E. Kiani-Azarbayjany, "Signal Processing Apparatus and Method." USA: Masimo Corporation, 2004.

[59] M. K. Diab and M. E. Kiani, "Signal Processing Apparatus and Method." USA: Masimo Corporation, 2004.

[60] J. M. Graybeal and M. T. Petterson, "Adaptive Filtering and Alternative Calculations Revolutionizes Pulse Oximetry Sensitivity and Specificity During Motion and Low Perfusion," presented at 26th Annual International Conference of the IEEE EMBS, 2004.

[61] Masimo, "Signal Extraction Technology," Technical Bulletin.

[62] S. Kaestle, "Method for Digitally Processing Signals Containing Information Regarding Arterial Blood Flow." USA: Hewlett-Packard Company, 1994.

[63] M. K. Diab, "Plethysmograph Pulse Recognition Processor." USA: Masimo Corporation, 2002.

[64] M. K. Diab, "Plethysmograph Pulse Recognition Processor." USA: Masimo Corporation, 2004.

[65] A. A. Ali, D. S. Breed, and J. J. Novak, "Pulse Oximetry Pulse Indicator." USA: Masimo Corporation, 2003.

[66] J. B. Goodman, "Physiological Signal Monitoring System." USA: Vitalsines International, Inc., 2003.

[67] S. C. Gates, "Peak Detection," in *Laboratory Automation Using the IBM PC*. Englewood Cliffs, NJ: Prentice Hall, 1989, pp. 188 - 209.

[68] J. L. Reuss and D. E. Bahr, "Period Domain Analysis in Fetal Pulse Oximetry," presented at Second Joint EMBS/BMES Conference, 2002.

[69] J. E. Corenman, R. T. Stone, A. Boross, D. A. Briggs, and D. E. Goodman, "Method and Apparatus for Detecting Optical Pulses." USA: Nellcor Inc., 1990.

[70] L. Bernardi, A. Radaelli, P. L. Solda, A. J. S. Coats, M. Reeder, A. Calciati, C. S. Garrard, and P. Sleight, "Autonomic Control of Skin Microvessels: Assessment by Power Spectrum of Photoplethysmographic Waves," *Clinical Science*, vol. 90, pp. 345 - 355, 1996.

[71] Task Force of the European Society of Cardiology and the North American Society of Pacing and Electrophysiology, "Heart Rate Variability: Standards of Measurement, Physiological Interpretation, and Clinical Use," *Circulation*, vol. 93, pp. 1043 - 1065, 1996.

[72] S. M. Wendelken, S. P. McGrath, M. Akay, and G. T. Blike, "Using a Forehead Reflectance Pulse Oximeter to Detect Changes in Sympathetic Tone," presented at 26th Annual International Conference of the IEEE EMBS, 2004.

[73] A. Hossen, B. A. Ghunaimi, and M. O. Hassan, "Subband Decomposition Soft-Decision Algorithm for Heart Rate Variability Analysis in Patients with Obstructive Sleep Apnea and Normal Controls," *Signal Processing*, vol. 85, pp. 95 - 106, 2005.

[74] R. McCraty, M. Atkinson, W. A. Tiller, G. Rein, and A. D. Watkins, "The Effects of Emotions on Short-Term Power Spectrum Analysis of Heart Rate Variability," *American Journal of Cardiology*, vol. 76, pp. 1089 - 1093, 1995.

[75] A. Marfella, M. Romano, M. Cesarelli, and M. Bracale, "The Cardiotocography: Frequency Analysis of the Fetal Heart Rate Variability," presented at 3rd European medical and Biological Engineering Conference, 2005.

[76] V. S. Murthy, S. Ramamoorthy, N. Srinivasan, S. Rajagopal, and M. M. Rao, "Analysis of Photoplethysmographic Signals of Cardiovascular Patients," presented at 23rd Annual EMBS International Conference, 2001.

[77] J. Vila, F. Palacios, J. Presedo, M. Fernandez-Delgado, P. Felix, and S. Barro, "Time-Frequency Analysis of Heart-Rate Variability," *IEEE Engineering in Medicine and Biology*, pp. 119 - 126, 1997.

[78] R. J. Winchell and D. B. Hoyt, "Analysis of Heart-Rate Variability: A Noninvasive Predictor of Death and Poor Outcome in Patients with Severe Head Injury," *Journal of Trauma: Injury, Infection, and Critical Care*, vol. 43, pp. 927 - 933, 1997.

[79] H. V. Huikuri, T. Makikallio, J. Airaksinen, R. Mitrani, A. Castellanos, and R. J. Myerburg, "Measurement of Heart Rate Variability: A Clinical Tool or a Research Toy?," *Journal of the American College of Cardiology*, vol. 34, pp. 1878 - 1883, 1999.

[80] D. Petry and J. L. B. Marques, "Software for Heart Rate Variability and QT Interval Variability Analysis," presented at 3rd European Medical and Biological Engineering Conference, 2005.

[81] Y. Y. Gu and Y. T. Zhang, "Reducing the Influence of Contacting Force Applied on Photoplethysmographic Sensor on Heart Rate Variability Estimation," presented at 25th Annual International Conference of the IEEE EMBS, 2003.

[82] W. Johnston and Y. Mendelson, "Extracting Heart Rate Variability from a Wearable Reflectance Pulse Oximeter," presented at IEEE 31st Annual Northeast Bioengineering Conference, 2005.

[83] L. Kalakutskiy, V. Kalakutskiy, and F. Belyanin, "Uncertainty of Heart Rate Variability Diagnostic Indices in Patient Monitoring Systems," presented at 3rd European Medical and Biological Engineering Conference, 2005.

[84] S. A. Atapattu and R. D. Mitrani, "A Telemedicine Application Utilizing DataSocket® to Remotely Track the Heart Rate Variability of Patients in a Clinical Research Environment," presented at 2000 IEEE EMBS International Conference on Information Technology Applications in Biomedicine, 2000.

[85] S. A. Atapattu, R. D. Mitrani, H. V. Huikuri, and P. P. Tarjan, "A Computer Program to Acquire, Analyze and Track the Heart Rate Variability of Patients in a Clinical Research Environment," presented at 22nd Annual EMBS International Conference, 2000.

[86] J. Schesser, P. Asselin, S. Reisman, and R. Rockland, "Are the Results Correct? - An Application of Wavelets to Analyze Heart Rate Variability," presented at IEEE 31st Annual Northeast Bioengineering Conference, 2005.

[87] R. A. Bates, M. F. Hilton, K. R. Godfrey, and M. J. Chappell, "Comparison of Methods for Harmonic Wavelet Analysis of Heart Rate Variability," *IEE Proc.-Sci. Meas. Technol.*, vol. 145, pp. 291 - 300, 1998.

[88] S. R. Seydnejad and R. I. Kitney, "Real-Time Heart Rate Variability Extraction Using the Kaiser Window," *IEEE Transactions on Biomedical Engineering*, vol. 44, pp. 990 - 1005, 1997.

[89] S. M. Wendelken, "Using a Forehead Reflectance Pulse Oximeter to Detect Changes in Sympathetic Tone," in *Biomedical Engineering*. Hanover, NH: Dartmouth College, 2004, pp. 108.

[90] J. Hayano, J. A. Taylor, A. Yamada, S. Mukai, R. Hori, T. Asakawa, K. Yokoyama, Y. Watanabe, K. Takata, and T. Fujinami, "Continuous Assessment of Hemodynamic Control by Complex Demodulation of Cardiovascular Variability," pp. H1229 - H1238, 1993.

[91] H. Husum, M. Gilbert, T. Wisborg, Y. van Heng, and M. Murad, "Respiratory Rate as a Prehospital Triage Tool in Rural Trauma," *Journal of Trauma: Injury, Infection, and Critical Care*, vol. 55, pp. 466 - 470, 2003.

[92] S. C. Tarrant, R. E. Ellis, F. C. Flack, and W. G. Selley, "Comparative Review of Techniques for Recording Respiratory Events at Rest and During Deglutition," *Dysphagia*, vol. 12, pp. 24 - 38, 1997.

[93] K. P. Cohen, D. Panescu, J. H. Booske, J. G. Webster, and W. J. Tompkins, "Design of an Inductive Plethysmograph for Ventilation Measurement," *Physiological Measurement*, vol. 15, pp. 217 - 229, 1994.

[94] W. S. Johnston and Y. Mendelson, "Extracting Breathing Rate Information from a Wearable Reflectance Pulse Oximeter Sensor," presented at 26th Annual International Conference of the IEEE EMBS, 2004.

[95] L. Nilsson, A. Johansson, and S. Kalman, "Macrocirculation is Not the Sole Determinant of Respiratory Induced Variations in the Reflection Mode Photoplethysmographic Signal," *Physiological Measurement*, vol. 24, pp. 925 - 937, 2003.

[96] A. Johansson and P. A. Oberg, "Estimation of Respiratory Volumes from the Photoplethysmographic Signal. Part I: Experimental Results," *Med. & Biol. Eng. & Comput.*, vol. 37, pp. 42 - 47, 1999.

[97] A. Johansson and P. A. Oberg, "Estimation of Respiratory Volumes from the Photoplethysmographic Signal. Part 2: A Model Study," *Med. & Biol. Eng. & Comput.*, vol. 37, pp. 48 - 53, 1999.

[98] J. M. Chang, S. P. McGrath, and G. T. Blike, "Investigating Respiratory Variation Using a Forehead Reflectance Pulse Oximeter to Identify Airway Obstruction for Automated Remote Triage," presented at IEEE 31st Annual Northeast Bioengineering Conference, 2005.

[99] C. Ahlstrom, A. Johansson, T. Lanne, and P. Ask, "A Respiration Monitor Based on Electrocardiographic and Photoplethysmographic Sensor Fusion," presented at 26th Annual International Conference of the IEEE EMBS, 2004.

[100] P. Z. Zhang, W. N. Tapp, S. S. Reisman, and B. H. Natelson, "Respiration Response Curve Analysis of Heart Rate Variability," *IEEE Transactions on Biomedical Engineering*, vol. 44, pp. 321 - 325, 1997.

[101] D. Barschdorff and W. Zhang, "Respiratory Rhythm Detection with Photoplethysmographic Methods," presented at 16th Annual International Conference of the IEEE EMBS, 1994.

[102] J. E. Whitney II and L. Solomon, "Respiration-Rate Signal Extraction from Heart Rate," presented at SPIE, 2001.

[103] L. Sornmo and P. Laguna, "ECG Signal Processing: Heart Rate Variability," in *Bioelectrical Signal Processing in Cardiac and Neurological Applications*, 2005, pp. 567 - 573.